EVGENIA RYABENKO

Nitrogen Isotopes in the Atlantic and Pacific Oxygen Minimum Zones

Nitrogen Isotopes in the Atlantic and Pacific Oxygen Minimum Zones

Dissertation zur Erlangung des Doktorgrades der
Mathematisch-Naturwissenschaftlichen Fakultät der
Christian-Albrechts-Universität zu Kiel

vorgelegt von Evgenia Ryabenko

Kiel 2011
Tag der mündlichen Prüfung: 23.05.2011
Finale Druckfassung Juni 2011

«А чем вы занимаетесь?» – спросил я.
«Как и вся наука, – сказал горбоносый. – Счастьем человеческим»

Аркадий и Борис Стругацкие.
«Понедельник начинается в субботу»

Referent:	Prof. Dr. Douglas W. R. Wallace
Koreferent:	Prof. Dr. Andreas Oschlies

Contents

List of Figures 9

List of Tables 11

Abbreviations 13

Summary 17

Zusammenfassung 15

1. Introduction 19

1.1. The Oxygen Minimum Zone 19

1.2. Nitrogen cycle investigation using stable isotopes 22
1.2.1. Fundamentals 22
1.2.2. Influence of nitrogen cycle processes on isotopic distributions 24

1.3. Processes of the nitrogen cycle 28
1.3.1. Nitrogen loss (denitrification and anammox) in the ocean 28
1.3.2. Nitrification 32
1.3.3. Nitrogen assimilation 34
1.3.4. Nitrogen fixation in the ocean 36

1.4. Synopsis of the chapters. 38

2. Effect of chloride on the chemical conversion of nitrate to nitrous oxide for $\delta^{15}N$ analysis 41

2.1. Introduction 42

2.2. Materials and Methods 44
2.2.1. Chemical conversion of nitrate to nitrous oxide 44
2.2.2. IRMS 45
2.2.3. NO_3^-, NO_2^- and NH_4^+ concentration analysis (DIN). 46
2.2.4. Nitrous oxide analysis. 46

2.3. Results 47
2.3.1. Influence of the salt concentration on $\delta^{15}N\text{-}NO_3^-$ determination 47
2.3.2. Influence of the salt concentration on second reduction step. 49
2.3.3. Efficiency and recovery of the first reduction step 51

2.4. Discussion and conclusions 56

3. Contrasting biogeochemistry of nitrogen in the Atlantic and Pacific OMZ's 57

3.1. Introduction. 58

3.2. Sampling and analytical methods. 59

3.3. Hydrographic setting of the two study regions 60

3.4. Results and discussion 63
3.4.1. Vertical distribution of nitrogen species and isotopes 63
3.4.2. Property-Property Distributions 68

3.5. Summary and conclusions. 76

4. Nitrogen isotope gradients off Peru and Ecuador related to upwelling, productivity, nutrient uptake and oxygen deficiency 79

4.1. Introduction 80

4.2. Regional setting 82

4.3. Sampling and analytical methods 83

4.4. Results 85
4.4.1. Surface sediments: $\delta^{15}N$ and export production proxies 85
4.4.2. Oxygen, nutrients and $\delta^{15}N$ water column distribution 88

4.5. Discussion 90
4.5.1. Latitudal distribution of $\delta^{15}N$ 90

4.6. Summary and conclusions 93

5. Eddy Enhancement of Nitrogen-Loss from an OMZ 95

5.1. Introduction 96

5.2. Supplementary Information 102
5.2.1. Methods 102
5.2.2. Use of N' to estimate NO_3^- removal and production of biogenic N_2 103
5.2.3. Anomaly in the $\delta^{15}N$ of N_2 104

6. Conclusions and Outlook 107

Author contributions 111

References 113

Acknowledgements 131

Eidesstattliche Erklärung 133

List of figures

Fig. 1.1. Physical model of Oxygen Minimum Zones 20
Fig. 1.2. Dissolved oxygen on the 26.5 sigma theta surface 21
Fig. 1.3. Marine nitrogen cycle 25
Fig. 1.4. $\delta^{15}N$ ranges of some important nitrogen compounds 26
Fig. 1.5. The impact of different processes on the $\delta^{15}N$ of oceanic NO_3^- 27
Fig. 1.6. $N^* = [NO_3^-] - 16\times[PO_4^{3-}] + 2.9$ on the 26.5 sigma theta surface 31
Fig. 2.1. Scheme of PRECON, GC, and the Cu/Ni metal reducer furnace 45
Fig. 2.2. Effect of salt concentration on the peak area and $\delta^{15}N_2O$ 48
Fig. 2.3. Salting out effect on the second reduction step and overall reduction 50
Fig. 2.4. DIN speciation of first reduction step without salt addition 53
Fig. 2.5. DIN speciation of first reduction step with 0.2 M salt addition 53
Fig. 2.6. DIN speciation of first reduction step with 0.5 M salt addition 54
Fig. 2.7. DIN speciation of first reduction step with 5 M salt addition 54
Fig. 3.1. Oxygen distribution at 200 m 59
Fig. 3.2. T-S diagrams with O_2 color coded for the Pacific and the Atlantic OMZ's 61
Fig. 3.3. Oxygen distribution in the Pacific and the Atlantic study regions 64
Fig. 3.4. Typical water column profiles 64
Fig. 3.5. Shallow vertical profiles of M80 stations in the Atlantic 67
Fig. 3.6. $[NO_3^-]$:$[PO_4^{3-}]$ relationships in the Pacific and the Atlantic study regions 68
Fig. 3.7. ΔN_2O vs. AOU in the Pacific and in the Atlantic study areas 70
Fig. 3.8. $\delta^{15}N$-NO_3^- vs. ΔN_2O to in the Pacific and in the Atlantic study areas 71
Fig. 3.9. $\delta^{15}N$ distribution vs. N' the Pacific 71
Fig. 3.10. Isotopic fractionation in the Pacific OMZ 72
Fig. 3.11. Satellite images of Aerosol Optical Depth at different time periods 75

Fig. 4.1. Latitudinal distribution of O_2 and NO_3^- along the South American coast 82

Fig. 4.2. Latitudal distribution of O_2 along the Peruvian margin 84

Fig. 4.3. a) Surface sediment $\delta^{15}N$ values and water column station positions 86

Fig. 4.3. b) C/N ratio and $\delta^{13}C$ data along the Peruvian margin 86

Fig. 4.3. c) Distribution of paleoproductivity proxies 87

Fig. 4.4. a) Water column distribution of O_2, $\delta^{15}N\text{-}NO_3^-$ and NO_3^- concentrations at for three stations, 5°S, 10°S and 17°S. 89

Fig. 4.4. b) Latitudal distribution of $\delta^{15}N_{sed}$ and $\delta^{15}N_{water\ column}$ 89

Fig. 4.5. $\delta^{15}NO_3^-$ vs. nitrate utilization in water column above the nitrocline 92

Fig. 5.1. Biogeochemical maps of the Peru OMZ 97

Fig. 5.2. Property vs depth profiles for stations 7 and 29 97

Fig. 5.3. Profiles at station 7. 99

Fig. 5.4. Satellite observations averaged for January 2009 100

Fig. 5.5. Profile for the offset between $\delta^{15}N\text{-}NO_3^-$ and $\delta^{15}N\text{-}NO_2^-$ at Station 7 105

Fig. 5.6. Parameter distribution off the Peru coast. 106

List of tables

Table 2.1. Effect of salt concentration in the sample on $\delta^{15}N_2O$ product. 47
Table 2.2. Calculation of N_2O partitioning and associated $\delta^{15}N$ fractionation 49
Table 2.3. $\delta^{15}N$ correlation between overall method and second reduction step 51
Table 2.4. Kinetics of first reduction step 52
Table 3.1. Summary of properties of water masses 62
Table 3.2. Predicted surface water $\delta^{15}N\text{-}NO_3^-$ under different scenarios 75

Abbreviations

13CW	13°C Equatorial Water
AAIW	Antarctic Intermediate Water
ADCP	acoustic doppler current profiler
AMO	ammonium monooxygenase
AOA	ammonium-oxidizing archaea
AOB	ammonium-oxidizing bacteria
AOU	apparent oxygen utilization
ATP	adenosine-5′-triphosphate
AVISO	Archiving, Validation and Interpretation of Satellite Oceanographic data
DIN	dissolved inorganic nitrogen
DIW	Deionized water
DON	dissolved organic nitrogen
ENSO	El-Niño-Southern Oscillation
ESW	Equatorial Surface Water
ETNA	eastern tropical North Atlantic
ETSP	eastern tropical South Pacific
EUC	Equatorial Undercurrent
GC-ECD	gas chromatography with electron capture detector
GEOSECS	Geochemical Ocean Section Study
HAO	hydroxylamine oxidoreductase
IRMS	ion ratio mass spectrometer
JGOFS	Joint Global Ocean Flux Study
LCPW	Lower Circumpolar Water
NACW	North Atlantic Central Waters
NADPH	nicotinamide dinucleotide phosphate
NADW	North Atlantic Deep Water
NASA	National Aeronautics and Space Administration

NECC	North Equatorial Counter Current
NEUC	North Equatorial Under Current
NifH	the enzyme catalyzing N_2 fixation
NiR	the enzyme catalyzing nitrite reduction
NOAA	US National Oceanic and Atmospheric Administration
NOB	nitrite-oxidizing bacteria
OM	organic matter
OMZ	oxygen minimum zone
PCU	Peruvian Coastal Upwelling
PN	particulate nitrogen
PRECON	Pre-concentration unit
SACW	South Atlantic Central Waters
SAMW	Subantarctic Mode Water
SCC	Southern Subsurface Counter Current
SEC	South Equatorial Current
SFB-754	Sonderforschungsbereich-754 "Climate-Biogeochemistry Interactions in the Tropical Ocean"
SICC	Southern Intermediate Counter Currents
SLA	sea level anomaly
SOPRAN	Surface Ocean Processes in the Anthropocene
SPDW	South Pacific Deep Water
SSC	sea-surface chlorophyll
STSW	Subtropical Surface Water
STUW	South Pacific Subtropical Underwater
TENATSO	Tropical Eastern North Atlantic Time-Series Observatory
TSW	Tropical Surface Water
WOA05	World Ocean Atlas 2005

Zusammenfassung

Stickstoff nimmt als ein limitierender Faktor in der biologischen Produktivität eine zentrale Rolle in der Biogeochemie des Ozeans ein. Die enorme Vielfalt der chemischen Verbindungen und Transformationen, an denen Stickstoff beteiligt ist, ist im Gegensatz zu vielen anderen Elementen einzigartig. Bei nahezu allen Stoffwechselprozessen mariner Organismen findet eine Isotopenfraktionierung statt. Folglich können durch stabile Isotope des Stickstoffs wichtige Rückschlüsse auf Quellen, Senken und Transformationen von Stickstoff innerhalb des Kreislaufes des Ozeans gezogen werden. Diese Dissertation untersucht speziell den Stickstoffkreislauf an zwei unterschiedlichen Regionen des Ozeans: den östlichen tropischen Nordatlantik und den östlichen tropischen Südpazifik. Diese zwei Regionen sind unteranderem bekannt für sauerstoffarme Zonen (OMZs), welche einen großen Einfluss auf den globalen Stickstoffkreislauf haben.

Zu Beginn der Arbeit wird die Methode zur Messung von Stickstoffisotopen beschrieben. Mit dieser Methode wurden die beiden OMZs soweit miteinander verglichen, dass eine Aussage über die dominierenden Prozesse in den jeweiligen Regionen und deren Auswirkungen auf den globalen Stickstoffkreislauf getroffen werden konnte. In der atlantischen OMZ dominieren Nitrifikation und die Ablagerung von Wüstenstaub den Stickstoffkreislauf, welches durch die Bestimmung des $\delta^{15}N$ Isotops festgestellt wurde. In der pazifischen OMZ lag der Schwerpunkt auf den Effekten der stickstoffreduzierenden Prozesse. Allerdings stellte sich ein kleinerer Fraktionierungsfaktor für Stickstoff als erwartet heraus (11.4‰ anstatt 20 – 30‰), was höchstwahrscheinlich für eine Denitrifikation im Sediment spricht.

Die letzten zwei Abschnitte der Arbeit sind der pazifischen OMZ gewidmet. Die Konzentration von $\delta^{15}N$ in der Wassersäule und in der Sedimentoberfläche zeigt einen zu den Breitengraden parallelen Anstieg von Norden nach Süden entlang der peruanischen Küste, was durchaus mit der Verstärkung der OMZ korreliert. Mit Hilfe der Daten aus der Wassersäule konnte gezeigt werden, dass die stickst-

offreduzierenden Prozesse indirekten Einfluss auf den in der Sedimentoberfläche bestimmten $\delta^{15}N_{sed}$ Werte haben. Die breitengradabhängige Verteilung von $\delta^{15}N_{sed}$ entlang der südamerikanischen Küste korreliert sehr gut mit der Nährstoffaufnahme, was die stickstoffreduzierenden Prozesse in den Schatten stellt. Dieser Zusammenhang ist wenig überraschend, da hauptsächlich die biologische Stickstoffaufnahme zur Entstehung von organischem Material und letztendlich zur Ablagerung im Sediment beiträgt.

Im letzten Kapitel sollen die Daten vom Pazifik zeigen, dass küstennahe mesoskalige Eddies zu einer Erhöhung des Stickstoffverlustes führen. Der Transport von nährstoffreichem Wasser vom Schelf in den offenen Ozean durch Eddies regt eine erhöhte Produktion von organischem Material an. Die sich ergebenen Impulse durch das organische Material tragen zur Förderung von stickstoffmindernden Vorgängen mit einer extremen Stickstofffraktionierung bis zu 40‰ bei. Diese Ergebnisse unterstreichen die Kopplung von physikalischen, chemischen und biologischen Prozessen in den tropischen OMZs.

Summary

As a limiting element for biological productivity, nitrogen occupies a central role in ocean biogeochemistry. It exists in more chemical forms than most other elements, with a myriad of chemical transformations that are unique to this element. Nearly all these transformations are undertaken by marine organisms as part of their metabolism, which involves isotopic fractionation. Thus stable isotopes of nitrogen carry important information on sources and sinks of nitrogen and its transformation within the oceanic cycle. This dissertation focused on the nitrogen cycle in two very different ocean regions: the Eastern Tropical North Atlantic and the Eastern Tropical South Pacific. These two basins are associated with Oxygen Minimum Zones (OMZs), which have a great influence on the global nitrogen cycle.

The first part of the thesis describes the method used for nitrogen isotope measurement. The method was used to contrast the two OMZs, to investigate what processes are dominating in each of them and how they influence the global nitrogen cycle. The nitrogen cycle in the Atlantic OMZ is dominated by nitrification and dust deposition, which could be detected in nitrogen isotope ($\delta^{15}N$) signatures. In the Pacific OMZ, effects of nitrogen loss processes were most pronounced. The nitrogen fractionation factor, however, was much smaller than expected (11.4‰ instead of 20 – 30‰), which was most probably was an effect of denitrification in sediments.

The last two parts are devoted to the Pacific OMZ nitrogen cycle. $\delta^{15}N$ in water column and surface sediments showed a parallel latitudinal increase from north to south along the Peru margin, which correlates with intensification of the OMZ. From water column data it was showed that N-loss processes indirectly influence the $\delta^{15}N$ found in the surface sediments ($\delta^{15}N_{sed}$). Latitudinal distribution of $\delta^{15}N_{sed}$ along the South American coast, however, showed a very good correlation with surface water nitrogen utilization, outshining N-loss

processes. This correlation is not surprising as utilization is the main biological process producing organic matter which is eventually buried in the sediments.

In the last chapter, the data from the Pacific are used to demonstrate that coastal mesoscale eddies lead to an enhancement of N-loss. Transport of nutrient rich waters from the shelf into the open ocean by eddies stimulates high organic matter production. Resulting pulses of organic matter stimulate N-loss events with an extreme N isotope fractionation, reaching 40‰. This observation emphasizes the coupling of physics, chemistry and biology in the tropical OMZs.

1 Introduction

Nitrogen is the most important element in the biogeochemical processes in the ocean. The study of nitrogen isotope distributions is central in order to understand the sinks and sources of nitrogen and the dominant processes in the ocean nitrogen cycle. The oxygen minimum zone is the most important basin for nitrogen sink, while nitrogen is produced by various processes in various basins. This chapter will briefly introduce the basic topics of the dissertation and present latest findings in the field.

1.1. The Oxygen Minimum Zone

The Oxygen Minimum Zone (OMZ) is a volume in the ocean where the oxygen concentration is close to zero. In the ocean oxygen is consumed via biogeochemical processes (e.g. respiration) and supplied by physical processes (e.g. mixing) and photosynthesis. From a biogeochemical viewpoint the OMZ's are located in eastern boundary upwelling areas with high productivity (HELLY, *et al.*, 2004), and thus can have a rather complex cycling of nutrients. From a physical point of view OMZ's are seen as a consequence of minimal lateral replenishment by surface waters (REID, *et al.*, 1965) being located in the so called 'shadow zones', which are unventilated by the basin scale wind-driven circulation (LUYTEN, *et al.*, 1983) (Fig. 1.1).

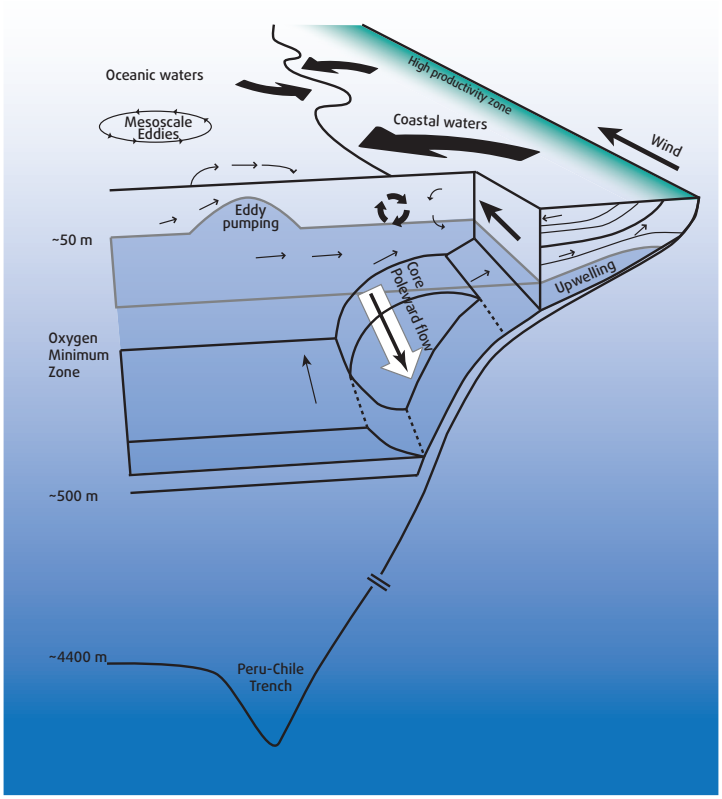

Fig. 1.1. Physical model of Oxygen Minimum Zones (adapted from webpage of Universidad de Concepción www. omz.udec.cl).

The geographical location of OMZ's are to first order determined by: (I) the patterns of upwelling, either via Ekman or equatorial divergence, (II) the regions of general sluggish horizontal transport at the eastern boundaries, and (III) to regions with high productivity (Karstensen, *et al.*, 2008) (Fig. 1.2).

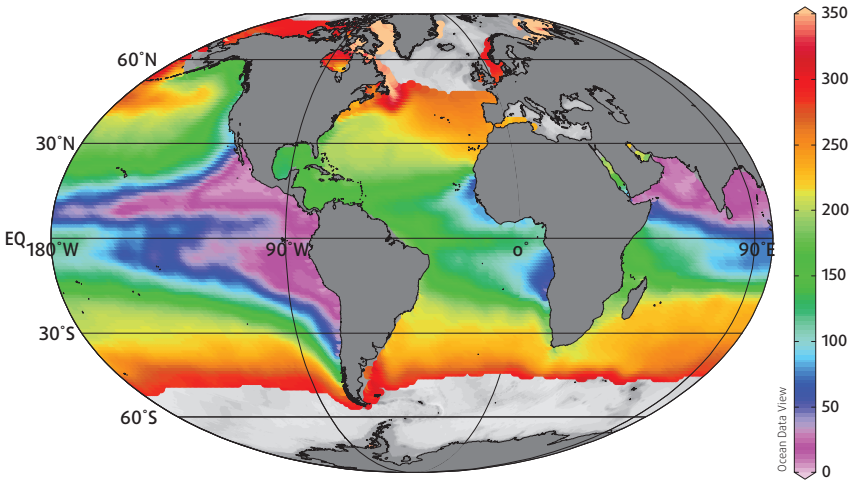

Fig. 1.2. Dissolved oxygen on the 26.5 sigma theta surface (World Ocean Atlas 2005).

It was shown that under low oxygen conditions high concentrations of nitrous oxide (N_2O) and other greenhouse gases (Naqvi, et al., 2010) are produced in the water column and in the sediments a release of iron (Fe) and phosphate into the ambient waters (Hupfer, et al., 2008) is observed. Fe is a limiting element in many parts of the global ocean and essential for many biochemical processes.

Under oxic conditions, but also at the upper boundary (oxycline) of an omz, nitrification transforms ammonium (NH_4^+) into nitrite (NO_2^-), and further to nitrate (NO_3^-). omz's are, however, especially associated with nitrogen loss processes in the ocean: denitrification (Cline, et al., 1972, Codispoti, et al., 2001, Ward, et al., 2009) and anammox (Galan, et al., 2009, Hamersley, et al., 2007, Lam, et al., 2009, Thamdrup, et al., 2006). The relative importance of denitrification, in comparison to anammox is debated (details of these processes are discussed below). Both result in molecular nitrogen (N_2) and are therefore associated with the removal of fixed-nitrogen from the ocean. Which of these processes dominates can be dependent on the amount of organic matter produced in the ocean basin (Voss, et al., 2009).

Oceanic dissolved oxygen concentrations have varied widely in the geologic past. For instance, paleoclimate records from the Cretaceous (145 – 65 million years ago) reveal profoundly altered biogeochemical cycles due to the reductions of oxygen with dramatic con-

sequences for the marine ecosystems (Jones, et al., 2001). However, the anoxic ocean at the end of the Permian (251 million years ago) is perhaps the most striking example, where elevated atmospheric CO_2 and massive terrestrial and oceanic extinctions were observed (Benton, et al., 2003). In the glacial/interglacial periods oxygen concentrations varied not only due to the strongly oscillating temperature but also due to the changes in oxygen supply into the omz's (Galbraith, et al., 2004). Recent studies show that omz's expand and deoxidize more in their cores (Stramma, et al., 2010, Stramma, et al., 2008). Further, some climate models predict an overall decline in oceanic dissolved oxygen concentration and a consequent expansion of the omz under global warming conditions (Matear, et al., 2003), with the largest declines occurring in the extratropical regions. These changes in the oxygen concentrations will inevitably cause changes in the nitrogen cycle.

1.2. Nitrogen cycle investigation using stable isotopes

1.2.1. Fundamentals

Isotopes and calculation of their ratio

Isotopes are atoms of an element that share the same number of protons but a different number of neutrons. In the scientific nomenclature isotopes are specified in the form, ${}^{m}_{n}E$, where the 'm' indicates the mass number (the sum of protons and neutrons in the nucleus) and the 'n' refers to the atomic number of an element the E. There are more than 10 nitrogen isotopes known. Most of them are radioactive and highly unstable with longest half-life time of 10 minutes. The only two stable nitrogen isotopes are ^{14}N and ^{15}N, which have seven protons and seven or eight neutrons in their nucleus, respectively. ^{15}N is the less frequent stable isotope, constituting of 0.365% of the global nitrogen pool (Nier, 1950). Consequently, it is more practical to measure the difference or ratio of two isotopes instead of the absolute quantity of each. Isotopic compositions are expressed in terms of 'delta' (δ) values which are given in parts per thousand or per mil (‰). Nitrogen isotope ratios, for example, are expressed as the ‰-difference to tropospheric N_2, which has a constant $^{14}N/^{15}N$ of 272 ± 0.3 (Coplen et al., 1992; Junk and Svec, 1958). The $\delta^{15}N$-value in the sample is then calculated by the following equation (1).

$$\delta^{15}N(vs.air) = \left(\frac{(^{15}N/^{14}N)_{sample}}{(^{15}N/^{14}N)_{air}} - 1 \right) \times 1000 \qquad (1)$$

The δ-values do not represent absolute isotope abundances but rather the ‰-difference to widely used reference standard, such as VSMOW (Vienna Standard Mean Ocean Water). The δ-value is then calculated from equation (2), by measuring the isotope ratios (*R*) for the sample and the reference standard:

$$\delta^{15}N = \left(\frac{R_{sample}}{R_{standard}} - 1\right) \times 1000 \quad (2)$$

where R_{sample} and $R_{standard}$ represent the isotope ratio $\delta^{15}N$(vs.air) in the sample and in the standard respectively, which is calculated with the help of equation 1. By convention, R is the ratio of the less abundant isotope over the most abundant isotope (i.e. $^{15}N/^{14}N$ for nitrogen).

The $\delta^{15}N$ value changes under the influence of chemical and physical processes. If the process is complete the resulting $\delta^{15}N$ value in the product is equal to the value of the reagent. Only if the reaction is incomplete the fractionation of isotopes happens, which means that the $\delta^{15}N$ values in the product and substrate differ.

Isotope fractionation effect

There are two different fractionation processes, both of which will be discussed here: equilibrium and kinetic fractionation processes.

Equilibrium fractionation processes are associated with reversible processes. They are mainly driven by changes in the internal energy of a molecule, i.e. vibrations of the atoms within a molecule with respect to each other and rotations around the molecular axes. The equilibrium fractionation factor α is related to the equilibrium constant k as shown in equation (3), where n is the number of exchanged atoms.

$$\alpha = k^{1/n} \quad (3)$$

During equilibrium reactions, the heavier isotope preferentially accumulates in the compounds with a higher number of bonds. During phase changes the ratio of heavy to light isotopes in the molecules in the two phases also changes. For example, as water vapor condenses in rain clouds (a process typically viewed as an equilibrium process), the heavier water isotopes (^{18}O and ^{2}H) become enriched in the liquid phase while the lighter isotopes (^{16}O and ^{1}H) remain in the vapor phase. In addition, the equilibrium isotopic effect decreases as the system temperature increases.

Kinetic fractionation processes are associated with incomplete processes like evaporation, dissociation reactions, biologically mediated reactions and diffusion (Hoefs, 2009). Kinetic isotope fractionation reflects the difference in the different bond strengths or motilities of the isotopic species. The degree of isotopic fractionation associated with a reaction is commonly expressed with α, which is the ratio of rate constants for molecules containing the different isotopes:

$$\alpha = {}^{14}k / {}^{15}k \quad (4)$$

where ${}^{14}k$ and ${}^{15}k$ are the rate constants for molecules containing the light and heavy isotopes, respectively. Most reactions discriminate against the heavier isotope, yielding $1.00 < \alpha < 1.03$. This makes it convenient to define an isotopic discrimination factor that highlights more clearly the range of variation:

$$\varepsilon = (\alpha - 1) \times 1000 \quad (5)$$

An alternative for calculating the enrichment factor (ε) is the Rayleigh equation. This is an exponential relation that describes the partitioning of isotopes between two reservoirs as one reservoir decreases in size. The equation can be used if the following conditions are met: 1) material is continuously removed from a mixed system; 2) the fractionation accompanying the removal process at any instance is described by the fractionation factor α, and 3) α does not change during the process. Under these conditions, the evolution of the isotopic composition in the residual (reactant) material is described by:

$$R = R_0 f^{(\alpha-1)} \quad (6)$$

where R is the isotopic ratio of the product, R_0 is the initial ratio of the reactant, f is the fraction of the substrate pool remaining and α is the kinetic fractionation factor.

1.2.2. Influence of nitrogen cycle processes on isotopic distributions

As a limiting element for biological productivity, nitrogen occupies a central role in ocean biogeochemistry. It exists in more chemical forms than most other elements, with a myriad of chemical transformations that are unique to this element (Fig 1.3). Nearly all these transformations are undertaken by marine organisms as part of their metabolism, either to obtain nitrogen to synthesize structural components, or to gain energy for growth. Figure 1.4 shows $\delta^{15}N$ ranges of some important natural samples in marine environments.

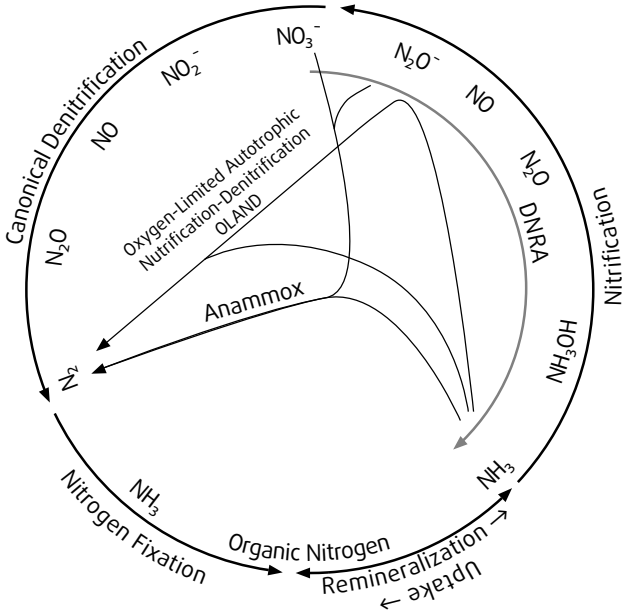

Fig. 1.3. Marine nitrogen cycle (Brandes, et al., 2007).

Nitrogen is cycled in the ocean in a complex manner, mainly through metabolic nitrogen transformations, that involve irreversible kinetic fractionation. The extent to which nitrogen isotope fractionation is observed varies, depending upon the kinetic mode of individual metabolic reactions, concentration of products and reactants, environmental conditions (i.e. anoxic or oxic) and species of the organisms. The following provides a brief overview of the processes of the nitrogen cycle, and how these processes alter the isotopic composition of the marine pool of inorganic nitrogen, especially nitrate. The isotopic composition of a pool of nitrogen can be used to identify the relative importance of sources that are isotopically distinct, or processes that add or remove nitrogen with a characteristic pattern of isotopic discrimination. Figure 1.5 presents a scheme showing the impact of the most important processes on nitrogen isotope distribution in oceanic nitrate.

Nitrogen assimilation (uptake) and denitrification processes decrease the concentration of ambient nitrate, while remineralization and N_2-fixation increase it (Fig. 1.5). The starting point on the scheme is the nitrate in the deep waters, with

an average oceanic value of $\delta^{15}N$ ~5‰ (Lehmann, et al., 2005, Sigman, et al., 2000, Wu, et al., 1997).

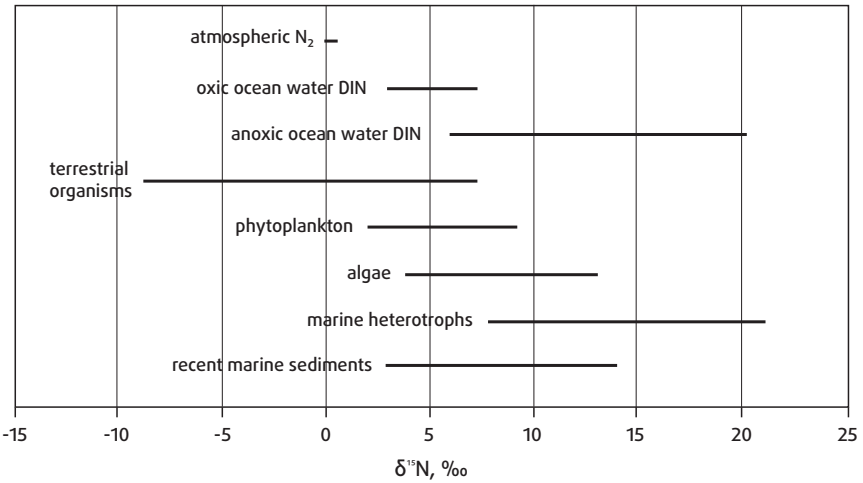

Fig. 1.4. $\delta^{15}N$ ranges of some important nitrogen reservoirs (Arthur, 1983)

Due to N-loss processes, i.e. denitrification and anammox, the $\delta^{15}N$ values increase to 15‰ or more. For the eastern tropical North Pacific omz Brandes et al. (1998) calculated the fractionation factors between 22‰ (Arabian Sea closed system model) and 30‰ (eastern tropical North Pacific open-system model). Altabet et al. (1999b), Cline and Kaplan (1975), Sigman et al. (2003), and Voss et al. (Voss, et al., 2001) have observed high nitrogen isotopic values and nitrate deficits in the Pacific omz's and estimated ε, which all cluster around a value of 25‰.

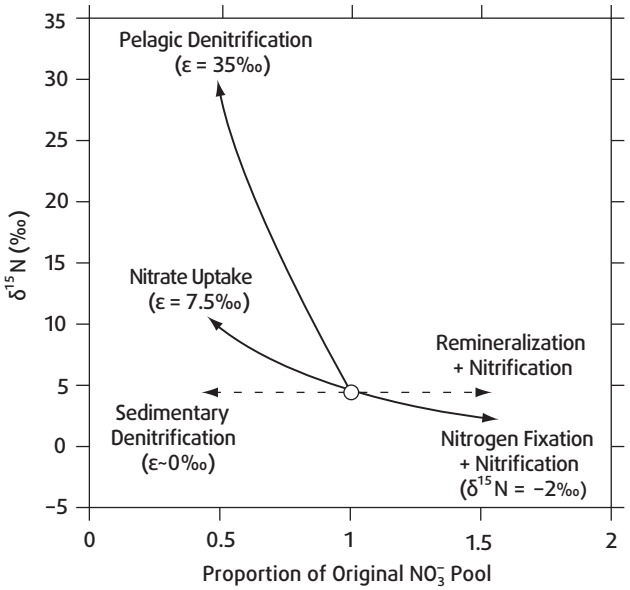

Fig. 1.5. The impact of different processes on the $\delta^{15}N$ of oceanic NO_3^- (Montoya, et al., 2002). Axis show deviation of $\delta^{15}N$ signal from oceanic average and loss/input of nitrogen due to different processes.

Nitrogen assimilation is the process of consumption of nitrate into a cell. Wada and Hattori (1978) first argued that N isotope fractionation by phytoplankton occurs during *nitrate reduction*, while Montoya and McCarthy (1995) ultimately favored fractionation associated with *nitrate transport* into the cell. In order to understand the isotope fractionation during nitrate assimilation it first requires knowledge of nitrate assimilation itself. The N isotope data presented in Granger at al. (2004) suggest that an isotope effect is driven solely by the reductase, and not by uptake at the cell surface and results in a fractionation factor of 5 – 10‰. Ammonium assimilation was shown to have higher fractionation factor of +14 – +27‰ (Hoch, et al., 1992, Waser, et al., 1998).

Nitrogen fixation is the process of incorporation of N_2 from the air into the cell. This process leads to an addition of bio-available N to the ocean via remineralization of dead cells, which had fixed N_2 from the air. As the $\delta^{15}N_{air}$ is set to 0‰, the kinetic isotope effect of the process is small (-2‰ to +2‰). Another process, which

increases nitrate concentrations in the ocean, is nitrification. One of the first studies of kinetic isotopic effect of nitrification in pure cultures of *Nitrosomonas europaea* was made by Mariotti group (1981), where a fractionation factor of 34.7 ± 2.5‰ was determined for conversion of $NH_4^+ \rightarrow NO_2^-$. The later work of Casciotti (2003) identified that the fractionation factor for different *Nitrosomonas* cultures of ammonia-oxidizing bacteria was linked to amino acid sequences. The isotopic effect in these cultures ranged from 14.2‰ to 38.2‰. The latest study of Karen Casciotti (2009) showed that the last step of nitrification (nitrite oxidation into nitrate) has a negative isotopic effect of -12.8‰. So far this is the only process known with preferential accumulation of the lighter isotope in the substrate.

1.3. Processes of the nitrogen cycle

Most nitrogen in marine environments is present in five forms: N_2, a quite stable molecule that requires specialized enzymatic systems to break and use it; NO_3^-, the most oxidized form of nitrogen and the dominant form of fixed-N within oxic environments; NH_4^+, the most reduced natural form of N and the dominant biologically available form found in anoxic environments; particulate nitrogen, predominant within sediments and primarily in the form of organic N, and dissolved organic N (don), which is a complex mixture of compounds with a wide range of compositions (Brandes, et al., 2007, McCarthy, et al., 1979, Seitzinger, et al., 2002, Ward, et al., 2001). Nitrate, nitrite, ammonium, and organic nitrogen are typically grouped together as "fixed N" in discussions about the availability of nitrogen. Although each form has a different level of reactivity, a complex web of reactions links these different compounds (Fig. 1.3). The most important processes discussed here are: N-loss (conversion of fixed N to N_2), nitrification, assimilation and N_2 fixation.

1.3.1. Nitrogen loss (denitrification and anammox) in the ocean

Canonical denitrification is a heterotrophic process in which nitrogen oxides serve as the terminal electron acceptor for organic carbon metabolism (Codispoti, et al., 2001). However, from a biogeochemical perspective any process that results in the loss of combined nitrogen from the biosphere is a denitrifying process. Henceforth, both canonical denitrification and anammox processes will be referred to as "N-loss processes".

Canonical denitrification

Canonical denitrification is carried out by heterotrophic bacteria during which nitrate (or nitrite) serves as the terminal electron acceptor for organic matter oxidation. The nitrogen oxides are reduced mainly to molecular nitrogen and some nitrous oxide may be formed as a side product. The sequential reduction is facilitated by four well-studied enzyme systems: nitrate reductase, nitrite reductase, nitric oxide reductase and nitrous oxide reductase (Zumft, et al., 1997) (eq. 7).

$$NO_3^- \xrightarrow{nitratereductase} NO_2^- \xrightarrow{nitritereductase} NO \xrightarrow{nitricoxide\ reductase} N_2O \xrightarrow{nitrousoxide\ reductase} N_2 \qquad (7)$$

The intermediate NO_2^- is known to escape the cell and is frequently found in denitrifying environments; likewise, N_2O also can accumulate externally (Codispoti, et al., 2005). In environments favorable for denitrification local maxima of both intermediates tend to occur near the boundaries of the suboxic zone.

Annamox

Anammox bacteria are chemoautotrophic bacteria that fix CO_2 using NO_2^- as the electron donor (Güven et al., 2005) and they are thought to be strict anaerobes. All anammox species found have evolved a membrane-bound intracytoplasmic compartment called the anammoxasome. The anammoxasome membrane is made up of high-density lipids, called ladderanes because of their ladder-like structure, that are thought to be specific to anammox bacteria. The proposed mechanism of anammox involves a hydrazine hydrolase, which catalyzes the combination of hydroxyl ammine and ammonium to form hydrazine. The hydrazine-oxidizing enzyme subsequently oxidized it to N_2 (Jetten, et al., 2003, van Niftrik, et al., 2004). The ladderane-lipid membrane is thought to act as a barrier to diffusion thus isolating the toxic intermediates of the anammox reaction within the anammoxasome.

Nitrate reduction to ammonium

The dissimilatory reduction of nitrate to ammonium is a bacteria-mediated heterotrophic process occurring under anaerobic conditions. Nitrate is first reduced to NO_2^- and then to NH_4^+. Bock et al. (1995) also showed that *N. europaea* and *N. eutropha* were able to nitrify and denitrify at the same time when grown under oxygen limitation ($[O_2]$ ~ 0.2 – 0.4 μmol/l). Under these conditions, oxygen and nitrite served simultaneously as electron acceptors and both N_2 and N_2O were produced,

whereas under anaerobic conditions N_2 was the predominant end product. This type of nitrification-denitrification pathway may help to explain why ammonium oxidizers remain active in nearly suboxic environments and enhanced N_2O production is observed (Blackmer, et al., 1980, Goreau, et al., 1980).

Controlling factors for denitrification

The controlling factor for denitrification is molecular oxygen. When the concentration of the denitrification intermediate NO_2^- is plotted against dissolved oxygen, we see that NO_2^- does not appear in the water columns of the eastern tropical Pacific until oxygen concentrations are reduced below about 2 μM (Cline, et al., 1972, Codispoti, et al., 1976). Another indication for the denitrification process is consumption of N_2O within the water column, where oxygen concentrations are reduced to levels less than c. 10 μM.

About less than half of the current marine denitrification of the global ocean is thought to occur in the three main pelagic oxygen minimum zones (omz's): eastern tropical North Pacific (etnp), the eastern tropical South Pacific (etsp) and the Northern Arabian Sea (Fig. 2). These zones occur in intermediate waters (~150 – 1000 m) in locations where the ventilation rate is insufficient to meet the oxygen demand (see above). This dissertation will concentrate on the South Pacific and North Atlantic omz's.

N-loss in the water column

To calculate nitrogen loss in the water column the amount of substrate which is consumed in N-loss processes or the amount of N_2 produced should be determined. The Redfield stoichiometry is used to calculate the expected NO_3^- ($NO_3^-{}_{exp}$) from apparent oxygen utilization (aou) and phosphate (PO_4^{3-}) data (Codispoti, et al., 1976). With the given $NO_3^-{}_{exp}$ and the measured concentration of the actual Dissolved Inorganic Nitrogen (din = $NO_3^- + NO_2^- + NH_4^+$), the amount of NO_3^-, which is removed by denitrification ($NO_3^-{}_{def}$), can be calculated as follows:

$$NO_3^-{}_{def} = NO_3^-{}_{exp} - \text{din} \quad (8)$$

An alternative stoichiometric method involves the quasi-conservative tracer N* (Deutsch, et al., 2001, Gruber, et al., 1997). Gruber and Sarmiento used high quality data from jgofs and geosecs databases to develop a general relationship between fixed inorganic nitrogen (din) and phosphate (PO_4^{3-}) for the world's oceans:

$$N^* = \text{DIN} - 16\times[PO_4^{3-}] + 2.90 \quad (9)$$

The value of 2.90 is the deviation from the amount of DIN predicted by the Redfield stoichiometry (N:P =16) and the world-ocean N:P regression relationship. Negative values of N* are interpreted to indicate the net *denitrification* whereas positive values imply the net *nitrogen fixation*.

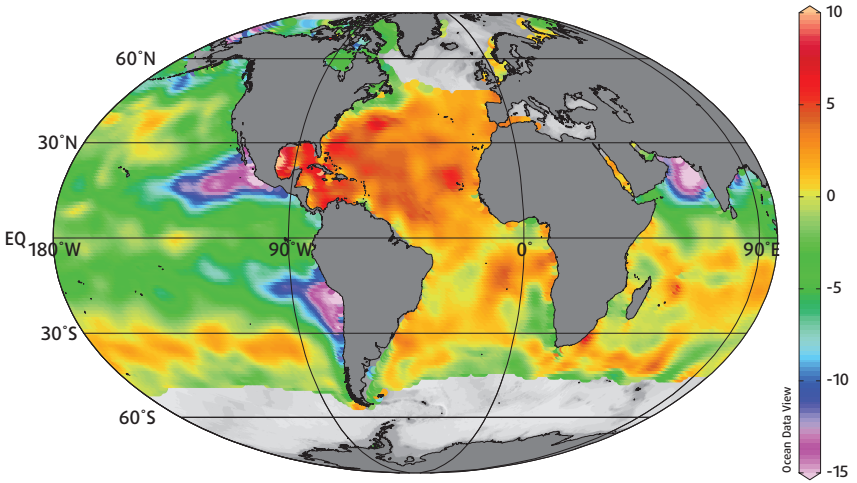

Fig. 1.6. $N^* = [NO_4^{3-}] - 16\times[PO_4^{3-}] + 2.9$ on the 26.5 sigma theta surface (World Ocean Atlas 2005). Note the large negative N* values in the Tropical Pacific and Arabian Sea and positive N* values in the Tropical Atlantic Ocean.

Devol et al. (2006) used N_2:Ar ratios in the Arabian Sea OMZ to determine the amount of N_2 produced during denitrification. The amount of N_2 excess in the OMZ was computed from the increase in the N_2:Ar ratio over that present in the source waters. Measurements of N_2 excess predicted a larger nitrogen anomaly than that estimated by nitrate deficit. The discrepancy is said to be due to incorrect assumptions of the Redfield stoichiometry (Van Mooy, et al., 2002). Inputs of new nitrogen through N-fixation, N_2 contributions from sedimentary denitrification along continental margins, the anammox reaction, or metal catalyzed denitrification reactions all lead to a shift of the N:P ratio from the Redfield stoichiometry.

Sedimentary denitrification

Another location where oxygen is typically depleted and denitrification takes place is in marine sediments, especially continental margin and hemipelagic sediments. This is because the source of nitrate is the local overlying water, while the respiratory processes within the sediments act as sinks. In most continental shelf sediments oxygen penetrates to less than 1 cm below the sediment–water interface and even in most deep-sea sediments oxygen penetration is restricted to the approximately upper 10 cm. Thus, there exist ample environments for denitrification in marine sediments.

All these N-loss processes result in N_2, which is lost from the ocean into the atmosphere.

1.3.2. Nitrification

Nitrification is a process whereby NH_4^+ is oxidized to NO_2^- and further to NO_3^-. Ammonium rarely occurs at significant concentrations in oxygenated habitats. It is recycled rapidly between heterotrophic and N_2 fixing organisms (which excrete NH_4^+ directly or release organic N that is microbially degraded to NH_4^+) and many heterotrophic and photosynthetic plankton (which utilize NH_4^+ as a N source) in the surface ocean. Similarly, NO_2^- rarely accumulates in oxygenated habitats, although NO_2^- is an essential intermediate in several oxidation and reduction processes in the N cycle (Fig. 1.3). Nitrate, which is the end product of nitrification, however, accumulates in the deep ocean.

There are two functionally distinct groups of nitrifying organisms: those that oxidize NH_4^+ to NO_2^- (ammonium-oxidizing bacteria and archaea, AOB and AOA) and those that oxidize NO_2^- to NO_3^- (nitrite-oxidizing bacteria, NOB). No organism is known, which carries out both reactions. The overall reaction of NH_4^+ oxidation for AOB shows (eq. 10) that the process consumes molecular oxygen and produces NO_2^- and hydrogen ions. Molecular oxygen is required in the first step of the reaction, which is catalyzed by a monooxygenase (NH_3 monooxygenase, AMO). Oxygen is also consumed by the terminal oxidase as a result of electron transport generating adenosine-5′-triphophate (ATP) for cellular metabolism. The immediate product of AMO is hydroxylamine, which is further oxidized by hydroxylamine oxidoreductase (HAO) to NO_2^-. In contrast, AOA apparently do not

possess the hydroxylamine reductase gene, so the pathway of ammonia oxidation in these organisms must be quite different.

$$NH_4^+ + O_2 + H^+ + 2e^- \xrightarrow{AMO} NH_2OH + H_2O \xrightarrow{HAO} NO_2^- + 5H^+ + 4e^- \quad (10)$$

Depending on the conditions nitric oxide (NO), N_2O and even N_2 have been reported as secondary products in autotrophic NH_4^+ oxidation by both marine and terrestrial strains (Schmidt, et al., 2004, Zart, et al., 1998). Although N_2O and NO can be produced in vitro by hao from hydroxylamine (Hooper, et al., 1979), the reduction of NO_2^- appears to be the dominant pathway in all cells (Hooper, et al., 1997, Poth, et al., 1985, Remde, et al., 1990).

The biochemistry of the NO_2^- oxidation is simpler than that of NH_4^+ oxidation because it is only involves a transfer of two electrons without intermediates (eq 11). The additional oxygen atom in NO_3^- is derived from water, and the molecular oxygen that is involved in the net reaction results from electron transport involving cytochrome oxidase.

$$NO_2^- + H_2O \xrightarrow[\text{oxydoreductase}]{\text{nitrite}} NO_2^- + 2H^+;\ 2H^+ + 0.5\ O_2 \xrightarrow[\text{oxydase}]{\text{cytochrome}} H_2O \quad (11)$$

In sum aoa, aob and nob require oxygen for the nitrification process. However, as a complex biological process it should be controlled by other factors, such as light intensity.

Controlling factors of nitrification

There is abundant evidence from culture studies that both aob and nob are photosensitive. Several studies of nitrification rates in surface seawaters from various geographical regions show profiles that are consistent with light inhibition of both NH_4^+ and NO_2^- oxidation (Lipschultz, et al., 1990, Ward, 1987, Ward, et al., 1984).

Nitrifying bacteria are traditionally considered to be obligate aerobes; they require molecular oxygen for reactions in the N oxidation pathways and for respiration. A significant positive correlation between aou and N_2O accumulation is often observed in marine systems (Cohen, et al., 1978, Nevison, et al., 2007, Yoshinari, 1976). The relationship implies that nitrification is responsible for N_2O accumulation in oxic waters where it is released as a byproduct. The relationship breaks down at very low oxygen concentrations (~6 mM, (Nevison, et al., 2003)), where N_2O is consumed by denitrification.

Distribution of nitrification in water column and sediments

The highest nitrification rates occur in a region near the bottom of the euphotic zone. It is in this interval where nitrifying bacteria can compete with phytoplankton for NH_4^+, as the rates of nutrient assimilation are reduced due to light limitation. A sharp peak of nitrification rate is often observed at water column depth where the light intensity is 5–10% of surface light intensity (Lipschultz, *et al.*, 1990, Sutka, *et al.*, 2004, Ward, 1987, Ward, *et al.*, 1984).

In both deep and shallow sediments, nitrification can be one of the main sinks for oxygen (Blackburn, et al., 1993, Grundmanis, et al., 1977). In continental shelf sediments, nitrification and denitrification are often closely linked. Coupled nitrification/denitrification is invoked to explain the observation that the rate of N_2 flux out of sediments can greatly exceed the diffusive flux of NO_3^- into the sediments (Devol, et al., 1993). Ammonium is produced during aerobic and anaerobic remineralization of organic matter. It is then oxidized to NO_3^- and subsequently reduced to N_2. Anaerobic oxidation of NH_4^+ can be a factor supporting the imbalance between supply and consumption of NO_3^-. Nitrification can supply up to 100% of the NO_3^-, which is later consumed by denitrification (Laursen, et al., 2002, Lehmann, et al., 2004).

Although oxygen and NH_4+ conditions likely differ between planktonic and sediment environments, there is no clear evidence from clone libraries that water column and sediment nitrifying communities are significantly different in composition and regulation.

Nitrification and nitrogen assimilation, discussed below, are usually found at similar depths in the ocean as they compete for the same reactants (NH_4^+). At the same time, nitrification, producing NO_2^- and NO_3^-, provides assimilation with additional reactants. Therefore, these two processes are bound to each other.

1.3.3. Nitrogen assimilation

Nitrogen assimilation is the process of incorporation of reactive nitrogen species (NO_3^-, NO_2^- and NH_4^+) into the bacterial cell. Nitrate concentrations in the surface ocean are usually maintained at low levels because phytoplankton assimilates NO_3^- more rapidly than can be supplied by mixing or diffusion from the deep NO_3^- reservoir. Ammonium, which is produced in the photic zone by heterotrophic processes, is also assimilated immediately by phytoplankton and heterotrophic

bacteria before it can be nitrified. The important physical and biological differences in the source functions of NH_4^+ and NO_3^- are the basis of a new production paradigm (Dugdale, et al., 1967, Eppley, et al., 1979). It is a framework to understand N demand and growth of phytoplankton in the surface ocean, and the subsequent flux of N to the deep sea and ocean floor.

Ammonium is often the dominant form of dissolved N taken up in a variety of marine and estuarine systems. This form of N is energetically efficient for cells to use, because it is already reduced and is a common cellular transient in N metabolism, requiring little additional energy for assimilation. Despite the low NH_4^+ concentrations in oceanic systems, uptake and regeneration of NH_4^+ are tightly coupled and result in rapid turnover times.

The assimilation of NO_3^- is more energetically demanding than NH_4^+, because it requires a synthesis of NO_3^- and NO_2^- reductases, associated active transport systems, and the turnover of cellular ATP and nicotinamide adenine dinucleotide phosphate (NADPH) (Mulholland, et al., 2008). In order to assimilate NO_3^- for growth, phytoplankton must first possess the genetic capacity to synthesize the necessary enzymes and transport systems, which not all phytoplankton do have. Further, the supply of NO_3^- is limited by nitrification and vertical mixing.

Since nitrite reductase (NiR) is required for NO_3^- assimilation, organisms that assimilate NO_3^- can by default assimilate NO_2^-. Consequently, some organisms that cannot use NO_3^- can still use NO_2^- (e.g., some clones of *Prochlorococcus*; (Moore, et al., 2002)). It has been suggested that this rather unique N physiology has arisen from the evolutionary loss of genes, which are necessary for the assimilation of NO_3^- (Garcia-Fernandez, et al., 2004a, Garcia-Fernandez, et al., 2004b). The resultant evolution of many ecotypes specifically adapted for unique environments where NO_2^- production can be high.

Factors controlling nitrogen uptake and assimilation

The most important factors controlling assimilation are the presence of oxygen for respiration, light for photosynthesis and enzymes, responsible for metabolic processes. Most of the enzymes involved in the uptake and assimilation of N are tied to energy sources and thus are affected by light, presence of oxygen, and the supply of enzyme co-factors and metabolic substrates. For example, uptake and reduction of NO_3^-, NO_2^-, and urea have been linked to the light supply in phytoplankton due

to the necessity for ATP and NADPH from photo-phosphorylation. While uptake and reduction of these compounds is thought to proceed at maximum rates only in the light under nutrient replete conditions, active uptake of these compounds may occur even in the dark (Antia, et al., 1991).

The accumulation of intracellular product pools, on the other hand, can result in the inhibition of uptake and assimilation. The posttranslational modification of enzymes can regulate uptake and assimilation by modulating the number of active sites available for catalyzing specific reactions. Studies examining the transcriptional activation of enzymes involved in the process have begun to demonstrate clear functional relationships between genomes and ecological capabilities. For example, the presence of NH_4^+ represses protein expression (i.e., enzymes) involved in the assimilation of alternative N sources (e.g., NO_3^- and N_2) in some organisms (Eppley, et al., 1969).

Overall, most factors controlling assimilation are directly connected with enzymes, which require substrate compounds or energy and oxygen supply for their metabolic activity. Another process, which can be found in the surface waters and which provides important reagents for assimilation is nitrogen fixation.

1.3.4. Nitrogen fixation in the ocean

Nitrogen fixation in general means the conversion of N_2 into ammonia. In the open ocean N_2 fixation research has focused most intensively on the cyanobacterium, *Trichodesmium* (Carpenter, 1973, Saino, et al., 1978), which often occur as aggregates (often referred to as colonies) visible to the naked eye ('sea sawdust'). It can also occur, however, as individual filaments. In early reports N_2 fixation was observed in the pelagic zone and associated with the cyanobacterial epiphytes (*Dichothrix fucicola*) of the brown macroalga, *Sargassum* (Carpenter, 1972) and cyanobacterial endosymbionts of certain oceanic diatoms (Mague, et al., 1977, Villareal, 1994).

The availability of molecular probes to the structural genes of nitrogenase has provided means with which to go beyond direct observation. The, so-called NifH genes are genes encoding enzymes involved in the fixation of atmospheric nitrogen and therefore represent the N_2-fixing bacteria. They have been found in the picoplankton, as well as in heterotrophic bacteria from the guts of copepods (Zehr, et al., 2000). To date, all marine nitrogen fixers are either isolated or identified by gene sequencing, and are members of the bacterial domain. Dense populations of

archaea also exist in the upper water of the marine environment (Fuhrman, et al., 1992, Karner, et al., 2001) and it is tempting to speculate that, in the low-nutrient upper layers of the ocean, archaea may also contribute to diazotrophy.

Controlling factors for N_2 fixation

Numerous factors, physical, chemical and biotic, can affect the extent of N_2 fixation in an ecosystem (Capone, et al., 1990, Howarth, et al., 1988a, Howarth, et al., 1988b, Karl, et al., 2002). Many factors which bear on nitrogenase activity are interdependent such as light, temperature, oxygen and turbulence. Indeed, a variety of different factors may limit the growth and activity of diazotrophs in various areas of the world's oceans at different times of the year.

One key factor for tropical diazotrophs may be water temperature. For example, the distribution of *Trichodesmium* spp. is roughly limited by the 20°C isotherm. Metabolically active populations of *Trichodesmium* have been observed at 18.3°C in the North Atlantic (McCarthy, et al., 1979), but activity was low, and substantial growth is typically not seen until water temperature exceeds 20°C (Carpenter, 1983). Maximum growth rates and maximum nitrogen fixation rates were measured within 24 to 30°C (Breitbarth, et al., 2007).

For photoautrophic diazotrophs, nitrogenase activity is intimately linked to photosynthesis (Gallon, 2001). Thus, light is an obvious and important factor potentially regulating or constraining this process. Carpenter (1983) has summarized much of the early marine work largely relating to *Trichodesmium* spp. with respect to their relationship to light. Whereas many non-heterocystous cyanobacteria fix nitrogen during the night, and thereby uncouple N_2 fixation from photosynthesis, *Trichodesmium* fixes nitrogen exclusively during the light period and shows a strong diel pattern of activity with maxima during midday (Berman-Frank, et al., 2001a, Berman-Frank, et al., 2001b, Capone, et al., 1990, Saino, et al., 1978). Natural populations of *Trichodesmium* which are often found in the upper layers of the euphotic zone appear to be adapted to high light with a relatively shallow compensation depth (typically 100–200 mmol quanta m^{-2} s^{-1}) for photosynthesis (LaRoche, et al., 2005).

A number of studies have speculated on diazotroph response to mineral dust Fe fertilization in the Atlantic (Mahaffey, et al., 2003), and Pacific Oceans (Johnson, et al., 2003). Circumstantial evidence for dust stimulation of marine diazotrophic biomass has recently been reported. A 1999 Saharan dust event coincided with

increases in dissolved Fe concentrations on the west Florida shelf and a 100-fold increase in *Trichodesmium* biomass. N_2 fixation rates were not measured, but DON concentrations doubled, presumably due to exudation by N_2 fixers (Lenes, et al., 2001). A recent Saharan dust addition experiment to surface water samples collected along a west African cruise transect (35°W–17°W), found a minimal increase in CO_2 fixation and a large stimulation in N_2 fixation, suggesting that diazotrophs were co-limited by both P and Fe (Mills, et al., 2004). It should be noted however, the analysis of aerosol dust shows that while providing Fe, the dust also supplies P and combined N (Baker, et al., 2003, Mills, et al., 2004, Ridame, et al., 2002).

Distribution of N_2 fixation

The observation of relatively high concentrations of DON in surface waters of regions of the tropical oceans have also been attributed to nitrogen fixation (Abell, et al., 2000, Hansell, et al., 2000, Hansell, et al., 1997, Vidal, et al., 1999). At the Hawaiian Ocean Time (HOT) series station, pools of DON increased during a period in which microbial nitrogen fixation also became more prominent (Karl, et al., 1997, Karl, et al., 1995). Similarly, patterns in the concentration of nitrate and phosphate in mid-waters of some areas of the ocean point towards nitrogen fixation (Gruber, et al., 1997, Michaels, et al., 1996), which are expressed in positive values of N*, as described above (3.1). Strong positive N* values have been observed in the tropical and subtropical North Atlantic and are proposed to be a result of the input into these areas of diazotrophic (i.e. nitrogen fixer) biomass with a higher N:P content than that typical of eukaryotic phytoplankton of the upper ocean (Deutsch, et al., 2001, Gruber, et al., 1997, Michaels, et al., 1996).

1.4. Synopsis of the chapters.

The main goal of this thesis is to study the nitrogen cycle from the isotopic perspective in very different Oxygen Minimum Zones and to investigate the influence of oxygen on the nitrogen cycle in the ocean. In chapter 2 the method for nitrogen isotopic analysis is presented. It is a purely chemical approach, where NO_3^- is converted to NO_2^- by Cd metal reduction and where NO_2^- is further converted to N_2O using azide. The method allows separate analysis of nitrite without interference from the isotopic signature of nitrate and was modified for quantitative and quick reduction.

Chapter 3 contains the description of the Atlantic and Pacific nitrogen cycle in theirs Oxygen Minimum Zones (OMZ's). The two oceanic OMZ's are very different with regard to the oxygen concentration and, as expected, show very different nitrogen cycles. In the Atlantic OMZ with oxygen concentration > 40 μmol/l we do not observe any significant denitrification. Instead, we find nitrification and a distinct signal of dust deposition which was not observed before. The surface waters in the Atlantic, which were exposed to atmospheric dry and wet deposition of nutrients, show an extremely low $\delta^{15}N$ signature. In contrast, we observe a very strong signal of N-loss processes in the Pacific OMZ. Isotopic fractionation of the denitrification is well known and is to be 20 – 30‰. Interestingly, the apparent fractionation factor in the Peruvian OMZ was 11.4‰, lower than expected. This lower fractionation effect is best explained with integrated signal from denitrification in sediments and water column.

The subsequent Chapter 4 of my thesis is devoted to the comparison of the nitrogen isotope distribution in the water column and surface sediments. Isotopic signature in the surface sediments is mainly hold the signature of organic matter, which is formed in the surface of the water column, and buried in the sea floor. Consequently, the highest input of the water column into the sediments happens in the most productive seasons in the year. The nitrogen isotope signal in sediments and water column differs first of all by the time scale: sediments show the signal of the region integrated over decades, while the water column can represent only one season. The water column samples used here were taken in austral summer (most productive season of the year) and were compared to the surface sediments collected on the same cruise. Nitrogen isotope distribution in both water column and surface sediments show a latitudal increase of the $\delta^{15}N$ signal southwards. Calculated $\delta^{15}N$ of particulate organic matter produced from the water column match the values measured in the surface sediments. This shows that the nitrogen cycles in the systems are connected and do influence each other. In the article we argue that the $\delta^{15}N_{sed}$ latitudinal gradient is driven by increasing nitrate utilization and N-loss processes in the water column.

Chapter 5 in my thesis resulted from the collaboration of physical and chemical oceanographers. We examine here the mesoscale eddies which are well known to be very important for the near surface ocean. Our observations reveal that coastal eddies create previously unrecognized spatial as well as temporal variability in

the biogeochemistry of the Peruvian OMZ. We assume that pulses of organic matter from eddy streamers produce temporal successions in the underlying OMZ microbial community. This would then cause an enhanced production of NH_4^+ and N_2O in the upper oxycline, as well as a reduction of NO_3^- and accumulation of NO_2^- and N_2O in the core of the OMZ. Overall, the Peruvian OMZ should be viewed as a dynamic system which is strongly affected by the physical forcing of organic matter flux. The latter, increasing a combined N-loss via transformations to biogenic N_2. This perspective may be critical to the design of future field programs. The findings underscore the importance of interdisciplinary linkages that may not be obvious to casual observation of the functioning of our Earth system.

2
Effect of chloride on the chemical conversion of nitrate to nitrous oxide for $\delta^{15}N$ analysis

Abstract

We investigate the influence of chloride concentration on the performance of the chemical reduction method for measurement of the nitrogen isotopic ratio ($\delta^{15}N$) in NO_3^- in natural waters (McIlvin and Altabet, 2005). In this method, NO_3^- is first reduced to NO_2^- using activated cadmium metal with further reduction to N_2O using sodium azide in an acetic acid buffer. N_2O is introduced into an isotope ratio mass spectrometer (IRMS) for isotopic measurement. Previously, it was recognized that the presence of halides was necessary for the speed and efficiency of the second step but not thought to be important for the first step. Whereas quantitative Cd reduction of NO_3^- to NO_2^- had been noted for seawater samples, here we report, for freshwater and low-salinity ($S < 30$) samples, a variable conversion efficiency (both under- and overreduction were observed) and significant variation in $\delta^{15}N$ determination. Addition of 5 M NaCl to all samples resulted in rapid (< 4 h) and quantitative (> 99%) reduction of NO_3^- to NO_2^- as well as stable $\delta^{15}N$ values that closely matched expected values for standards (within 0.3‰ of standard value). The positive effect of NaCl is likely due to a decrease in free Cd^{2+} produced over the course of the reaction due to formation of $CdCl_2$.

This chapter is based on:

Ryabenko, E., Altabet, M.A., Wallace, D.W.R, 2009. Effect of chloride on the chemical conversion of nitrate to nitrous oxide for $\delta^{15}N$ analysis. In: *Limnology and Oceanography: Methods* **7**: 545-552

Acknowledgements: The authors thank Frank Malien, Annette Kock and Gert Petrick for technical assistance. The work was supported by the DFG-funded "Future Ocean" Excellence Cluster and Sonderforschungsbereich 754 "Climate-Biogeochemistry Interactions in the Tropical Ocean."

2.1. Introduction

The nitrogen and oxygen isotope ratios of nitrate ($\delta^{15}N\text{-}NO_3^-$, $\delta^{18}O\text{–}NO_3^-$) provide powerful tools to investigate nitrate sources (Aravena et al. 1993, Böttcher et al. 1990, Casciotti et al. 2002, Schmidt et al. 2004) as well as mechanisms in the nitrogen cycle (Brandes et al. 2007). A number of important biogeochemical processes result in isotopic fractionation and alteration of $\delta^{15}N$ values that can be measured using isotope ratio mass spectrometry (irms). This allows for studies of NO_3^-– cycling (e.g., assimilation, remineralization, and nitrification) as well as identification of sinks and sources of nitrogen in the ocean (e.g., nitrogen fixation and denitrification).

Within the past two decades, several approaches have been developed to analyze nitrogen and oxygen isotope ratios in dissolved nitrogen compounds. Usually, these methods contain a step transforming NO_3^- via chemical reduction into a gaseous compound suitable for irms analysis. Various studies have been published that use the conversion of NO_3^- into N_2 (Silva et al. 2000, Voss et al. 1997), NH_4^+ (Sigman et al. 2000, Slawyk and Raimbault 1995, Thunell et al. 2004), or N_2O (Casciotti et al. 2002; Kaiser et al. 2007; Sigman et al. 2001, 2005). As part of a "chemical only" approach, Cd metal reduction to NO_2^- has been adapted from the methodology for colorimetric NO_3^- concentration determination (Burakham et al. 2004, Gal et al. 2004, Hales et al. 2004, Nydahl 1976, Thabano et al. 2004). All of these methods have advantages and disadvantages. Pyrolytic methods (Silva et al. 2000) have been useful only in the analysis of freshwater samples, and their application is unsuitable for measuring oceanic nitrate isotope compositions. Chemical reduction methods have the potential for over- or underreduction and corresponding difficulty in maintaining stable 100% reduction yield (Gal et al. 2004). In the ammonia diffusion method (Slawyk and Raimbault 1995), both nitrate and nitrite are converted to ammonia, and then the N isotopic composition is measured. Similarly, the denitrifier method (Casciotti et al. 2002, Sigman et al. 2001) does not distinguish between the respective signals imparted by nitrite and nitrate. In our laboratory, we have applied the method developed by McIlvin and Altabet (2005), which uses azide for quantitative nitrite conversion to N_2O for the isotopic analysis of seawater and freshwater. The method allows separate analysis of nitrite without interference from the isotopic signature of nitrate and has a standard de-

viation of less than 0.2‰ for $\delta^{15}N$ in nitrate samples ranging in concentration from 40 to 0.5 μM. We refer to the McIlvin and Altabet method as MA (2005).

For NO_3^- concentration measurements (e.g., by an autoanalyzer), a quantitative (100%) reduction is not necessary, because NO_3^- standards are run under exactly the same conditions as the samples, so that sample concentrations are corrected for any over- or under-reduction. For ^{15}N analysis, on the other hand, a quantitative (100%) reduction of NO_3^- is essential to avoid potentially large and variable isotopic fractionation.

Application of the MA (2005) method at IFM-GEOMAR includes analysis of samples collected from the Atlantic and Pacific Oceans and the Baltic Sea covering a wide range in salinity (equivalent to 0 – 0.5 M NaCl). A salinity effect on NO_3^- reduction yields has been discussed in several articles, which examined the effect of Cd column methods for NO_3^- concentration measurements (Gal et al. 2004, Nydahl 1976). For example, Nydahl (1976) argued: "Considering the reaction equation for the reduction, the reducing power of cadmium should increase when the concentration of cadmium ions decreases, in this case by complex formation with the chloride ions, and the reduction should be accelerated instead of retarded."

The MA (2005) method has two independent reduction steps. The first reduction step consists of a NO_3^- to NO_2^- reduction using cadmium metal. In the second step, the NO_2^- is reduced further to N_2O using a reaction with sodium azide in an acetic acid buffer.

$$NO_3^- + Cd + H_2O \rightarrow NO_2^- + Cd(OH)_2 \qquad \text{(First reduction step)}$$

$$NO_2^- + HN_3 + H^+ \rightarrow N_2O + N_2 + H_2O \qquad \text{(Second reduction step)}$$

The mechanism of the azide reaction was described by Stedman (1959a, 1959b). First, the nitrous acidium ion is formed, followed by slow nucleophilic attack by the azide ion on the nitrous acidium ion to form nitrosyl azide. This decomposes in a fast step to nitrogen and nitrous oxide.

$$NO_2^- + H^+ \leftrightarrow HNO_2 \qquad (1)$$

$$HNO_2 + H_2O \leftrightarrow H_2NO_2^+ + OH^- \qquad (2)$$

$$H_2NO_2^+ + N_3^- \xrightarrow{slow} N_3NO + H_2O \xrightarrow{fast} N_2O + N_2 \qquad (3)$$

Addition of chloride, bromide and thiocyanate ions catalyzes the reaction, via the formation of the corresponding nitrosyl compounds, thereby improving competition with exchange of $H_2NO_2^+$ with water:

$$H_2NO_2^+ + Cl^- \xrightarrow{slow} NOCl + H_2O \quad (4)$$

$$NOCl + N_3^- \xrightarrow{fast} N_3NO + Cl^- ; N_3NO \xrightarrow{fast} N_2O + N_2 \quad (5)$$

Until now, no systematic treatment of the effect of salt concentration on the reduction yield, especially for first reduction step, appears to have been conducted. This article presents results of experiments designed to investigate the efficiency of the first reduction step and the influence of salinity on the chemical reduction method for $\delta^{15}N\text{-}NO_3^-$ analysis.

2.2. Materials and Methods

2.2.1. Chemical conversion of nitrate to nitrous oxide

Off the shelf cadmium powder (Alfa Aesar, -325 mesh, 99.5%) was found to be as effective as lab-generated spongy Cd. It was prepared by washing with 10% HCl to activate particle surfaces followed by multiple rinsing with deionized water (DIW) until the pH became neutral. After use, the cadmium could be collected for reuse, by repeating the acid wash and rinse steps. Samples containing 70 ml of 0.5 – 20 μM NO_3^- were reduced to NO_2^- by adding 3 g (dry weight) activated cadmium powder. Effectiveness of Cd powder is likely sensitive to the activation process and pH. On the one hand, if Cd is not properly activated, the reduction process will take longer. On the other, if Cd is not brought to pH neutral, there is the risk of NO_2^- loss under acidified conditions. NaCl used for manipulating sample Cl^- concentration was precombusted for 20 h to remove contaminants.

After the addition of Cd and NaCl (where indicated), the sample bottles were capped tightly with Teflon-faced rubber septa (Macherey-Nagel, rubberstoppers N20 gray, 702931) and aluminum crimp seals. The pH was adjusted to 9 by addition of 1 ml of 1 M imidazole solution, via a medical syringe. Samples were shaken on a horizontal shaker (GFL 3018) for between 2 and 20 h at a rate of ~220 cycles/min. Sample volumes of 70 ml were decanted into fresh 120-ml bottles with Teflon-lined septa.

For the next stage (second reduction step), the samples were reduced to nitrous oxide using sodium azide in an acetic acid buffer, exactly as described in the MA (2005) method. For a separate analysis of $\delta^{15}N\text{-}NO_2^-$, the first reduction step can be bypassed.

2.2.2. IRMS

In contrast to the MA (2005) method, we did not quantitatively purge the samples by bubbling He through the liquid, but rather performed a N_2O headspace analysis. Inoue and Mook (1994) reported isotopic fractionation between dissolved and gaseous N_2O that may accordingly influence our observations. Under equilibrium conditions at 25°C, they found a small but significant fractionation of -0.75‰ for nitrogen and -1.06‰ for oxygen isotopes that did not vary from 0 to 44.5°C. The heavier isotopes (^{15}N and ^{18}O) were concentrated in the aqueous solution.

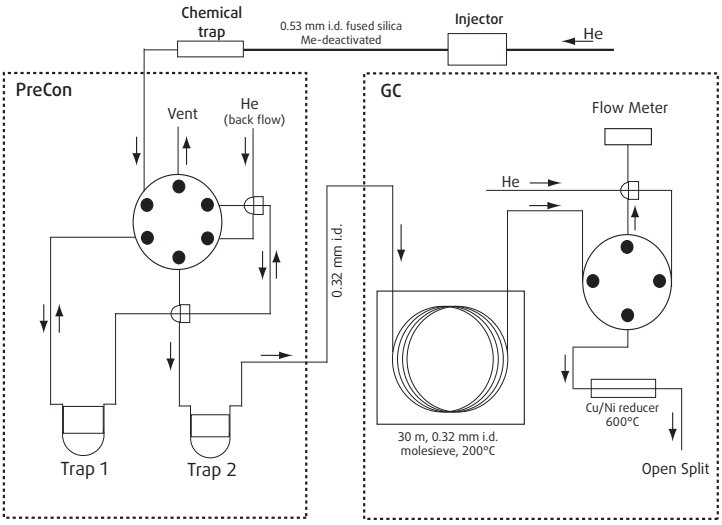

Fig. 2.1. Scheme of PRECON, GC, and the Cu/Ni metal reducer furnace

For $\delta^{15}N$ measurements (IRMS), 2 ml of the headspace, containing N_2O released in the reaction, were injected with a syringe into a PRECON system (Nuss 2007) and transferred onto a gas chromatography column (Fig. 2.1). Unlike the MA (2005) method, N_2O was further reduced to N_2 at the end of the chromatographic column, using a Cu/Ni metal reducer at 640°C with Pt added as catalyst before reaching the continuous-flow isotope

ratio mass spectrometer (CF-IRMS) via an open split. Quantitative conversion of N_2O to N_2 was tested and verified. We run N_2 and N_2O standards every day for a minimum of 5 times for validation of the signal and $\delta^{15}N$ data. It is also verified through monitoring mass 44. When N_2O standard is injected, there is no detectable mass 44 peak, only a stable background signal. Subsequently, the conversion efficiency was tracked by monitoring the $\delta^{15}N$ value and peak height of the N_2O standards on a daily basis. If the response was changed, then the efficiency of the reducing furnace was checked. This approach allowed N_2 from a gas cylinder, calibrated against atmospheric N_2, to be used as a direct reference standard for nitrogen isotopic analysis. Disadvantages of this approach are that oxygen isotope information is lost and care must be taken to ensure 100% conversion of N_2O into N_2 to avoid further fractionation.

2.2.3. NO_3^-, NO_2^- and NH_4^+ concentration analysis (DIN).

To examine the reduction kinetics of the first reaction step, we measured the concentration of the NO_2^- product and the remaining NO_3^- as well as NH_4^+ on an autoanalyzer equipped with a Cd-copperized column (GRASSHOFF et al. 1999). NO_3^- in the sample is reduced to NO_2^- in a column packed with copperized cadmium granules. Nitrite and ammonium concentrations were detected and measured spectrophotometrically. The NO_3^- concentration was calculated as the difference between the NO_2^- + NO_3^- and the NO_3^- absorbance data.

2.2.4. Nitrous oxide analysis.

A gas-chromatography method was used to determine N_2O. An aliquot (10 ml) of the sample headspace was used to flush a 2-ml sample loop after passing through a moisture trap (filled with Sicapent; Merck). The gas chromatographic separation was performed at 190°C on a packed molecular sieve column (6 feet by 1/800 inch, 5 A, mesh 80/100; Alltech GmbH), and N_2O was detected with an electron capture detector (GC-ECD). A mixture of argon and methane (95:5 by volume) was used as carrier gas with a flow of 21 ml/min. For the two-point calibration procedure, we used standard gas mixtures with 311.8 ± 0.2 ppb and 346.5 ± 0.2 ppb N_2O in synthetic air (Deuste Steininger GmbH). The standard mixtures have been calibrated against the US National Oceanic and Atmospheric Administration (NOAA) standard scale in the laboratories of the Air Chemistry Division of the Max Planck Institute for Chemistry, Mainz, Germany (WALTER et al. 2006).

2.3. Results

2.3.1. Influence of the salt concentration on $\delta^{15}N\text{-}NO_3^-$ determination

To check the effect of salt concentration on the first reduction step, test samples with five replicates were prepared. Samples containing 20 μM $\delta^{15}N\text{-}NO_3^-$ standard of initial concentration and $\delta^{15}N = 14.67 \pm 0.03$‰, 1 ml imidazole buffer, and 3 g Cd were diluted to 70-ml volume with distilled water and placed in a 120-ml bottle. NaCl was added to the samples to produce solutions with concentrations ranging from 0.5 to 5 M. The NaCl was precombusted for 20 h before sample preparation. The samples were shaken for 20 h. Sample volumes of 60 ml were then decanted into fresh 120-ml bottles. The NO_2^- produced was converted into N_2O using the azide ($\delta^{15}N = -2.69 \pm 0.08$‰) reaction step and injected into the IRMS-PRECON system.

Table 2.1. Effect of salt concentration in the sample on $\delta^{15}N_2O$ product.

NaCl conc (M)	N_2O peak area	Standard deviation	n	$\delta^{15}N_2O$ (‰)	Standard deviation	n
0.5	20.9	0.8	5	2.3	0.5	5
1	20.4	1.6	5	3.8	0.9	5
2.5	22.8	1.1	5	3.9	0.5	5
5	27.0	0.8	5	4.5	0.4	5

Along with an increase of peak area, there is a trend in the measured $\delta^{15}N\text{-}N_2$ with salt concentration. Assuming that the conversion to NO_2^- is quantitative and that there is 1:1 combination of nitrite-N and azide-N without fractionation, a theoretical value of $\delta^{15}N$ in the N_2O produced from the NO_3^- standard would be +5.99‰ (McIlvin and Altabet 2005), assuming no isotopic fractionation with respect to the N contributed by the azide reagent. The N_2O produced is partitioned between liquid and gas phases (1:1 volume ratio in our study). Under equilibrium conditions at 25°C, the fractionation of -0.75‰ between dissolved and gaseous N_2O (Inoue and Mook 1994) implies a theoretical $\delta^{15}N_2O$ value of +5.24‰ in the headspace. With increasing NaCl concentration in the sample solution, progressively more N_2O was detected in the headspace and there was an increase in its measured $\delta^{15}N$ value, which became closer to the theoretical $\delta^{15}N_2O$ value expected for the headspace. With 5 M salt concentration, the difference between the measured and

calculated $\delta^{15}N$-N_2O headspace values was about 1.4‰. This offset, which we attribute to isotopic fractionation of the N originating from azide, is still significant but much smaller than the offset in MA (2005) (ca. 4.4‰) (see Table 1 and Fig. 2.2).

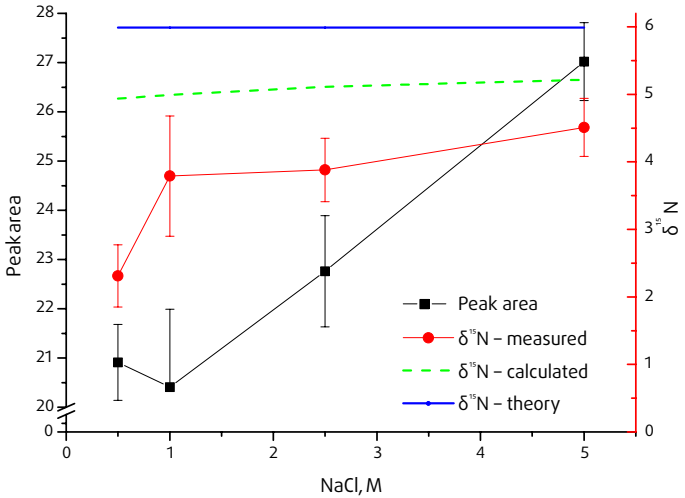

Fig. 2.2. Effect of salt concentration on the peak area and $\delta^{15}N_2O$. $\delta^{15}N$-theory shows the calculated value, assuming 1:1 combination of nitrite-N and azide-N and no isotopic fractionation. $\delta^{15}N$-calculated takes account of fractionation between dissolved and gaseous N_2O and changes in headspace–liquid partitioning as a function of salt concentration ($\delta^{15}N_{calculated} = \delta^{15}N_{theory} - 0.75\alpha$). Error bars represent standard deviations.

With an increasing NaCl concentration, there is a ca. 30% increase in the peak area associated with N_2O in the headspace. This could be explained by either incomplete conversion of initial NO_3^- to NO_2^- at low salt concentrations or the "salting out" effect: i.e., the decrease of N_2O solubility due to an increase of the salt concentration. Blank samples showed that there was no NO_3^- or NO_2^- contamination from the salt (data not shown; see also "Efficiency and recovery of the first reduction step" under "Results").

The effect of the salt concentration on the solubility of gases was first described by Sechenov (1889) and was modified for mixed electrolyte solutions (Schumpe 1993):

$$\log(c/c_0) = \sum(h_i+h_G)c_i$$

where h_i is an ion-specific parameter, h_G a gas-specific parameter, and c_i the ion concentration. Table 2 shows the predicted effect of N_2O solubility change on the expected headspace concentration in relation to the salt concentration. $\delta^{15}N_{total}$ presented in the table is calculated under different solubility conditions as

$$\delta_{total} = \alpha\delta_{gas} + (1-\alpha)\,\delta_{liq} = \alpha\,\delta_{gas} + (1-\alpha)\,(\delta_{gas} + 0.75)\,,$$

$$\delta_{total} = \delta_{gas} + 0.75 - 0.75\alpha$$

where α is N_2O solubility under different salt concentrations, calculated from the Sechenov equation.

Table 2.2. Calculation of N_2O partitioning into the gas phase and associated $\delta^{15}N$ fractionation. ($h_i(Na^+) = 0.1171\ M^{-1}$, $h_i(Cl^-) = 0.1171\ M^{-1}$ and $h_G(N_2O) = 0.011\ M^{-1}$ (Schumpe, 1993)) for a headspace volume that is 58% of the total volume. Calculated from 1:1 combination of nitrite-N and azide-N.

	NaCl conc, M	N_2O in the headspace, %	$\delta^{15}N_{gas}$	$\delta^{15}N_{liq}$	$\delta^{15}N_{total}$	$\delta^{15}N_{offset}$
Overall method	–	–	–	–	6.0*	–
	0.5	51.76	2.3	3.1	2.7	3.3
	1	58.95	3.8	4.6	4.1	1.9
	2.5	74.71	3.9	4.7	4.1	1.9
	5	88.72	4.5	5.3	4.6	1.4

The calculated increase of N_2O in the headspace of about 30% correlates well with our results. However this does not explain the shift in $\delta^{15}N$ values. The $\delta^{15}N$ could be altered via changes in fractionation for the N contributed from HN_3 during the second step or by incomplete conversion and isotopic fractionation of NO_3^- during the first reduction step (e.g., at low salt concentrations). To further study the source(s) of isotopic fractionation for the resulting N_2O, we designed a set of experiments that would outline kinetics and pathways for both reduction steps.

2.3.2. Influence of the salt concentration on second reduction step.

$$NO_2^- + HN_3 + H^+ \rightarrow N_2O + N_2 + H_2O$$

To check the effect of salt concentration on the fractionation effect and the N_2O peak area for the second reduction step, test samples were prepared (60 ml) con-

taining an initial concentration of 20 μM NO_2^- ($\delta^{15}N$ = -16.67 ± 0.07‰), which was converted into N_2O and injected into the IRMS-PRECON system.

These experiments showed that with an increase of the NaCl concentration in the sample solution there is a ca. 30% increase in the peak area associated with the N_2O concentration in the sample headspace, as was seen with the overall method and which is consistent with the salting-out effect. Comparison of the salting out effect with the result from the overall method and the second step are also shown in Fig. 2.3.

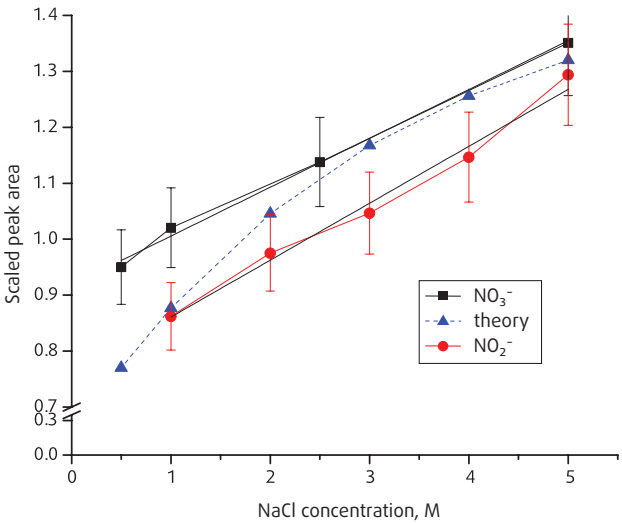

Fig. 2.3. Salting out effect on the second reduction step (NO_2^-) and overall reduction (NO_3^-). Scaled peak area is calculated from peak area divided by the initial concentration or [NO_2^-]). Dashed line shows the theoretical increase of N_2O in the headspace with an increase of the salt concentration.

The slopes of both curves are close to the predicted trend. $\delta^{15}N_{total}$ in Table 3 represents the isotope ratio for the N_2O in both the gas and liquid phases and has been calculated for the different solubility conditions as described earlier. Increasing NaCl does not change $\delta^{15}N_{total}$ when only the second reduction step is carried out.

Table 2.3. $\delta^{15}N$ correlation between the overall method and the second reduction step. Standard deviation of 0.3‰ was calculated for n=3. Calculated from 1:1 combination of nitrite-N and azide-N.

	NaCl conc, M	N_2O in the head-space, %	$\delta^{15}N_{gas}$	$\delta^{15}N_{liq}$	$\delta^{15}N_{total}$	$\delta^{15}N_{offset}$
Second step	–	–	–	–	-9.7*	–
	1	58.95	-11.7	-11.0	-11.4	1.7
	2	70.28	-11.0	-10.3	-10.8	1.1
	3	78.48	-11.7	-11.0	-11.5	1.9
	4	84.42	-11.3	-10.6	-11.2	1.5
	5	88.72	-11.4	-10.7	-11.3	1.6
Overall method	–	–	–	–	6.0*	–
	0.5	51.76	2.3	3.1	2.7	3.3
	1	58.95	3.8	4.6	4.1	1.9
	2.5	74.71	3.9	4.7	4.1	1.9
	5	88.72	4.5	5.3	4.6	1.4

The similar offset of 1.6‰ for the overall method with 5 M NaCl addition (NO_3^- standard) and the second reduction step (NO_2^- standard) suggests that this offset is a result of azide fractionation, which was also observed by McIlvin and Altabet (2005).

This result suggests that the source of the increase of $\delta^{15}N$ with an increase of salt concentration in the overall method (Table 1) is due to fractionation during the first reduction step, especially at salt concentrations below or close to 0.5 M which correspond, very approximately, to salinities < 30 – 32 psu. (We note that the exact equivalent salinity cannot be calculated without knowledge as to whether it is $[Cl^-]$ or the ionic strength of the solution that controls the reduction efficiency).

2.3.3. Efficiency and recovery of the first reduction step

$$NO_3^- + Cd + H_2O \rightarrow NO_2^- + Cd(OH)_2$$

To measure the reduction efficiency of the first reduction step, we measured the concentration of the NO_2^- product and the remaining NO_3^- on an autoanalyzer. The samples, which we made up in distilled water, initially contained 60 ml of 20 μM NO_3^-, 1 ml imidazole buffer, and 3 g Cd in a 120-ml bottle. NaCl was added to samples at concentrations varying from 0 to 5 M, and the time on the shaker was

varied from 1 to 18 h to investigate reduction kinetics under different salt concentrations. The reference samples contained 20 μM NO_3^- standard solution that did not undergo reduction with Cd (Table 4).

Table 2.4. Kinetics of first reduction step.

NaCl concentration (M)	Time (hrs)	NO_3^- (μM)	NO_2^- (μM)	NH_4^+ (μM)	Sum (μM)
No salt addition	Reference	19.23	0.13	0.33	19.69
	1	1.90	16.87	0.01	18.78
	2	0.88	17.53	0.01	18.42
	3	0.91	14.03	0.01	14.95
	4	0.77	11.93	0.02	12.72
	18	1.22	2.17	0.80	4.19
0.2M	Reference	20.23	0.01	0.00	20.24
	1	12.96	7.33	0.05	20.34
	2	12.03	8.00	0.04	20.07
	3	9.82	10.47	0.06	20.35
	4	11.61	9.25	0.13	20.99
	18	10.34	10.17	0.39	20.90
0.5M	Reference	20.06	0.43	0.01	20.50
	1	15.78	4.33	0.03	20.14
	2	13.93	7.00	0.04	20.97
	3	14.15	6.37	0.04	20.56
	4	13.40	7.25	0.04	20.69
	18	8.68	11.95	0.05	20.68
5M	Reference	19.58	0.13	1.30	21.01
	1	4.73	15.84	0.21	19.78
	2	1.55	18.27	1.32	21.14
	3	0.25	19.53	1.27	21.05
	4	0.01	20.20	0.10	20.31
	18	0.14	20.53	0.20	20.87

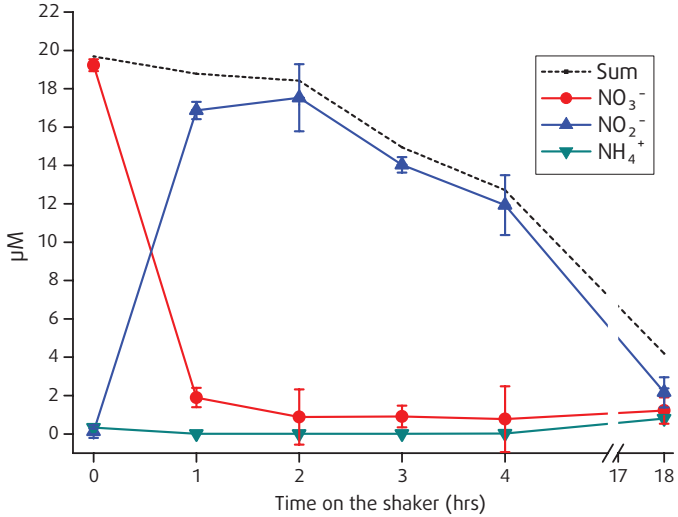

Fig. 2.4. DIN speciation of first reduction step without salt addition. Standard deviation of 1 µM was calculated for n=3.

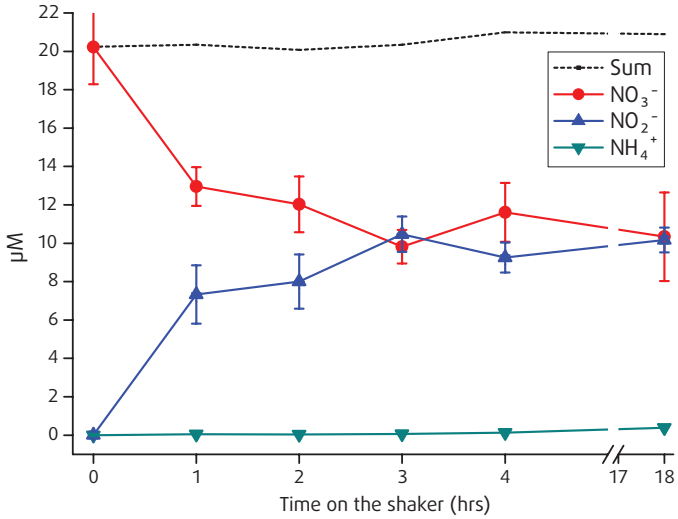

Fig. 2.5. DIN speciation of first reduction step with 0.2 M salt addition. Standard deviation of 1 µM was calculated for n=3.

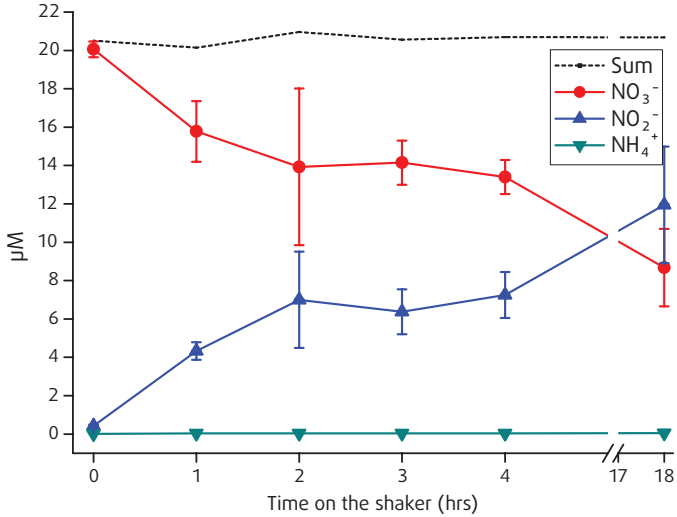

Fig. 2.6. DIN speciation of first reduction step with 0.5 M salt addition. Standard deviation of 3 µM was calculated for n=3

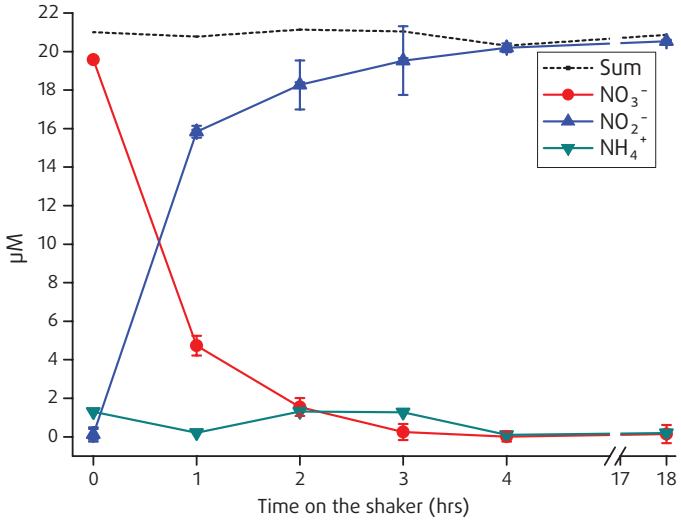

Fig. 2.7. DIN speciation of first reduction step with 5 M salt addition. Standard deviation of 0.5 µM was calculated for n=3

From these results, it is obvious that *without* salt addition, the recovery of DIN decreases with time and the loss of DIN to an unknown form is very large after 18 h (ca. 80%) (Fig. 2.4). Moreover, there is a measurable increase (0.8 μM) of dissolved NH_3, which may suggest an over-reduction of NO_3^-. From these measurements, however, it is not clear which nitrogen species are being produced. With intermediate NaCl concentrations (0.2 and 0.5 M; see Fig. 2.5 – 2.6, respectively), all the added nitrogen can be accounted for; however, reduction to NO_2^- is incomplete even after 18 h (ca. 50%).

Quantitative yields for this step are routinely obtained overnight in the laboratory at SMAST, and we suspect that this step is very sensitive to details of the Cd preparation. For example, previous work done at IFM-GEOMAR (Nuss 2007) showed that complete NO_3^- conversion with 0.5 M NaCl was achieved only after 35 h.

These results demonstrate over-reduction of NO_3^- (i.e., beyond NO_2^-) in freshwater, with N_2O or N_2 as the most likely products. A set of experiments was therefore designed and conducted in our laboratory to measure N_2O accumulated during the first reduction step. The samples contained 60 ml NO_3^- solution of 20 μM initial concentration, 1 ml imidazole buffer, 5 M NaCl, and 3 g Cd in a 120-ml bottle and were left on the shaker for 2 and 18 h. The reference samples contained no NO_3^- standard solution but had 3 g Cd and imidazole buffer in the solution. All bottles were flushed with an N_2 flow for 5 min before closing the bottles and placing them on the shaker.

The results from the GC-ECD measurements show some production of N_2O *without* salt addition, but it was very small, representing only about 13 nmol N_2O or 0.07% of the initial NO_3^- concentration. This cannot explain the loss of more than 90% of the DIN after 18 h (Fig. 2.3). N_2O is probably an intermediate product in the reduction mechanism to N_2.

From these data, it is also clear that already (after only 4 h on the shaker) there is a complete conversion of NO_3^- to NO_2^- performed with salty samples (5 M NaCl, Fig. 2.7), whereas without salt addition we risk either overreduction to N_2 or incomplete reduction to NO_2^-.

2.4. Discussion and conclusions

Whereas it was recognized previously that Cl^- was needed for the azide reaction, in this work we show that it promotes the efficient reduction of NO_3^- to NO_2^- by Cd. Therefore [Cl^-] has a significant influence on the overall reduction mechanism and the resulting $\delta^{15}N$ values. Very low salt concentrations can lead to overreduction of NO_3^- and significant fractionation of $\delta^{15}N$ in the products. By adding 5 M NaCl, a quantitative reduction to NO_2^- after only 4 h of treatment with Cd on the shaker is achieved and overreduction on the first reduction step is excluded.

We hypothesize the sequence for overreduction by Cd is:

$$NO_3^- \rightarrow NO_2^- \rightarrow N_2O \rightarrow N_2$$

Without salt addition, Cd metal likely reduces NO_3^- to N_2, whereas with 5 M NaCl the reduction of NO_3^- effectively stops with NO_2^-. With intermediate salt concentrations, there is no overreduction apparent, but the conversion to NO_2^- is not complete. At 5 M NaCl, there is quantitative conversion of NO_3^- to NO_2^-, as required by the method. We speculate that the effect of Cl^- on acceleration and completion of the reaction may be associated with formation of a complex between the Cd^{2+} and Cl^- during the reduction.

Addition of 5 M NaCl in our experiments sped up the conversion to NO_2^- and resulted in avoidance of fractionation effects along with improved yield of N_2O from the headspace (due to the salting out effect). The salting out effect resulted in a sensitivity of the headspace method comparable to that of the purge/trap method of MA (2005).

Thus we suggest a modification of the MA (2005) method for $\delta^{15}N$ analysis by adding 5 M NaCl into the initial samples to achieve quantitative and rapid reduction. The modified method is suitable for water analysis over a wide range of salinities.

3 Contrasting biogeochemistry of nitrogen in the Atlantic and Pacific Oxygen Minimum Zones

Abstract

We present new data for the stable isotope ratio of inorganic nitrogen species from the contrasting oxygen minimum zones (OMZ's) of the Eastern Tropical North Atlantic, south of Cape Verde, and the Eastern Tropical South Pacific off Peru. Differences in minimum oxygen concentration and corresponding N-cycle processes for the two OMZ's are reflected in strongly contrasting $\delta^{15}N$ distributions. Pacific surface waters are marked by strongly positive values for $\delta^{15}N\text{-}NO_3^-$ reflecting fractionation associated with subsurface N-loss and partial NO_3^- utilization. This contrasts with negative values in NO_3^- depleted surface waters of the Atlantic which are lower than can be explained by N-supply via N_2-fixation. We suggest the negative values reflect inputs of nitrate, possibly transient, associated with deposition of Saharan dust. Strong signals of N-loss processes in the subsurface Pacific OMZ are evident in the isotope and N_2O data, both of which are compatible with a contribution of canonical denitrification to overall N-loss. However the apparent N-isotope fractionation factor observed is relatively low (ε_d = 11.4‰) suggesting an effect of influence from denitrification in sediments. Identical positive correlation of N_2O vs. AOU for waters with oxygen concentrations $[O_2] > 50$ μmol/l in both regions reflect a nitrification source. An inverse correlation in the Pacific OMZ due to denitrification is observed for oxygen concentrations $O_2 < 5$ μmol/l.

This chapter is based on:

E. Ryabenko, A. Kock, H.W. Bange, M.A. Altabet, D.W.R. Wallace: Contrasting biogeochemistry of nitrogen in the Atlantic and Pacific Oxygen Minimum Zones

Acknowledgements: The authors thank Frank Malien, Gert Petrick and Karen Stange for technical assistance and Andreas Oschlies helpful discussion. The work was supported by the DFG-funded Sonderforschungsbereich 754 "Climate-Biogeochemistry Interactions in the Tropical Ocean" and SOPRAN (Surface Ocean Processes in the Anthropocene: www.sopran.pangea.de | FKZ 03F0462A)

3.1. Introduction.

Nitrogen is a key limiting element for biological productivity and occupies a central role in ocean biogeochemistry. Although most chemical forms of nitrogen in the ocean are bio-available (i.e. fixed nitrogen or "fixed-N") the most abundant form, N_2 is generally not. The sources of fixed-N include river inputs, atmospheric deposition (Duce, et al., 2008) and N_2 fixation. Sinks of fixed-N, producing N_2, include microbial denitrification and anammox processes, both requiring very low [O_2] (Gruber, 2008). Hence Oxygen Minimum Zones (omz's) are the oceanic regions especially associated with denitrification (Cline, et al., 1972, Codispoti, et al., 2001, Ward, et al., 2009) and anammox (Galan, et al., 2009, Hamersley, et al., 2007, Lam, et al., 2009, Thamdrup, et al., 2006) and play a particularly important role in the global nitrogen cycle. They are located typically in areas of upwelling with high productivity which exhibit complex cycling of nutrients (Helly, et al., 2004).

The relative importance of heterotrophic denitrification (a stepwise reduction process involving a number of intermediates, $NO_3^- \rightarrow NO_2^- \rightarrow NO \rightarrow N_2O \rightarrow N_2$), compared to anammox (a chemosynthetic process, $NO_2^- + NH_4^+ \rightarrow N_2$) is debated (Voss, *et al.*, 2009). Absence of ammonium in omz's that should have accumulated from organic matter breakdown could be indicative of anammox, while the consumption of N_2O requires the denitrification process (Naqvi, *et al.*, 2010).

Although omz's are found in all major ocean basins, the associated nitrogen cycle processes can vary dramatically due to contrasting minimum oxygen levels. In the Eastern Tropical South Pacific (etsp), suboxic ([O_2] < 5 μmol/l) conditions are found, whereas in Eastern Tropical North Atlantic (etna), hypoxic ([O_2] < 60 μmol/l) conditions exist. In addition, fixed-N inputs associated with atmospheric deposition and, possibly, N_2-fixation, vary between the two regions (Chavez, *et al.*, 2009).

Cruises carried out during the collaborative research project sfb-754 (www.sfb754.de) of the German Research Foundation and the bmbf-supported project sopran (Surface Ocean Processes in the Anthropocene: www.sopran.pangaea.de) provided unique opportunities to sample nitrogen species in these two contrasting regions. Here we present a comparison of N_2O concentration and stable nitrogen isotope distributions, which were measured in both omz's to highlight the similarities and differences in nitrogen cycling between the two regions.

3.2. Sampling and analytical methods.

In the Pacific OMZ, samples were collected onboard the FS Meteor (M77 Legs 3 and 4) in December 2008 and January 2009 (Fig. 3.1). In the Atlantic OMZ, samples were collected on the R/V L'Atalante during February 2008 from Dakar to Cape Verde Islands and on the FS Meteor (M80) in December 2009 covering the region south to Cape Verde Islands. At each station, water samples were collected using 12 l Niskin bottles on a CTD rosette system equipped with temperature, pressure, conductivity and oxygen sensors. Nutrients and oxygen were determined onboard according to GRASSHOFF et al. (1999). Triplicate water samples were taken from the CTD/rosette casts and were analyzed for dissolved N_2O onboard using a static equilibration method. For details concerning the N_2O method, see WALTER et al. (2006).

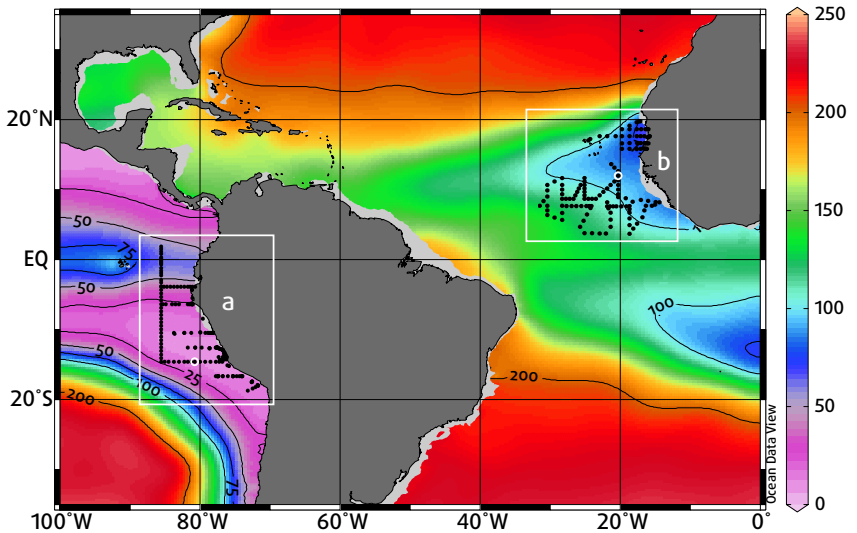

Fig. 3.1. Oxygen distribution at 200 m (Schlitzer, R., Ocean Data View, World Ocean Atlas 2005, http://odv.awi.de/en/data/ocean/world_ocean_atlas_2005/) with CTD station locations in the Pacific (a) and Atlantic (b) study regions referred to in the text. White circles indicate station 84 (a) and station 5 (b).

Water samples for $d^{15}N$ analysis were collected in 100 ml HDPE bottles and kept frozen prior to analysis. For logistical reasons, samples from the M77 cruise that contained low to negligible levels of nitrite ($[NO_2^-] < 0.1$ µmol/l) were acidified and

stored at room temperature, whereas samples with significant [NO_2^-] were kept frozen prior to the $\delta^{15}N\text{-}NO_2^-$ analysis. Aliquots of these samples were treated in the laboratory with sufficient sulfanilic acid to remove [NO_2^-] prior to $\delta^{15}N\text{-}NO_3^-$ analysis with any remaining sample stored at room temperature.

The isotopic composition of dissolved nitrate ($\delta^{15}N\text{-}NO_3^-$) and nitrite ($\delta^{15}N\text{-}NO_2^-$) was measured using the Cd-reduction/azide method (McIlvin, et al., 2005) with addition of NaCl as described by Ryabenko et al (2009). All the samples from the Atlantic study region and 50% of the Pacific samples were analyzed at the IFM-GEOMAR in Germany, while c. 50% of the Pacific samples were analyzed at SMAST in the USA, using the same method. The only difference was that at SMAST N_2O produced by this method was analyzed isotopically, whereas at IFM-GEOMAR N_2O was converted on-line to N_2 for isotopic analysis. The detection limit at IFM-GEOMAR was 0.2 μmol/l of nitrate or nitrite with the precision of the $\delta^{15}N$ measurements being ± 0.2‰. The detection limit at SMAST was slightly higher, 0.5 μmol/l, with the same precision of ^{15}N measurements.

The analyses of the Pacific deep water samples (> 1500 m) from both labs gave near identical values of $\delta^{15}N\text{-}([NO_2^-]+[NO_3^-])$ of 5.69 ± 0.7‰ (IFM-GEOMAR; n = 31) and 5.62 ± 0.4‰ (SMAST; n = 8) respectively. The Fisher test showed that we can merge the two data sets with a confidence level > 95%. The resulting mean value of 5.64 ± 0.7‰ (n = 39) lies between previously published values of 6.5‰ Voss (2001) and 4.5‰ Sigman (1997) for the deep North Pacific Ocean. Deep waters of the Atlantic showed very similar values as those of the Pacific (5.3‰ ± 0.5 for > 2000 m, see table 1).

3.3. Hydrographic setting of the two study regions

In the North Equatorial Atlantic region, the eastward flow of the North Equatorial Counter Current (NECC) and North Equatorial Under Current (NEUC) supplies oxygen rich waters to the Atlantic OMZ (Glessmer, et al., 2009). The water mass distribution in this Atlantic OMZ study region (Fig. 3.1, square b) is affected by the Cape Verde Frontal Zone, which marks the boundary between *North* and *South Atlantic Central Waters* (NACW, SACW). This separates well-ventilated waters of the subtropical gyre in the north from less-ventilated waters to the south. Our CTD data (Fig. 3.2) show water mass properties < 500 m intermediate between those of NACW and SACW. *Antarctic Intermediate Water* (AAIW: 3 – 5°C, S = 34.5) is found at ~1000 m with *North Atlantic Deep*

Water (NADW) filling the depth range between ~1000 and 4000 m (Fig. 3.2b). A summary of the water masses properties found in both study regions is presented in Table 1.

In the South Pacific, the Equatorial Undercurrent (EUC), Southern Subsurface Counter Currents (SCC), and the Southern Intermediate Counter Currents (SICC) supply 13°C Equatorial Water (13CW, $25.8 < \sigma_\theta < 26.6$) to the eastern Pacific OMZ (STRAMMA, et al., 2010). The westward flowing South Equatorial Current (SEC) may recirculate some 13° water from the OMZ by returning eastward as the South Subsurface Counter Current at 3 – 5°S (SCHOTT, et al., 2004). The origin of 13CW is remote from the equator (QU, et al., 2009) mostly as *Subantarctic Mode Water* (SAMW; TOGGWEILER et al, 1991) and transports very oxygen depleted waters to the OMZ , due to its relative old age. The *South Pacific Subtropical Underwater* (STUW) is a likely O_2 source from the south which is centered on the $\sigma_\theta = 25.0$ isopycnal and is well-ventilated across nearly the full width of the subtropical gyre (O'CONNOR, et al., 2002). The low-salinity water ($S < 34.5$) found between c. 500 and 1000 m southward of 10°S is *Antarctic Intermediate Water* (AAIW). *South Pacific Deep Water* (1.2 – 2°C) is found between c. 1500 – 3000 m and is underlain by *Lower Circumpolar Water* (LCPW) (FIEDLER, et al., 2006) (Fig. 3.2a).

Because of the differences in hydrography and significantly lower oxygen supply, the Pacific OMZ is much more intense as compared to the Atlantic (KARSTENSEN, et al., 2008). The resulting very low oxygen concentrations favor metabolic pathways that convert nitrogen from biologically reactive "fixed" forms (for example nitrate, nitrite or ammonium) to N_2 via denitrification and/or anammox.

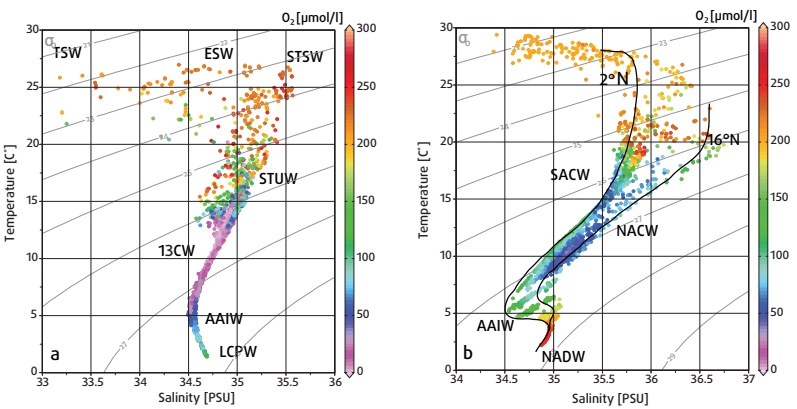

Fig. 3.2. T-S diagrams with O_2 color coded for the Pacific (a) and the Atlantic (b) study regions from CTD data collected during the M77, M80 and L'Atalante cruises.

Table 3.1. Summary of properties of water masses based on data collected during M77, M80 and L'Atalante cruises. Tropical Surface Water (TSW: T>25°C, S<34), Equatorial Surface Water (ESW: T<25°C, S>34), Subtropical Surface Water (STSW: S>35), South Atlantic Central Water (SACW: 5<T<20°C, 34.3<S<36.0), North Atlantic Central Water (NACW: 7<T<18 °C, 35<S<36.7), Subtropical Underwater (STUW: 13<T<22°C, 34.3–35.5), 13°C Equatorial Water (13CW: 12<T<14°C, 34.8<S<35), Antarctic Intermediate Water (AAIW: 3<T<5°C, 34.4<S<34.5), South Pacific Deep Water (SPDW: 1.2<T<2°C), Lower Circumpolar Water (LCPW: 0.5<T<0.9°C, S<34.7), North Atlantic Deep Water (NADW: T<4°C, S~35)

	Water mass		Temp. [C°]	Salinity [PSU]	Nitrate	Phosphate [µmol/l]	Oxygen	$\delta^{15}N$ [‰]
PACIFIC	TSW	Range	20.4–26.1	32.9–34.6	0.8–15.9	0.3–1.4	96.8–233.0	5.7–10.4
		Average	24.1	33.7	6.4	0.7	192.4	8.7
			n=24	n=24	n=19	n=19	n=19	n=5
	ESW	Range	20.2–24.8	34.9–34.2	0.2–18	0.6–1.4	96.8–271.7	5.8–10.7
		Average	22.5	34.6	8.3	0.9	199.6	8.1
			n=43	n=43	n=38	n=38	n=42	n=6
	STSW	Range	23.6–26.8	35.5–35.6	1.4–5.1	0.3–0.7	220.0–244.0	14.6–29.1
		Average	24.9	35.5	3.3	0.5	226.7	18.5
			n=47	n=47	n=28	n=28	n=31	n=10
	STUW	Range	13.0–16.5	34.7–35.0	0.3–33.7	1.1–3.8	1.8–201	1.5–19.4
		Average	13.6	35.0	26.3	2.4	24.0	7.5
			n=374	n=374	n=315	n=317	n=340	n=135
	13CW	Range	12.1–13.9	34.8–35.0	0.0–34.5	1.1–3.9	1.8–74.3	3.8–25.2
		Average	13.1	34.9	23.2	2.6	10.9	9.1
			n=657	n=657	n=526	n=526	n=604	n=207
	AAIW	Range	4.2–6.0	34.5–34.6	42.0–51.6	3.1–3.6	17.9–62.6	5.4–8.4
		Average	4.9	34.5	46.8	3.3	44.2	6.7
			n=134	n=134	n=96	n=95	n=103	n=39
	SPDW	Range	1.9–2.9	34.6–34.7	38.2–45.7	2.7–3.2	68.5–136.0	5.1–7.2
		Average	2.2	34.6	40.5	2.9	106.4	5.8
			n=73	n=73	n=62	n=62	n=70	23
	LCPW	Range	1.8	34.7	34.9–38.0	2.6–2.7	139.0–158.0	5.1–6.1
		Average	1.8	34.7	36.6	2.7	148.1	5.4
			n=21	n=21	n=18	n=18	n=18	n=4

	Water mass		Temp. [C°]	Salinity [PSU]	Nitrate	Phos-phate [µmol/l]	Oxygen	$\delta^{15}N$ [‰]
ATLANTIC	NACW	Range	9.7–16.8	35.2–36.3	13.4–33.8	0.8–2.0	57.7–135.0	3.4–7.0
		Average	12.7	35.6	26.4	1.6	77.3	5.4
			n=24	n=24	n=17	n=17	n=24	n=16
	SACW	Range	9.7–17.4	35.0–35.8	16.4–37.1	0.8–2.1	52.9–134.2	2.0–7.1
		Average	12.3	35.2	26.7	1.5	101.4	5.3
			n=60	n=60	n=40	n=42	n=60	n=33
	AAIW	Range	5.0–7.2	34.7–34.9	33.9–44.9	1.9–2.4	76.9–140.6	4.8–6.8
		Average	5.8	34.8	38.2	2.2	113.1	5.5
			n=13	n=13	n=10	n=10	n=13	n=8
	NADW	Range	2.5–3.9	34.9–35.0	21.8–23.0	1.4–1.6	220.9–249.1	4.8–5.6
		Average	3.1	34.9	22.5	1.5	238.6	5.3
			n=22	n=22	n=10	n=10	n=10	n=13

3.4. Results and discussion

3.4.1. Vertical distribution of nitrogen species and isotopes

General

Dissolved O_2 varies considerably in its depth distribution between the Atlantic and Pacific study regions as shown in Figure 3.3. Figure 3.4 presents typical water column profiles for oxygen and several nitrogen related properties from both study regions (outside of the upwelling zones). Stations 5 (Atlantic, M80) and 84 (Pacific, M77) were chosen due to synoptic availability of N_2O, $\delta^{15}N$ and $[NO_2^-]$ data. The geographic positions of the stations are indicated on Figure 3.1 by white circles.

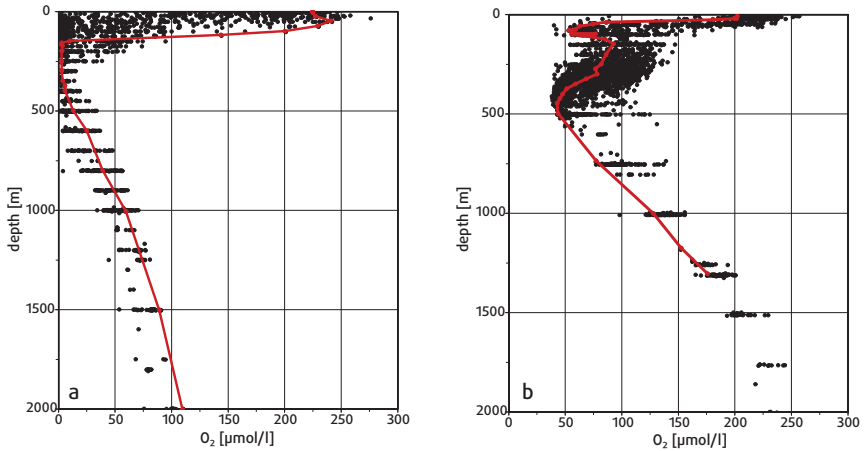

Fig. 3.3. Oxygen distribution in the Pacific (a) and the Atlantic (b) study regions, as measured on the cruises M77, M80 and L'Atalante. The red lines show the water-column profiles for M77 station 84 in the Pacific and M80 station 5 in the Atlantic

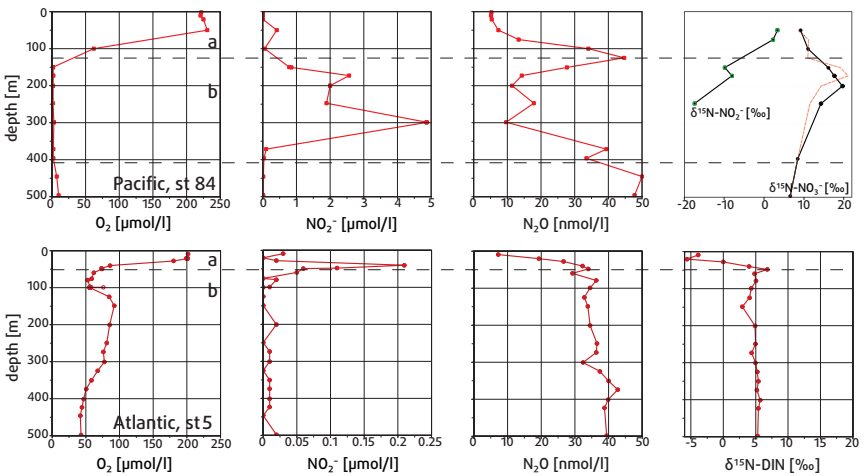

Fig. 3.4. Typical water column profiles from the SE Pacific OMZ (st. 84, 81°W/14°S) from the M77 cruise (upper panels) and the NE Atlantic OMZ (st. 5, 20.5°W/12.3°N) from the M80 cruise (lower panels). Black lines in the Pacific indicate $\delta^{15}N\text{-}NO_3^-$ and $\delta^{15}N\text{-}NO_2^-$, and the red line indicates $\delta^{15}N\text{-}DIN$ (NO_3^- + NO_2^-). Note the different of scales for $\delta^{15}N$: -20 to +20‰ in the Pacific and -5 to +20‰ in the Atlantic.

Pacific Study Region

In the Pacific study region, the OMZ contains mostly 13CW, with oxygen concentrations < 2 μmol/l at depths as shallow as ~50 m and as deep as ~550 m. The Pacific station (Fig. 3.4, upper panels) is also characterized by a broad oxygen minimum with $[O_2]$ < 2 μmol/l (170 – 400 m). Two $[NO_2^-]$ maxima are located in the upper oxycline (50 m) and the core of the oxygen minimum (300 m). We divide the Pacific profile into layers a and b to focus the discussion of nitrogen transformations at OMZ boundaries and its core.

Layer (a) (0 – 120 m) includes a ~70 m deep mixed layer and the 50 m deep euphotic zone (Chavez, et al., 2009), and contains water with the highest oxygen concentrations as well as a very sharp oxycline at 80 – 120 m in which $[O_2]$ drops from ~150 to 20 μmol/l. The primary nitrite maximum lies close to the base of the euphotic zone and can be a consequence of two processes (Lomas, et al., 2006): light-limited, incomplete assimilatory reduction of nitrate by phytoplankton and microbial ammonium oxidation (nitrification). Near-surface N_2O is close to saturation and increases within the oxycline from ~12 to ~45 nmol/l. The observed increase in nitrous oxide increase within the oxycline and upwards is likely a by-product of ammonia oxidation (Codispoti, 2010) with a net flux from the mixed layer to the atmosphere via gas exchange. The concentrations of $[NO_3^-]$ and $[NO_2^-]$ above 80 m in layer (a) at this station were below our detection limit for $\delta^{15}N$ measurement (0.2 μmol/l). Higher near-surface DIN concentrations were observed at other stations along the 86°W transect and the corresponding $\delta^{15}N\text{-}NO_3^-$ values were as high as 20‰. High surface $\delta^{15}N\text{-}NO_3^-$ is likely the result of incomplete nutrient utilization and fractionation during nitrate assimilation (Granger, et al., 2004). $\delta^{15}N\text{-}NO_2^-$ is generally much lower and its difference from $\delta^{15}N\text{-}NO_3^-$increases with depth, coming close to a value of ~30‰ in layer (b). Relative ^{15}N depletion in nitrite can be explained by isotopic fractionation during nitrate reduction to nitrite. A smaller difference between $\delta^{15}N\text{-}NO_3^-$ and $\delta^{15}N\text{-}NO_2^-$ observed in the oxycline is likely due to nitrification as the fractionation effect of the process is significantly smaller (~13‰) (Casciotti, 2009, Casciotti, et al., 2007). Thus there is evidence for a clear switch from nitrification to denitrification with depth.

Layer (b) (120 m to 400 m). O_2 concentrations in this layer drop below 2 μmol/l and there is a strong increase in $[NO_2^-]$ towards a "secondary" maximum at the core of OMZ. N_2O concentrations drop sharply within the OMZ core to ~10 nmol/l and

increase again only towards the lower border of the layer. Denitrification is the only N-removal process which is known to consume N_2O, hence it is likely that both the increase in [NO_2^-] and the increase and decrease in [N_2O] within this layer can be attributed to different stages of canonical denitrification ($NO_3^- \rightarrow NO_2^- \rightarrow N_2O \rightarrow N_2$) (Bange, 2008). The vertical profiles, especially the minimum in N_2O within the OMZ's core, provide strong evidence that all stages of canonical denitrification influence nitrogen speciation in this layer. The observed increase in $\delta^{15}N\text{-}NO_3^-$ and decrease in $\delta^{15}N\text{-}NO_2^-$ at the base of the layer (b) are also consistent with denitrification, which leaves [NO_2^-] depleted in ^{15}N. On the other hand, the deep [NO_2^-] maximum can also support anammox, which has been observed in several previous studies of this region (Galan, et al., 2009, Hamersley, et al., 2007, Lam, et al., 2009).

Atlantic Study Region

In the Atlantic study region, the oxygen profile has two minima at ~70 m and ~400 m (Fig. 3.3b). The shallow minimum is strongest between Senegal and the Cape Verde Islands and is probably caused by enhanced subsurface remineralization associated with high biological productivity and a shallow mixed layer (Karstensen, et al., 2008). The deeper minimum is more prominent south of Cape Verde and is associated with the water mass boundary between Central Water and AAIW (Stramma, et al., 2005). The double oxygen minimum (Fig. 3.3) is therefore caused by the mixing of two water masses from the North and South (NACW and SACW) of the Atlantic region.

The profiles from the Atlantic station (Fig. 3.4, lower panels) are considerably simpler, with fewer subsurface features. Once again, two layers have been distinguished based on oxygen concentration and its influence on dominant nitrogen cycle processes.

Layer (a) (0 – 50 m) includes the surface mixed layer which extends to c. 30 m. This layer includes the steepest part of the oxycline, a strong increase in N_2O with depth, and a primary nitrite maximum which lies at the base of this layer. The $\delta^{15}N$ of DIN increases steadily throughout this layer and reaches a maximum at a depth close to the primary nitrite maximum. These features can be attributed to a combination of remineralization of organic matter, nitrite excretion by phytoplankton after nitrate reduction and nitrification. In contrast to the Pacific study region, the surface layer has minimum values of $\delta^{15}N$ in DIN, with some values being strongly negative (e.g. -5.6‰ at 20 m).

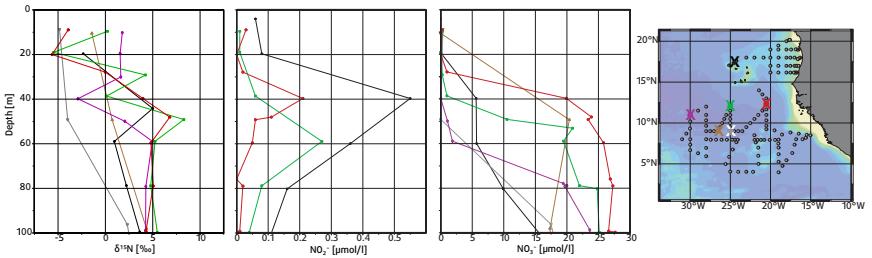

Fig. 3.5. Shallow vertical profiles of M80 stations south to Cape Verde islands in the Atlantic. Stations: 1 (TENATSO) and 5, 67, 76, 81 and 87 located between 12°N and 9°N.

Examination of near-surface profiles from the Atlantic (Fig. 3.5) reveals negative values of $\delta^{15}N$ in DIN within the surface mixed layer at stations located South of Cape Verde and at the TENATSO station. There is a tendency for the values to be most negative at the shallowest depths (20 m). The $[NO_2^-]$ concentrations at these depths on these stations are very low (mostly below 0.1 nmol/l), while $[NO_3^-]$ concentrations in the region are about 0.1 – 0.5 µmol/l. In regions more influenced by upwelled waters, the near-surface values were in the range +4 – +7‰. Even though these concentration levels lie close to our detection limit for $\delta^{15}N$ measurements (0.2 µmol/l), all surface water samples were measured 5 times and gave reliable values with > 95% reliability and ± 0.3‰ standard deviation. Further, laboratory tests with dilutions of $\delta^{15}N$ standards showed no suggestion of any systematic change of measured $\delta^{15}N$ values with decreasing $[NO_3^-]$ concentrations.

Layer (b) (below 50 m) includes the core of the Atlantic OMZ. In contrast to the Pacific OMZ, the Atlantic profiles had no secondary nitrite maximum, and $\delta^{15}N$ values and N_2O concentrations remained relatively constant with depth. The N_2O profiles show no evidence for consumption as was seen in the Pacific. This is a clear indication for the absence of significant denitrification in this region. A slight increase in N_2O with depth below 500 m can be explained by nitrification (WALTER, et al., 2006).

3.4.2. Property-Property Distributions

Nitrate to Phosphate

Figure 3.6 presents the NO_3^- to PO_4^{3-} relationship (with dissolved oxygen concentrations as the color code) for the Atlantic and Pacific study regions. According to Redfield stoichiometry, the average ocean ratio of N:P is 16:1. The deviation from this ratio can is an indicator for which processes are dominating in the ocean region of interest. Waters in the Pacific study region are highly N-deficient (N:P < 16), with the highest deficits found in oxygen minimum waters (purple coloring, Fig 3.6a) and associated with N-removal processes: denitrification and/or anammox (Deutsch, et al., 2001). Data from the Atlantic study region show strong positive deviations from the 16:1 Redfield stoichiometry, which can be a result of N_2-fixation (Gruber, et al., 1997, Hansell, et al., 2004, Michaels, et al., 1996) and/or nutrient uptake and/or remineralization with non-Redfield stoichiometry (Monteiro, et al., 2006). Positive deviation from Redfield stoichiometry can also, potentially, be caused by atmospheric deposition of nitrogen (Duce, et al., 2008). Note that our treatment of deviations in $[NO_3^-]$:$[PO_4^{3-}]$ does not include nitrite (NO_2^-) produced under low oxygen. Including NO_2^- in the calculation, however, does not change significantly the ratios (average DIN:$[PO_4^{3-}]$ = 15.04 in the Pacific and 16.92 in the Atlantic regions).

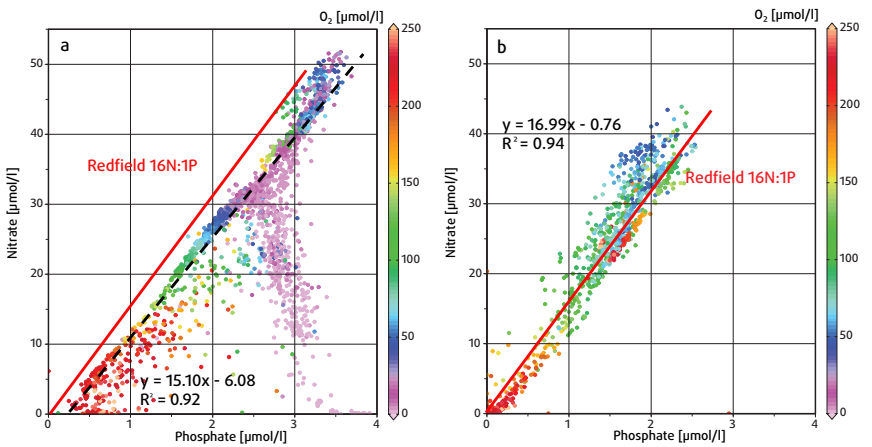

Fig. 3.6. $[NO_3^-]$:$[PO_4^{3-}]$ relationships in the Pacific (a) and the Atlantic (b) study regions. The data are color-coded by oxygen concentration. Note that the average $[NO_3^-]$:$[PO_4^{3-}]$ relationship in the Pacific was calculated for $[O_2]$ > 50 µmol/l.

N_2O vs. AOU

Property-property plots of ΔN_2O to AOU (with pressure as the color code) are presented in Figure 3.7. ΔN_2O is the excess nitrous oxide over concentrations in equilibrium with atmospheric N_2O levels. It is calculated as the difference between the contemporary equilibrium concentration N_2O (i.e. calculated for an atmospheric mole fraction of N_2O of 322 x 10^{-9} for Pacific data and 323 x 10^{-9} for Atlantic data, http://agage.eas.gatech.edu) and the measured concentration (Walter, et al., 2006).

An overall linear relationship of ΔN_2O to AOU (Fig. 3.7) was observed previously in both regions (Elkins, et al., 1978, Oudot, et al., 1990). However, the Pacific relationship is linear only for $[O_2] >$ c. 50 μmol/l (which corresponds here to an AOU of c. 208 μmol/l) after which there is a marked change in slope. The slope of the ΔN_2O to AOU relation for $5 < [O_2] < 50$ μmol/l is 0.14 ± 0.03, which is significantly higher than the slope for $[O_2] > 50$ μmol/l (0.10 ± 0.006). This is suggestive of a higher yield of N_2O per mole NO_3^- produced by nitrification at low oxygen levels (Goreau, et al., 1980, Stein, et al., 2003). In Pacific waters with $[O_2] < 5$ μmol/l (AOU of c. 248μmol/l), ΔN_2O concentrations decrease again to near-zero values, indicative of the N_2O consumption at very low oxygen levels mentioned above. Corresponding changes in slope are not visible in the Atlantic data, likely because there are so few data with $[O_2] < 50$ μmol/l. The slopes of the ΔN_2O vs. AOU relationships for $[O_2] > 50$ μmol/l are remarkably similar in both regions: 0.104 ± 0.006 and 0.111 ± 0.003 in the Pacific and Atlantic, respectively. These values lay between the values of 0.078 (Walter, et al., 2006) and 0.211 (Oudot, et al., 2002) measured for tropical Atlantic.

This higher yield of N_2O under reduced concentrations of oxygen was observed earlier (Goreau, et al., 1980) and was attributed to increasing N_2O yield when ammonia oxidizing microbes become O_2 stressed. This view was challenged by Frame and Casciotti (2010), who showed that ammonia-oxidizing bacteria do not have increased N_2O yield under low O_2 conditions under environmentally relevant culture conditions. The most recent findings from both the Atlantic and Pacific oceans indicate however that archaeal ammonia-oxidizers (AOA) rather than bacteria may be key organisms for the production of oceanic nitrous oxide and can exhibit higher production rates under low oxygen conditions (Löscher, et al., 2011).

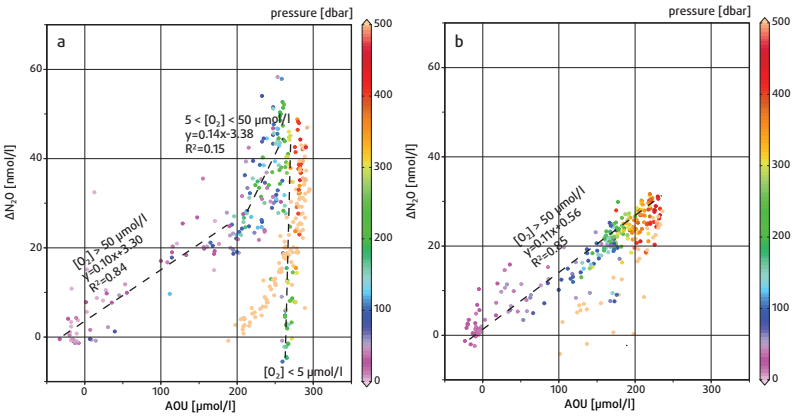

Fig. 3.7. ΔN_2O vs. AOU in the Pacific (a) and in the Atlantic (b) study areas. Black dashed lines show the correlation between ΔN_2O and AOU.

Regarding the Pacific observations at very low O_2, N_2O removal provides strong evidence for the occurrence of denitrification given its specificity for this process (Bange, et al., 2005). However, the amount of N_2O removed (c. 50 nmol/l) is an order of magnitude lower then the observed amount of NO_3^- removal. Hence it gives no indication of the quantitative significance of this process for overall fixed nitrogen removal (e.g. compared to anammox). Additional insight into N-loss processes is gained here from nitrogen isotope ($\delta^{15}N\text{-}NO_3^-$) and fixed nitrogen deficit (N′) data.

N_2O vs. $\delta^{15}N\text{-}NO_3^-$

Figure 3.8 shows ΔN_2O vs. $\delta^{15}N\text{-}NO_3^-$ (with color coding indicating the oxygen concentration) in the two study regions which help to reveal the processes responsible for the production or consumption of nitrous oxide. In the Atlantic, the profiles and property-property plots show no evidence of N_2O consumption and the nitrogen isotope values stay close to the oceanic average of 5‰, which is also consistant with a lack of denitrification. As discussed above, the dominant process affecting N_2O in the Atlantic study region is production due to nitrification. For Pacific oxygenated waters ($[O_2] > 5$ µmol/l) the ΔN_2O vs. $\delta^{15}N\text{-}NO_3^-$ relationship is similar to that found in the Atlantic. High $\delta^{15}N\text{-}NO_3^-$ values in the Pacific study region (Fig 3.8a) can be associated with denitrification at lower O_2 concentrations ($[O_2] < 5$ µmol/l, purple coloring) or with nitrate assimilation in surface waters ($[O_2] > 200$ µmol/l, red color-

ing). These two processes cannot be distinguished in Figure 3.8a as the ΔN_2O is close to zero both under $[O_2] < 5$ μmol/l due to denitrification and under $[O_2] > 200$ μmol/l due to N_2O gas exchange with the atmosphere. In order to differentiate between these two processes the correlation between $\delta^{15}N\text{-}NO_3^-$ and N-deficit was calculated.

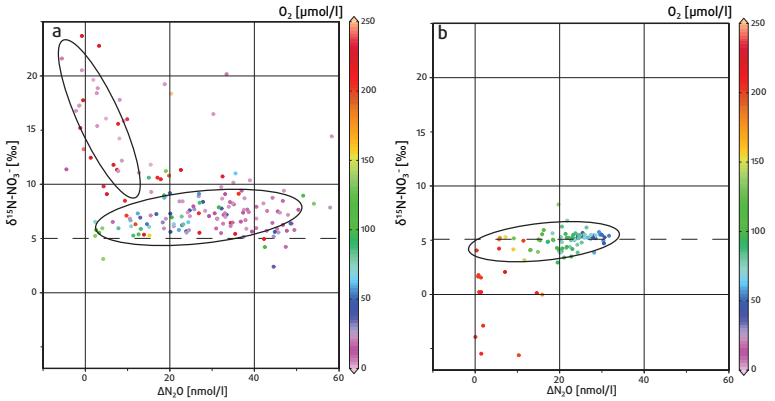

Fig. 3.8. $\delta^{15}N\text{-}NO_3^-$ vs. ΔN_2O to in the Pacific (a) and in the Atlantic (b) study areas.

$\delta^{15}N$ vs. N′

Figure 3.9 presents the distribution of $\delta^{15}N$ of DIN as a function of N′ for the Pacific study regions (where $N' = [NO_3^-] + [NO_2^-] - 16\times[PO_4^{3-}]$). The data are again color-coded by the O_2 concentration.

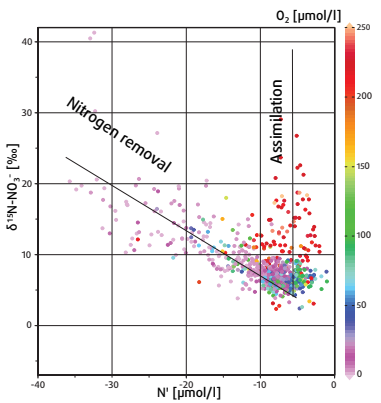

Fig. 3.9. $\delta^{15}N$ distribution vs. N′ the Pacific.

$\delta^{15}N$ vs. N′ data reveal two clear trends in the Pacific study region. In the core of the OMZ, the $\delta^{15}N$ of DIN is inversely correlated with N′ (mainly negative values) and hence with N-removal, whereas in high-oxygen, near-surface waters, $\delta^{15}N\text{-}NO_3^-$ increases independent of N′, reflecting fractionation during NO_3^- assimilation by phytoplankton in the euphotic zone (Granger, et al., 2004). The reduction of nitrate to nitrite is the first step of the denitrification process and is also an essential source of NO_2^- for fuelling anammox (Lam, et al., 2009). We will next examine the isotope fractionation signal associated with this reduction step.

Isotope fractionation and N-loss in the Pacific OMZ

The kinetic isotope fractionation factor can be represented as either $\alpha_r = {}^{15}R/{}^{14}R$ or $\varepsilon_r = (1 - \alpha) \times 1000$, where ^{15}R and ^{14}R are the rates of denitrification for $^{15}NO_3^-$ and $^{14}NO_3^-$, respectively. An effective or "apparent" value for the fractionation factor for nitrate reduction (ε_r) can be calculated through application of the Rayleigh model to the field data. This model assumes isotope removal from a closed pool of nitrate with constant isotopic fractionation. Hence:

$$\delta^{15}N\text{-}NO_3^-{}_{(f)} = \delta^{15}N\text{-}NO_3^-{}_{(f=1)} - \varepsilon^* \times \ln(f), \qquad (2)$$

where f is the fraction of consumed NO_3^-, $f = [NO_3^-]/(16\times[PO_4^{3-}])$, the ε^* is an "apparent" fractionation factor, in this case for a nitrogen removal process.

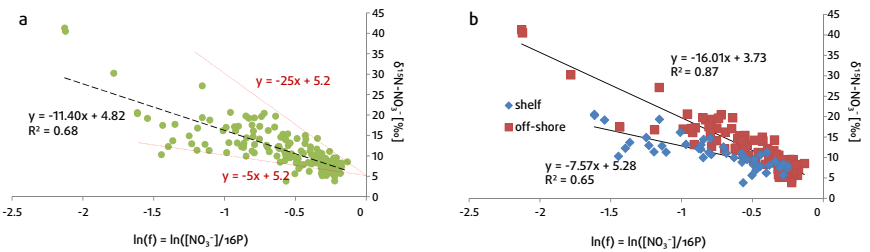

Fig. 3.10. (a) Application of Rayleigh model to assess fractionation in the Pacific OMZ for all waters with $[O_2] < 50$ µmol/l. Dashed lines indicate relationships calculated for $\varepsilon_d = 5$ and 25‰. The average calculated or "apparent" fractionation factor for the entire region is 11.4‰. (b) Apparent fractionation factors calculated separately for shelf (stations shallower then 200 m) and offshore (stations deeper then 200 m) stations. The shelf stations show a lower apparent fractionation factor of 7.6‰, while the value for off-shore stations is 16.0‰.

Least squares fitting of all data from the Pacific OMZ (i.e. $[O_2] < 50$ µmol/l) is shown in Figure 3.10a, with the "apparent" isotopic enrichment factor (ε^*) estimated to be

+11.4‰ (standard error of the fit is 0.7, Fig. 3.10). The data are scattered between relationships defined by ε* = 5 and 25 ‰ (assuming a common initial value for $\delta^{15}N_{initial}$ of 5.2‰). This value of ε* of +11.5‰ is significantly lower than values estimated from data from the Eastern Tropical North Pacific (22.5 – 30‰) and Arabian Sea (22-25‰) (Brandes, et al., 1998, Sigman, et al., 2003, Voss, et al., 2001) and from denitrifier cultures (28.6‰) (Barford, et al., 1999). However the value lies close to a values determined 30 years ago for 2 stations off southern Peru using much less sensitive analytical techniques (13.8‰) (Liu, 1979)

Separating data for shelf and offshore stations (Fig. 3.10b) results in fits with significantly different values of ε* of 7.6‰ and 16.0‰, respectively. Similar observations have been made in Santa Barbara Basin as compared to the open etnp (Sigman, et al., 2003). This was attributed to a larger contribution from sedimentary denitrification input into the water column in the Basin, which has significantly smaller fractionation effect of ~1.5‰ due to control of overall NO_3^- removal rate by transport through the sediments (Brandes, et al., 2002)

In marked contrast to the Pacific study region, most $\delta^{15}N\text{-}NO_3^-$ values from the Atlantic (Fig. 3.8b) stay close to the ocean average value of 5.2‰ (Table 1, (Sigman, et al., 2009b)). In part this can be explained by the absence of significant fixed-N removal in this region. Notable also was the complete absence of any trend towards higher values associated with partial nitrate utilization in fully-oxygenated, near-surface waters on the M80 samples (stations south to Cape Verde). Significant increases of $\delta^{15}N$ (up to 12‰) in surface waters were only observed at shallow stations very close to the African coast (data from L'Atalante cruise in 2008, not shown) that are likely associated with partial phytoplankton uptake of upwelled NO_3^-.

Decreasing values of $\delta^{15}N$ of din towards the surface have been reported previously for Monterey Bay (Wankel, et al., 2007), and for near-surface samples collected close to the Azores Front (30 – 35°N) (Bourbonnais, et al., 2009) and at Bermuda (Knapp, et al., 2010). The lowest values published from this general region (Bourbonnais, et al., 2009) were ~3.5‰ at a depth of 100 m. Our data indicate very similar values at this depth. The relatively low values of 3.5‰ were attributed by Bourbonnais et al (2009) to the effects of nitrogen fixation, which can result in remineralised din with typical values of -1‰ (-2‰ to +2‰) (Carpenter et al., 1997, 1999; Montoya et al., 2002). The strongly negative $\delta^{15}N$ values measured in surface waters south of Cape Verde (e.g. down to -5.5‰, Fig. 3.5) have not been

observed before in oceanic surface waters and cannot be explained by ammonification and nitrification of organic nitrogen produced by nitrogen fixers. On the other hand, very low values of $\delta^{15}N$ (~ -7‰) of aerosol nitrate have been measured in samples of atmospheric dust from this region (Baker, et al., 2007, Morin, et al., 2009). Similarly low, negative values have been measured in samples of atmospheric dust originating in the Sahara that were collected from the eastern Mediterranean (Wankel, et al., 2010). Recent work (Knapp, et al., 2010) shows that the wet deposition flux of fixed-N at Bermuda can be comparable to estimates of biological N_2 fixation rates in surface waters. The $\delta^{15}N\text{-}NO_3^-$ in wet deposition at Bermuda was significantly lower (-4.5‰) then $\delta^{15}N$ added by oceanic N_2 fixation (-2 to 0‰) (Hastings, et al., 2003, Knapp, et al., 2010). For our study region, dry deposition of dust from the Sahara is likely to dominate the N-flux (Duarte, et al., 2006).

The N-flux due to diapycnal mixing of NO_3^- from below in this region has been estimated to be 140 μmol/m²/day and was statistically indistinguishable from the integrated rate of nitrate assimilation (Lewis, et al., 1986). Later calculations come to values of about 7 mg N m^{-2} d^{-1} (or ~500 μmol/m²/day) (Bourbonnais, et al., 2009, Klein, et al., 1995). According to Baker et al. (2007) the dry deposition N flux of soluble aerosol at 20°W in the Atlantic ocean is 80 – 120 μmol/m²/day, while wet deposition is 50 – 70 μmol/m²/day. In an earlier article (Baker, et al., 2003), however, the dry deposition N flux was significantly lower (~20 μmol/m²/day), which emphasizes that the flux can be highly variable. Duarte (2006), for example, estimated a dry deposition N flux of 280 ± 70 μmol/m²/day in tropical Atlantic region, which is significantly higher than the diapycnal flux. This deposition flux is sufficient to supply the observed DIN inventory of the top 20 m (0.2 μmol/l) within two weeks. The most negative $\delta^{15}N$ values in surface water were observed at stations south of the Cape Verde Islands, which is also the region with the highest Saharan dust deposition (Schepanski, et al., 2009, Tanaka, et al., 2006). A few days before our samples were collected on M80, an intensive dust event took place, and this may have influenced the $\delta^{15}N$ values observed. Satellite imagery from November and December 2009 are shown in Figure 3.11 and indicate a significant dust event in the region over the period immediately prior to our samples being collected (between 26th November and 12th December 2009).

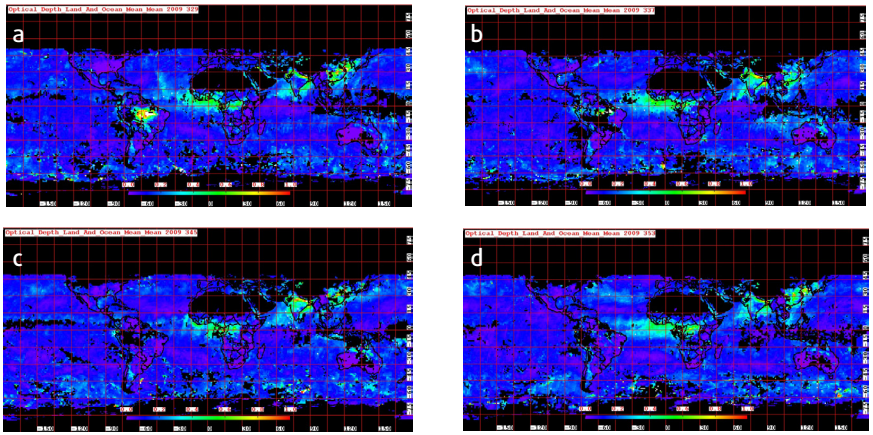

Fig. 3.11. Satellite images of Aerosol Optical Depth at different time periods of 2009: a)25 Oct–2 Dec; b)3 Dec–10 Dec; c)11 Dec–18 Dec; d)19 Dec–26 Dec. (http://ladsweb.nascom.nasa.gov/browse_images/l3_browser.html)

Under these conditions, the nitrogen loading to the surface layer cannot be considered to be in a steady state. We therefore examined extreme scenarios with dry deposition N flux dominating and for balance with diapycnal mixing and assimilation (table 2). In the first scenario, 90% of total nitrogen originates from dust deposition with initial $\delta^{15}N$ values of -7‰, and only 10% are coming from diapycnal mixing from the underlying waters with $\delta^{15}N$ values of +5‰. This scenario results in $\delta^{15}N$ value of -5.8‰, very close to observations. The second scenario assumes equal contribution from those two nitrogen sources, while third includes the assimilation process as nitrogen sink with +5‰ isotopic effect. This isotopic effect would be relevant, however, only when $f = [NO_3^-]_{obs}/[NO_3^-]_{initial}$ is close to 1, which is not usually the case in the open ocean. Both scenarios increase resulting $\delta^{15}N$ value (Table 3.2).

Predicted surface water $\delta^{15}N\text{-}NO_3^-$ under different scenarios. $F_{total} = F_{dustx} + F_{mixing} + F_{assimilation}$. The end members for $\delta^{15}N$ surface water calculation were: $\delta^{15}N$-dust = -7‰, $\delta^{15}N$-mixing =5‰ and $\delta^{15}N$-assimilation = 5‰.

Scenario	$\delta^{15}N\text{-}NO_3^-$ surface water	F_{dust}/F_{total} [%]	F_{mixing}/F_{total} [%]	$F_{assimilation}/F_{total}$ [%]
I	-5.8	90	10	0
II	-1	50	50	0
III	1	33%	33%	33%

These scenarios do not take into consideration an isotopic signal from N_2 fixation. They do show, however, that under non-steady state conditions, such as shortly after dust deposition events, the $\delta^{15}N$ for NO_3^- in surface waters can decrease to -5.8‰. Thus, atmospheric dust N deposition should be taken into account, together with the oceanic N_2 fixation, in explaining the low $\delta^{15}N\text{-}NO_3^-$ pool observed in subtropical thermoclines (Brandes, et al., 1998, Karl, et al., 2002, Knapp, et al., 2005, Wannicke, et al., 2010).

3.5. Summary and conclusions.

In this paper we have presented an extensive amount of new data for nitrogen isotope and key nitrogen species, such as N_2O, collected from OMZ regions in the NE Atlantic and SE Pacific. These regions have strongly contrasting O_2 concentrations and N-cycling processes. Measurements with near identical techniques in both oceans, reveal that whereas deep waters (> 2000 m) share near-identical values of $\delta^{15}N\text{-}DIN$ (5.3 ± 0.4 ‰), there are significant to major differences between the two OMZ's in both surface and intermediate waters. The same AAIW water mass, for instance, has in the Pacific $\delta^{15}N\text{-}DIN$ average value of 6.7 ± 0.8 ‰ and in the Atlantic of 5.5 ± 0.6 ‰ (table 1). Strongest differences in $\delta^{15}N\text{-}DIN$ in the two study regions are located in depth 100 – 500 m in the OMZ's. In the Pacific $\delta^{15}N$ values tend towards strongly positive values as a result of N-loss processes within the OMZ and partial NO_3^- utilization in surface waters, while in the Atlantic the values stay close to ~5.4‰ on average.

Co-located measurements of N_2O and stable N-isotopes in waters with $[O_2] < \sim 5$ µmol/l reveal a clear signal of canonical denitrification, although its quantitative significance for overall N-loss, relative to anammox, cannot be assessed. The correlations of N_2O with $\delta^{15}N\text{-}DIN$ and AOU for waters with $[O_2] > 50$ µmol/l are similar in both OMZ's, reflecting similar sources of N_2O via nitrification. However waters with $5 < [O_2] < 50$ µmol/l in the Pacific exhibit correlations that are suggestive of a 50% higher relative N_2O yield, that may be associated with nitrification by AOA (Löscher, et al., 2011).

Whereas $\delta^{15}N\text{-}NO_3^-$ values in surface waters of the Pacific OMZ region are strongly positive, being controlled by partial nutrient utilization and a ^{15}N-enriched NO_3^- supply affected by subsurface denitrification, the oligotrophic surface waters south

of Cape Verde in the Atlantic exhibit negative values of $\delta^{15}N$ (-5 to +2 ‰). The negative values are too low to be explained by N-fixation and we show that they are most likely the result of a transient input of NO_3^- associated with atmospheric deposition of Saharan dust. This implies that atmospheric dust input as well as nitrogen fixation should be considered in budgets and explanations of upper ocean stable N isotope data, especially in the Atlantic region.

Within the Pacific oMz, correlation of $\delta^{15}N$ with measures of N-loss gives a calculated apparent fractionation factor for $\delta^{15}N\text{-}NO_3^-$ ($\varepsilon_d = 11.4 \pm 0.3$ ‰) which is low compared to canonical values, but close to a value estimated by the only prior study in this region (Liu, 1979). Sub-division of the data into shelf and offshore stations resulted in improved correlations and very different apparent fractionation factors for the two depth-regimes ($\varepsilon_{d\text{-offshore}} = 16 \pm 0.5$‰; $\varepsilon_{d\text{-shelf}} = 7.6 \pm 0.6$‰). Whereas the offshore value lies close to the ~20‰ fractionation factor of denitrification (Brandes, et al., 1998, Granger, et al., 2008), the much lower apparent fractionation factor for shelf waters likely reflects a larger contribution from sedimentary denitrification (fractionation factor of 1.5‰; (Brandes, et al., 2002). We note that the fractionation effect from the complete set of stations ($\varepsilon_d = 11.4 \pm 0.3$‰) lies reasonably close to an apparent global fractionation factor for oMz denitrification of 12‰ which was calculated for a steady state 50:50 balance between water column and sedimentary denitrification (Altabet, 2007).

4
Nitrogen isotope gradients off Peru and Ecuador related to upwelling, productivity, nutrient uptake and oxygen deficiency

Abstract

We present new results from surface sediments collected along the Peruvian margin between 1°N and 17°S. Bulk sediment organic carbon, total nitrogen, biogenic opal, C37 alkenone concentrations and $\delta^{15}N_{sed}$ were measured at more than 60 locations within and below the present-day Peruvian OMZ. Modern biological production and NO_3^- uptake is maximal between 10°S and 15°S, the current position of local and perennial upwelling cells. Due to strong oxygen minimum conditions, local denitrification also reaches maximal intensity resulting in the highest surface-sediment and water-column nitrate $\delta^{15}N$ values observed in our study. Within OMZ's occurred denitrification, which is an O_2 sensitive process and increases the $\delta^{15}N$ of residual dissolved NO_3^-. The sediment data set ($\delta^{15}N_{sed}$) is compared to $\delta^{15}NO_3^-$ in the overlying water column in order to better understand how the regional oceanography transfers the water column $\delta^{15}N$ signal to the core-top. The high $\delta^{15}N$ values south of 10°S contrast with much lower values from the northern part of our study area (1°N – 10°S), associated with less intense export production and nitrate uptake, together with a diminished OMZ. Our mapping effort provides a baseline for further down core studies to reconstruct past changes in the Peruvian OMZ dynamics over the Holocene and its relationship to regional oceanography and global climate change.

This chapter is an adapted draft version of

Elfi Mollier-Vogel, Evgenia Ryabenko, Philippe Martinez, Douglas Wallace, Mark Altabet, Ralph Schneider: Nitrogen isotope gradients off Peru and Ecuador related to upwelling, productivity, nutrient uptake and oxygen deficiency.

4.1. Introduction

The Humboldt Current System in the Eastern South Pacific is one of the most productive ecosystem in the world ocean, with permanent or seasonal upwelling cells along the coasts of Peru and Chile (Pennington, et al., 2006). It is also very sensitive to enso events which cause significant changes of the physical, chemical and biogeochemical environment (Barber and Chavez, 1986, Huyer, et al., 1987). This oceanographic system is characterized by large exchanges of heat and CO_2 between the ocean and the atmosphere because of the upwelling of cold, nutrient rich and CO_2 saturated subsurface waters. Associated with this current system, a zone of shallow oxygen minimum zone (omz) is present and extends far offshore, as the result of the interplay between high export production, weak ventilation and sub-surface circulation. Off Peru where the omz is the most intense, the oxygen content ranges from saturated values at the surface to values lower than 10 μmol/l at very shallow water depths (< 50 m), and reaching less than 1 μmol/l at its core (Karstensen, et al., 2008, Paulmier and Ruiz-Pino, 2009). On average, this omz is located between 30 – 70 m and 300 – 400 m.

The omz is associated with processes of water column denitrification when dissolved oxygen concentrations are sufficiently low (O_2 concentrations below 2-10 μmol/l; (Codispoti, et al., 2005)). In such conditions, nitrate will be used as an oxidant during the degradation of the organic matter, leading to the loss of bioavailable nitrogen in the global ocean and the production and efflux of greenhouse gases such as CO_2 to the atmosphere. Water column denitrification process lead to isotopically heavy sedimentary $\delta^{15}N$ values because denitrification occurs with a large isotopic fractionation, producing isotopically light N_2 that can be largely lost to the atmosphere, and isotopically heavy residual nitrate (Cline and Kaplan, 1975, Liu and Kaplan, 1989). Supply of some of this nitrate to surface waters by upwelling and its utilization by plankton can then enrich the particulate organic matter in the heavy isotope and finally the organic matter buried in the sediments (Cline and Kaplan, 1975, Liu and Kaplan, 1989, Saino and Hattori, 1987).

Following these findings, and using sedimentary $\delta^{15}N$ records as a tool to reconstruct past water-column denitrification, several studies have shown that the omz's of the global ocean varied in response to climate fluctuations on millennial and glacial-interglacial time-scales over the last thousands of years (Altabet, et al., 1995, 2002, De Pol-Holz, et al., 2006, 2007, Ganeshram, et al., 2000, Ganeshram, et

al., 1995, Hendy, et al., 2004, Martinez and Robinson, 2010, Pichevin, et al., 2007, Pride, et al., 1999, Robinson, et al., 2007). All these studies have shown that cold climatic intervals were characterized by a contraction of the OMZ, and warm climatic intervals experienced an expansion of the OMZ. Many mechanisms have been proposed as candidates for explaining this variability, such as local and remote changes in oxygen demand and/or oxygen supply from the high latitudes (Galbraith, et al., 2004, Ganeshram, et al., 2000, Hendy and Pedersen, 2006, Martinez and Robinson, 2010, Meissner, et al., 2005).

In addition to the intensification of denitrification, many other factors influence sedimentary $\delta^{15}N$, such as nitrate utilization, remineralization and diagenesis and potentially control or alter the isotopic signature of organic matter (OM) as it is produced, exported to the deep sea, and buried in the sediments. The isotopic signature of plankton and OM is firstly controlled by the degree of nutrient uptake. Phytoplankton preferentially takes up NO_3^- containing the lighter nitrogen isotope ($^{14}NO_3^-$) during photosynthesis and thus becomes depleted in ^{15}N relative to the nitrogen substrate (Cline and Kaplan, 1975, Wada and Hattori, 1978). Thus, a low relative utilization of NO_3^- will tend to drive the OM signal toward light values, whereas an increase in nutrient utilization will tend to drive the signal toward ^{15}N-enriched values leading to low or high $\delta^{15}N$ in particulate OM, depending on intensity of utilization (Altabet and Francois, 1994, Freudenthal, et al., 2001).

Utilization process can significantly mash or even hide the signature of water colum denitrification in areas characterized both by a strong OMZ at subsurface and incomplete nitrate utilization at the sea-surface (Farrell, et al., 1995). The purpose of the present study is to investigate the main process and examine the robustness of $\delta^{15}N$ proxy for further paleoclimatic and paleoceanographic reconstructions. We present here nitrogen isotopic data from both water column and surface sediment, along with several other proxies related to export production (C_{org}, %N, Opal, [Alk]), off the entire Peruvian and Ecuadorian OMZ. This data set compliment very well to previously published work along Chile margin (De Pol-Holz, et al., 2009), where the data only reached as far north as to 21°S.

4.2. Regional setting

The area presented in this study is situated in the Peruvian-Ecuadorian margin, from 1°N to 17°S. Peruvian Coastal Upwelling (PCU) well developed between 4°S and 15°S is by far the richest in the world in terms of chlorophyll a concentration and biomass, up to 100 km offshore (Chavez and Barber, 1987, Chavez and Messié, 2009, Echevin, et al., 2008, Pennington, et al., 2006). The upwelled waters are derived from the first ~50 m of the water column during periods of moderate upwelling and from ~200 m depth during periods of strong upwelling (Strub, et al., 1998). Between 12° – 15°S, the shelf becomes narrower inducing stronger upwellings (Echevin, et al., 2004, Strub, et al., 1998), which are not a continuous band from North to South but more similar to active cells spread near shore along the margin (Echevin, et al., 2004). Some of these are also perennial and located particularly around 7° – 8°S, 11° – 12°S and 14° – 16°S (Strub, et al., 1998, Suess, et al., 1987).

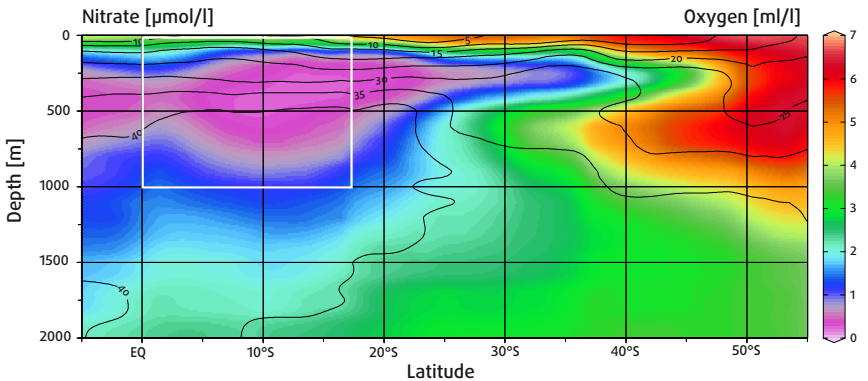

Fig. 4.1. Latitudinal distribution of oxygen (color code) and nitrate concentration (contours) along the South American coast, average values on 300 km width from the coast (woa05). The white rectangle shows the study area.

The PCU is strongly seasonal and reaches its maximum intensity during austral winter (Jun-Jul-Aug) (Echevin, et al., 2008, Strub, et al., 1998). Strong winds and turbulence within the mixed layer decreases the luminosity and prevents photosynthesis of the organisms (Messié, et al., 2009, Pennington, et al., 2006) during the season. Thus, highest levels of chlorophyll *a*, associated to primary production, occur in austral summer, in anti phase to the upwelling season (Chavez, et

al., 1996, Echevin, et al., 2008). As a result of sinking and decay of surface-derived primary production and in addition to the poor ventilation, surface oxygenated waters overlie an intense and extremely shallow omz (Chavez, et al., 2008). The maximum productivity and seasonal variability take place between 8 – 15°S (Fig. 4.3b), where the core of the omz is the most extended (Fig. 4.1).

Offshore, strong winds coming from the South push the surface waters to the West, North-West (Humbolt Current, hc). On the contrary, equatorial waters, Equatorial Under Current (euc) and Subtropical Surface Water (stsw), are pulled to the surface along the coast and feed coastal upwelling cells during the intense season (Wyrtki, 1981). euc southward-flowing from the equator up to 5°S has low salinity (S < 34 psu), is well-oxygenated and nutrient rich. Further South, from 5°S to 20°S, stsw is saltier (S > 35 psu), more oxygen depleted, nutrient rich and extends from the surface down to 500 m depth (Fig. 4.1).

These nutrient rich waters, when upwelled, involve large primary production and consequently enhance omz, which the core (< 5 μmol/l) extended from 8°S to 17°S with at 50 to 700 m depth (Fig. 4.1). Below 500 m, the Antarctic Intermediate Water (aaiw) coming from the South and sinking under the stsw around 20°S, is fresher (S < 34.5 psu), better oxygenated but poorer in nitrate (Fig. 4.1) (Lavín, et al., 2006).

4.3. Sampling and analytical methods

The physical, chemical, and biological dynamics of the Peru omz were studied in a series of cruises carried out as part of the Climate - Biogeochemistry Interactions in the Tropical Ocean program of the German-Research Foundation (www.sfb-754.de). Surface sediments were collected during cruises aboard the research vessel Meteor (M77 legs 1 and 2, 2008). The study area extended from 1°N to 17°S and covered the Ecuadorian and Peruvian margin with 57 stations along the coast, between 60 m and 2080 m depth (Fig. 4.2). This sampling enabled construction of latitudinal and a longitudinal transects. At each of these stations, 6 multicores (1 m each) were retrieved. An additional set of 13 samples from imarpe (Instituto Del Mar del Perù, Lima), located between 5°S and 14°S, were also analysed and included into this study.

Water samples were also collected on 77 stations during the 3rd and 4th Legs of M77 cruise onboard the R/V Meteor (Fig. 4.2), using 12 l Niskin bottles on a ctd rosette

system equipped with oxygen sensors. Nutrients and oxygen concentrations were determined according to the method of (Grasshoff, et al., 1983). Samples for the measurement of $\delta^{15}N$ of nitrates were collected into 100 ml plastic bottles. Samples containing nitrite concentration below 0.1 µmol/l were acidified with 0.5 ml of 25% HCl, otherwise samples were kept frozen until analysis.

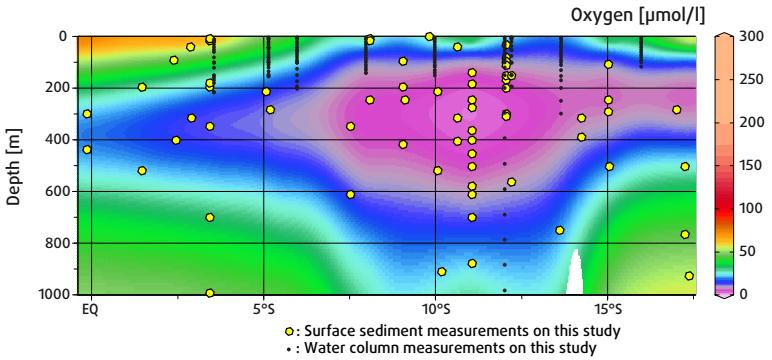

Fig. 4.2. Latitudal distribution of oxygen concentration (color code) along the Peruvian margin. Black dots represent water samples measured; yellow ones stand for surface sediment samples.

Nitrogen isotope ratios ($\delta^{15}N_{sed}$,‰) and total nitrogen content (%N, wt %) were measured on ~5 to 60 mg of homogenized and dried bulk sediment, using a Carlo-Erba CN analyser 2500 interfaced directly to a Micromass-Isoprime spectrometer. The precision of the isotopic analyses based on repeated measurements of some surface sediment samples as well as routine international and in-house standards measurements is ± 0.23‰ (Martinez and Robinson, 2010). Organic carbon (C_{org}, wt %) measurements were carried out using a LECO C-S 125 analyzer after treatment of ~80 – 100 mg of sediment with hydrochloric acid to remove calcium carbonate, with precision on repeated measurements better than ± 0.5%. The isotopic composition of dissolved nitrate and nitrite was measured using Cd-reduction method with NaCl addition as described by (Ryabenko, et al., 2009) in Germany (ifm-geomar) and in USA (smast) with the precision of the $\delta^{15}N$ values being ± 0.2‰ (Ryabenko, et al., 2009). Alkenones were extracted from 0.5 g freeze-dried and homogenized sediment samples using accelerator solvent extraction (Dionex ase) prior to analysis of the C_{37} group by a double column multidimensional gas chromatograph (Agilent 6890N). Using the commonly accepted $U^{k'}_{37}$ index, SSTs

were calculated using global calibration (Müller, et al., 1998, Müller and Schneider, 1993). Standard deviation based on repeated measurements on sediment samples, was ± 0.29‰, and standard deviation based on sediment reference standards was ± 0.3‰. Biogenic opal was measured on 20 mg of freeze-dried and homogenized bulk sediment by using an automated extraction method and wet chemical leaching as described in (Müller and Schneider, 1993). Standard deviation based on repeated measurements was ± 0.5%.

4.4. Results

4.4.1. Surface sediments: $\delta^{15}N$ and export production proxies

The surface sediment $\delta^{15}N_{sed}$ data along the margin can be separated into northern (1°N to 8°S) and southern (8°S – 17°S) groups (Fig. 4.3a). In the North, $\delta^{15}N_{sed}$ values are light, stable (4 – 5.2‰.) In the southern part the values increase southward from 4.5‰ to 10‰ and present a greater scatter. The North-South gradient is not a monotonic function of the latitude and highest values, ± 10‰, are located near shore at 12°S, 15°S and 17°S.

Proxies of export production show the same latitudinal and cross-shelf trends as $\delta^{15}N_{sed}$. Organic carbon (C_{org}) values vary between 0.3% and 3% of the sediment in the north and between 2.2% and 15.6% in the southern part (Fig. 4.3b). Highest nitrogen content (%N) values are located between 8°S and 15°S, ranging from 0.2% to 1.7% and decrease to the North and the South of this area (Fig. 4.3b). Opal (SiO_2) data show highest values, from 1% to 21%, between 10°S and 15°S and lower values ranging between 1.5% and 11.5%, North and South of this area. Alkenones content ([Alk]) values show the same trend as the other export productivity proxies, with higher values from 1 ng/g to 50 ng/g between 10°S and 15°S. North and South of this area values are lower ranging between 1 ng/g and 20.5 ng/g (Fig. 4.3b). Organic matter $\delta^{13}C$ and C/N ratio are stable all along the Peruvian margin with values respectively equal to ~ -21‰ and ~6 – 11 (Fig. 4.3c).

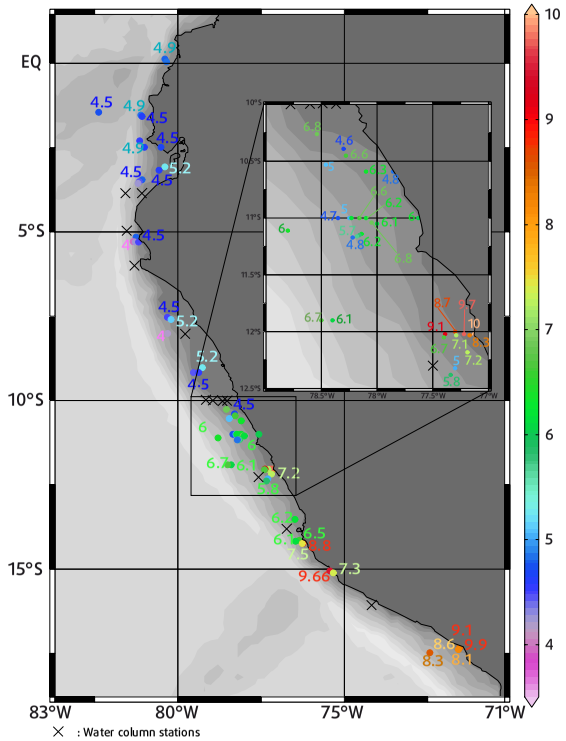

Fig. 4.3. a) Surface sediment $\delta^{15}N$ values and water column station positions along the Ecuadorian and Peruvian margin. Gray shading is the topography of the bottom. On the right side is the color scale for the $\delta^{15}N$ data of the map and the zoom area. (Data are available in the Pangaea database).

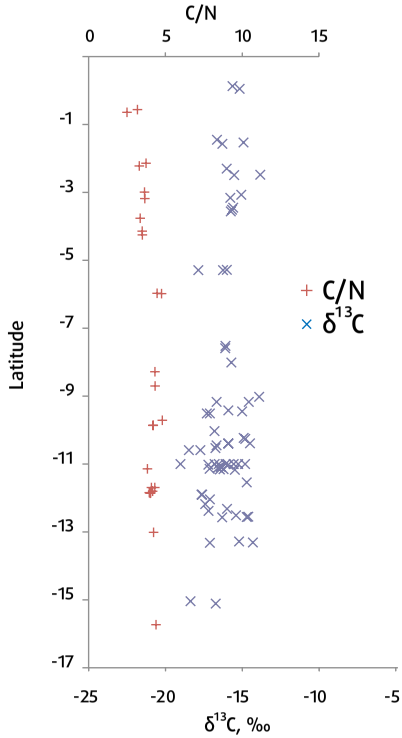

Fig. 4.3. b) C/N ratio (blue cross) and $\delta^{13}C$ data (red stars) along the Peruvian margin.

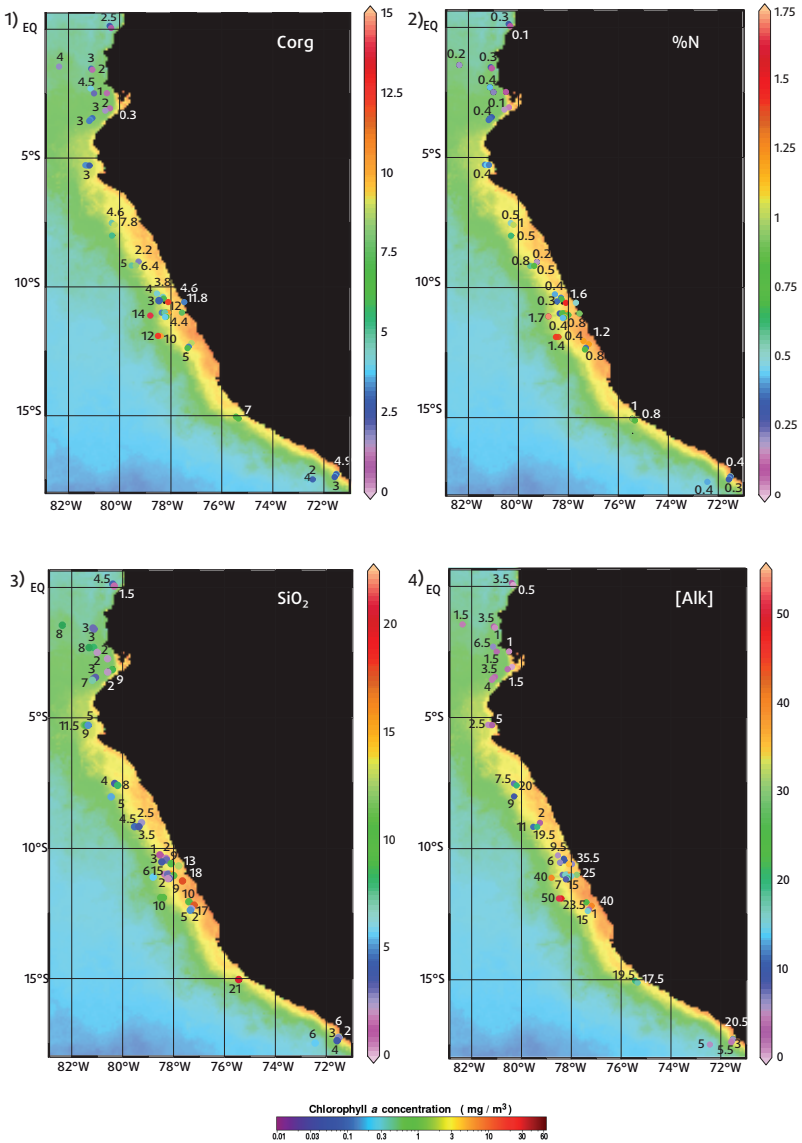

Fig. 4.3. c) Distribution of paleoproductivity proxies in the sediment sampled during the METEOR cruise (2008) along the Ecuadorian-Peruvian coast. 1) Organic carbon C_{org}, 2) Nitrogen content % N, 3) Opal SiO_2, 4) Alkenones content [Alk]. The background represents chlorophyll a concentrations averaged during austral summers from 2003 until 2010. (cf. http://oceancolor.gsfc.nasa.gov/cgi/l3).

4.4.2. Oxygen, nutrients and $\delta^{15}N$ water column distribution

In spite of the water column data being a seasonal snapshot, it was sampled during the austral summer, the season of highest primary production and therefore it should be the representative of the sediment OM. At 8°S we observe an intensification of OMZ, which seems to change the nitrogen cycle in the water column. Figure 4.4a shows water column properties in three stations along Peruvian coast: at 3.5°S, 10°S and 17°S. Oxygen concentrations show the transition from a relatively weak OMZ in the Equatorial region ($[O_2] > 20$ μmol/l) to a well developed and broad OM OMZ Z South of 8°S ($[O_2] < 5$ μmol/l) (Fig. 4.2 and 4.4a). Decreasing oxygen concentrations trigger N-loss processes, which are reflected in nitrate and $\delta^{15}N$ profiles. In the northern stations NO_3^- stay stable below the oxycline at about 25 μmol/l ,while in the southern stations NO_3^- concentrations decrease in the OMZ (Fig. 4.4a) . Nitrogen isotope distribution in the water column show similar transition from stable values of ~5‰ (close to ocean average) in the northern stations to high values of ~20‰ in the southern stations. $\delta^{15}N$ distribution in the sea-surface waters, and surface sediments, shown in figure 4.4b. Water column $\delta^{15}N$ data from upper 200 m are presented in box-whisker plot, with 25% of lowest and highest data cut off the box and mean values marked with black dots in the box. Such a data presentation allows us to evaluate the change of scatter and of mean values along the Peruvian coast. North to 8°S both $\delta^{15}N_{sed}$ and $\delta^{15}N_{water\ column}$ have low scatter and does not seem to change much with latitude. Water column $\delta^{15}N$ values are few per mil higher than in the sediments. This offset could be explained by nitrate utilization, leading to higher $\delta^{15}N$ values in the water and lower $\delta^{15}N$ in the OM produced (see below). South to ~8°S both $\delta^{15}N_{sed}$ and $\delta^{15}N_{water\ column}$ increase in their values and variability. The water column $\delta^{15}N$ increase is caused by N-loss processes in the OMZ, while increase in $\delta^{15}N_{sed}$ values can be caused by various processes, which are discussed below.

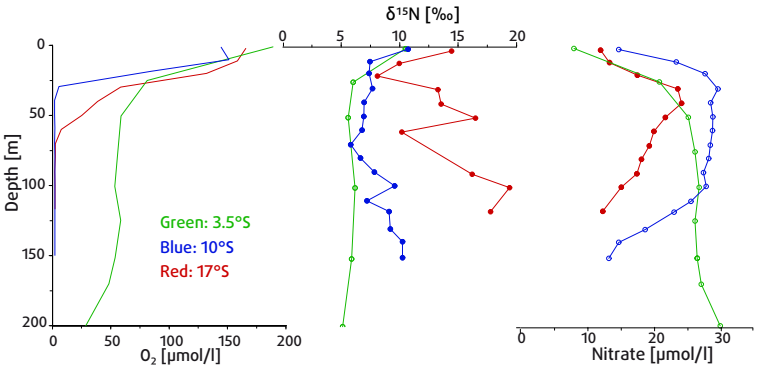

Fig. 4.4. a) Water column distribution of oxygen, $\delta^{15}NO_3^-$ and NO_3^- concentrations at for three stations, 5°S, 10°S and 17°S.

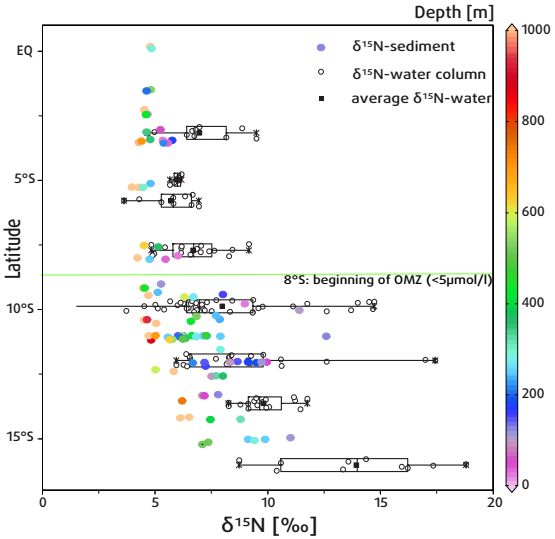

Fig. 4.4. b) Latitudal distribution of $\delta^{15}N_{sed}$ (colored dots) and $\delta^{15}NO_3^-$ in upper 200 m in whisker box, showing statistical distribution of the water column data. Color scale represents sediment sample depths. Water column data presented in box-and-whisker plot. The box cuts off 25% of lowest and highest data set with mean values marked as black dots in the center of the box.

4.5. Discussion

4.5.1. Latitudal distribution of $\delta^{15}N$

The inorganic nitrogen (mainly ammonium) component in the sediments is assumed to be negligible compared to the organic nitrogen. The sedimentary organic matter of Peru and Ecuador might include a contribution of continental-derived (terrestrial) organic matter, especially in the northern part of the studied area. In general, terrestrial organic matter is characterized by low $\delta^{13}C_{org}$ (2 – 3‰) and high C/N ratios (> 20), whereas marine organic matter has typical $\delta^{13}C_{org}$ values of -19 to -22‰ and C/N ratios close to the Redfield ratio of 6 – 7 (Emerson and Hedges, 1988, Hebbeln, 1992, Jasper and Gagosian, 1989, Meyer, 1997, Peters, et al., 1978, Schubert and Calvert, 2001). Along the Peruvian and Ecuadorian margins, C/N ratios ranges between 6 – 11 and $\delta^{13}C_{org}$ between -21 and -22‰ indicating that organic matter is likely to be of marine planctonic origin (Fig. 4.3c).

It is also possible that the degree of alteration of organic matter during settling through the water column and burial within the sediment may alter the $\delta^{15}N_{sed}$signal up to several per mil. For example, some studies have shown an enrichment in ^{14}N with water depth in sinking particles, others have found the opposite (Altabet, 2001, Altabet and Francois, 1994, Altabet and McCarthy, 1985). Yet, these studies have shown that this water column degradation effect is smaller in continental margin settings. During remineralization in the water column, organisms preferentially use light isotope (^{14}N) (Altabet, et al., 1999b, Holmes, et al., 1998). As a result, particles in off-shore locations stay longer in the water column and $\delta^{15}N$ signal in the sediment. We observe $\delta^{15}N_{sed}$ values off shre to be slightly lighter than inshore $\delta^{15}N_{sed}$ values (Fig. 4.3a). Therefore, remineralization could not explain observed the decrease of $\delta^{15}N_{sed}$ with the depth from our study.

Diagenesis can alter the primary signal of $\delta^{15}N_{sed}$ via dissolution-crystallization related and redox processes (Froelich, et al., 1979, Martinez, et al., 2000). However, a Peruvian coast environmental setting is similar to those off North-West Africa and Mexico, where no change in downcore $\delta^{15}N$ in the first 10 cm of sediment was observed (Ganeshram, et al., 1995, Martinez, et al., 2000). Hence, we assume that diagenesis does not affect $\delta^{15}N_{sed}$. Denitrification in the sediments, which can be associated wuth extremely low oxygen concentrations, also would not influence

on $\delta^{15}N_{sed}$ as the fractionation factor for this process is ~0‰ (Brandes and Devol, 1997, Lehmann, et al., 2007, Sigman, et al., 2003).

The source of latitudal change in $\delta^{15}N_{sed}$ is most likely associated with water column processes. The Peruvian omz is associated particularly with nitrogen loss processes: denitrification (Altabet, et al., 1999b, Brandes, et al., 2007, Gruber and Galloway, 2008, Lehmann, et al., 2007) and anammox (Dalsgaard, et al., 2003, Galan, et al., 2009, Kuypers, et al., 2005, Lam, et al., 2009, Thamdrup, et al., 2006). The relative importance of denitrification, the stepwise reduction process involving a number of intermediates ($NO_3^- \rightarrow NO_2^- \rightarrow NO \rightarrow N_2O \rightarrow N_2$), compared to anammox (a more direct process, $NO_2^- + NH_4^+ \rightarrow N_2$) is debated (Voss, 2009). The $\delta^{15}N_{water\ column}$ represents the isotopic composition in the nitrate and nitrite pool. The reduction of nitrate to nitrite is the first step of denitrification process and also is essential for anammox being the source of NO_2^- (Lam, et al., 2009). Thus, isotopic fractionation of nitrate reduction to nitrite is common for both N-loss process. $\delta^{15}N_{water\ column}$ omz shows the southward increase of $\delta^{15}N$ south of 8°S(Fig. 4.4a) correlating with oxygen decrease and the intensification of N-loss processes in the water column. In addition to N-loss processes in mid-depths, nitrate utilization can increase $\delta^{15}N$ values in surface waters (Granger, et al., 2004).

As long as nitrate utilization is not complete, an increase in nitrate utilization should involve an increase of the $\delta^{15}N\text{-}NO_3^-$ in the water column as well as in the $\delta^{15}N$-om and in the sediment. High nitrate availability along Peruvian coat leads to intensive utilization of it in the surface waters. The utilizing organisms use ambient nitrogen for organic matter formation, which is eventually buried in the sediments. According to sedimentation rates of our study area (Chazen, *et al.*, 2009, Rein, 2007) $\delta^{15}N_{sed}$ represents an integrated average of surface and subsurface water conditions over several years. In previous work the Equatorial Pacific data was modeled using the Rayleigh equation for instantaneous product (Altabet and Francois, 1994). The same approach is used here:

$$\delta^{15}NO_3^- = \delta^{15}NO_3^-_{initial} - \varepsilon_u \times \ln([NO_3^-]/[NO_3^-]_{initial}), \quad (1)$$

$$\delta^{15}N\text{-}PN = \delta^{15}NO_3^- - \varepsilon_u \quad (2)$$

The nitrate supply ($\delta^{15}NO_3^-_{initial}$) and isotope effect of nitrate uptake (ε_u) are the key parameters in the Rayleigh fractionation model. $[NO_3^-]_{initial}$ would be the nitrate concentration of newly upwelled water or, alternatively, the highest concentration

in the nitrocline. δ^{15}N-PN is the nitrogen isotopic signature of particulate nitrogen produced via utilization, which we assume eventually determine $\delta^{15}N_{sed}$.

Figure 4.5 shows the isotope effect of nitrate uptake (ε_u), given by the slope of the relation, which is very similar (3.80 and 3.85‰) in the north and south stations. High nitrate availability might explain ε_u being slightly lower than the 5 – 6‰, observed previously in the Pacific (Altabet, 2001, Holmes, et al., 1998, Waser, et al., 1998). The initial $\delta^{15}N\text{-}NO_3^-$ signal, given by the offset in the relation, is 5.2‰ in the north and is coming from upwelled waters from the deeper water column, which are close to the oceanic average of 5-6‰ (Sigman, et al., 2009a). In the south the $\delta^{15}N$ of initial NO_3^- rise up to 7.64‰. The increase of 2.44‰ is significant as it is about 64% of ε_u. This increase in the initial value of $\delta^{15}N\text{-}NO_3^-$ may reflect the N-loss processes in the water column discussed above. To determine how the surface ocean signals are translated to the sedimentary record along the Peru margin we calculated the theoretical $\delta^{15}N$ of the particles ($\delta^{15}N\text{-}PN$). Applying the equation (2) to calculate it, we found out that $\delta^{15}N\text{-}PN$ values rise from 4‰ at 6°S up to 12‰ at 16°S, which is in agreement with measured $\delta^{15}N_{sed}$ increase (Fig. 4.4b).

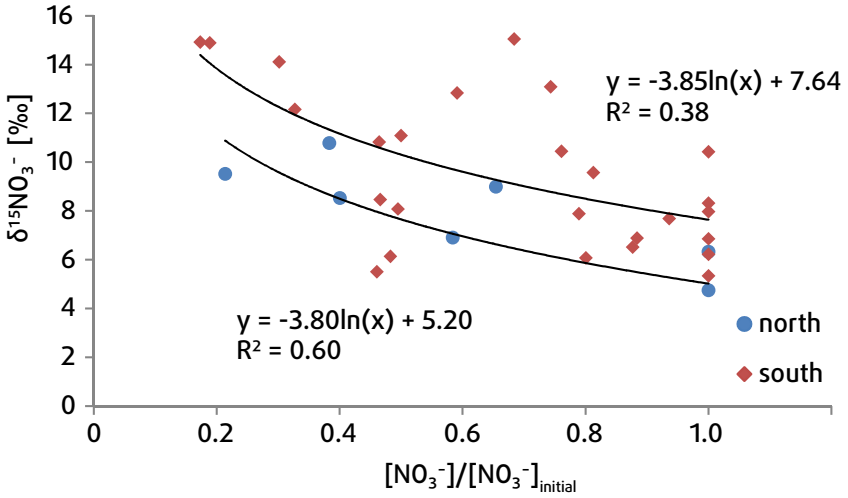

Fig. 4.5. $\delta^{15}N\text{-}NO_3^-$ vs. nitrate utilization in water column above the nitrocline.

4.6. Summary and conclusions

In this paper we have presented new data for surface sediments and the water column along the Peruvian coast, which complement very well previously published data along the Chile margin (De Pol-Holz, et al., 2009). $\delta^{15}N$ signal in the sediments along Peruvian margin correlates very well to water column nitrogen isotope distribution and the intensification of the OMZ from north (1°N) to south (18°S). We were able to show quantitatively that the latitudal increase of $\delta^{15}N$ signal in the surface waters, caused by denitrification process in the water column, is transported into the PN and sediments. This result is very important for future interpretations of the sedimental records in the region, showing the influence of the present day processes on the record in the sediments

5
Eddy Enhancement of Nitrogen-Loss from an Oceanic Oxygen Minimum Zone

Abstract

Microbially-mediated nitrogen (N) loss in intense oceanic O_2 minimum zones (OMZ) accounts for a large fraction of the global N sink and is an essential control on the ocean's N budget. However, major uncertainties exist regarding pathways and net impact on the magnitude of N-loss. Here we demonstrate the importance of coastal mesoscale eddies for enhancing N-loss in the Peru OMZ. Eddies transport productive, nutrient-rich coastal water offshore that stimulate subsurface ocean N-loss 'events' with extreme N isotope fractionation. The associated temporal/spatial heterogeneity of N-loss, mediated by a local succession of microbial processes, would explain inconsistencies observed among prior studies. Similar transient enhancements of N-loss likely occur within all other major OMZ's exerting a major influence on global ocean N and N isotope budgets.

This chapter is based on:

Mark A. Altabet, Evgenia Ryabenko, Lothar Stramma, Douglas Wallace, Martin Frank, Patricia Grasse, & Gaute Lavik: Eddy Enhancement of Nitrogen-Loss from an Oceanic Oxygen Minimum Zone.

Acknowledgements Enrique Montes aided in sample collection and Jen Larkum and Laura Bristow provided critical technical assistance. Funding to MAA was provided by the US Nation Science Foundation. Funding to ER, LS, DW, MF, PG and GL was provided by the Deutsche Forschungsgemeinschaft-supported project SFB754 (www.sfb754.de). The RV Meteor M77 Pacific cruise ship time was granted by the DFG. The crews and captain of "RV Meteor" are thanked for their help during cruises M77/3 and M77/4.

5.1. Introduction

In intense oceanic OMZ's, microbial processes rely on oxidants other than O_2 and include those that result in the production of N_2 gas from combined forms of N. These processes in sum account for a large portion of N-loss from the oceans (Codispoti, 2007). Key pathways include heterotrophic denitrification ($NO_3^- \rightarrow N_2$ via NO_2^-) and dissimilatory nitrate reduction to ammonia ($NO_3^- \rightarrow NH_4^+$ via NO_2^-) (Lam, et al., 2009) as well as the chemosynthetic anammox process ($NO_2^- + NH_4^+ \rightarrow N_2$) (Kuypers, et al., 2003, Thamdrup, et al., 2006). Recent studies vary widely in concluding whether heterotrophic denitrification or anommox is the dominant process for producing biogenic N_2 (Bulow, et al., 2010, Lam, et al., 2009, Ward, et al., 2009). Insufficient supply of NH_4^+ has been cited as a limitation on the relative importance of anammox (Koeve, et al., 2010) but dissimilatory nitrate reduction to ammonia has been detected as possible source via relatively abundant NO_3^-. In addition, N stable isotope effects produced by OMZ N-loss have been used to estimate their global contribution (the rest from microbial processes in sediments) but assuming heterotrophic denitrification as the only N-loss pathway (Brandes, et al., 2002).

To address these issues, relevant biogeochemical properties were mapped throughout the Peru OMZ in winter 2009. South of 7 to 10°S, O_2 concentrations in the upper Peru OMZ (σ_θ = 26.3, 100 to 170 m depth) were sufficiently low to enable N-loss processes (< 5 μmol kg^{-1}; Fig. 5.1a), similar to prior observations (Codispoti, et al., 1985). Southward intensification of the OMZ is associated with the poleward flow of the Peru Undercurrent (PUC) comprising the OMZ's core in this region (Strub, et al., 1987). Onset of dissimilatory NO_3^- reduction in the OMZ is marked by the appearance of NO_2^- in the OMZ, which is both an intermediate for heterotrophic denitrification and dissimilatory nitrate reduction to ammonia, as well as a substrate for anammox (Fig. 5.1b). For most of the open ocean portion of the Peru OMZ, maximal [NO_2^-] is < 5 μmol kg^{-1}. The corresponding negative N anomaly ($N' = NO_3^- + NO_2^- - 16 \times PO_4^{-3}$; see Suppl. Info) provides an estimate of N-loss to biogenic N_2 gas (Devol, et al., 2006) and has a similar geographic pattern (Fig. 5.1c).

Our biogeochemical maps reveal one offshore station (12°S 82°W, Station 7) with extreme N-loss indicators. Station 7 is characterized by strongly elevated [NO_2^-] and negative N′ (up to 9 and down to -35 μmol kg^{-1}, respectively; Fig. 5.2a) as compared to surrounding stations (Fig. 5.1). Although the maxima are relatively

shallow, these N-loss indicators extend broadly over the water column from 80 to 400 m depth. One other deep ocean station has signals of equally extreme N-loss (Station 29, 16°S 76° 27′W, Fig. 5.2a) but does not stand out as clearly in the property maps due to its proximity to the coast. N′ and [NO_2^-] sections at 12° and 16°S confirm Stations 7 and 29 to be distinct as compared to neighboring stations whereas the intervening section at 14°S shows no such offshore feature (Suppl. Info. Fig. 5.6).

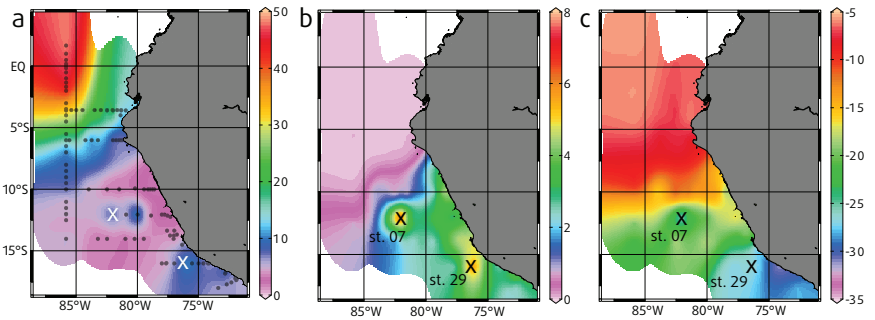

Fig. 5.1. Biogeochemical maps of the Peru OMZ from a series of stations constituting 6 transects normal and 1 transect parallel to the coast occupied during cruises M77/3 and M77/4 of the German research vessel "RV Meteor" in January and February of 2009. a) O_2 concentration (µmol kg^{-1}). b) NO_2^- concentration (µmol kg^{-1}) and c) Nitrogen anomaly – N′ (µmol kg^{-1}) calculated as [NO_3^-] + [NO_2^-] + [NH_4^+] – 16 × [PO_4^{-3}]. Properties are shown along a constant density surface (σ_θ = 26.3) within the upper portion of the OMZ corresponding to a depth range of 100 to 170 m. When southward intensification of O_2- poor conditions reaches [O_2] < 5 µmol kg^{-1}, the onset of N loss processes is evident. Station and transect locations discussed in text are as indicated.

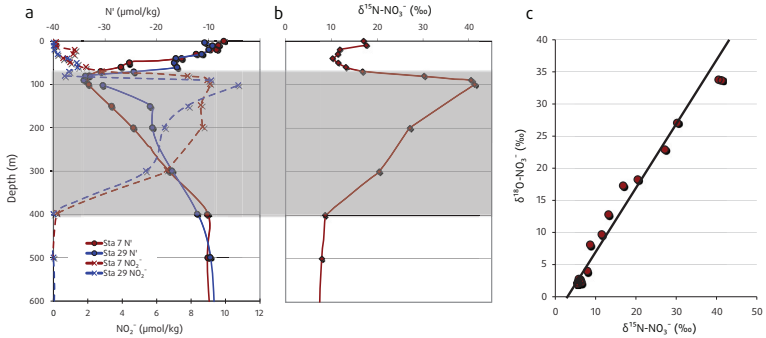

Fig. 5.2. Property vs depth profiles for stations 7 and 29 showing extreme values for N loss indicators. Oxycline indicated as a shaded depth interval. a) NO_2^- and N anomaly (N′) concentration profiles (µmol kg^{-1}) b) profiles for $\delta^{15}N\text{-}NO_3^-$ (‰ relative atmospheric N_2) for station 7. c) crossplot of $\delta^{18}O\text{-}NO_3^-$ vs $\delta^{15}N\text{-}NO_3^-$ for station 7.

Dissimilatory NO_3^- reduction to NO_2^- is the first biochemical step for heterotrophic denitrification and dissimilatory nitrate reduction to ammonia. It is known to produce strong N and O isotopic fractionation (Granger, et al., 2008) leaving residual NO_3^- isotopically enriched and the product NO_2^- depleted (Casciotti and McIlvin, 2007). Accordingly, the largest reported isotopic enrichments for OMZ NO_3^- (Altabet, et al., 1999a) were observed at Station 7 (Station 29 data not available) where $\delta^{15}N$ and $\delta^{18}O$ values reached 40 and 34‰ in comparison to oceanic averages of near 5 and 2‰, respectively (Sigman, et al., 2009b) (Fig. 5.2b). The dominance of NO_3^- reduction is evidenced by the strong 1:1 co-variation between $\delta^{15}N$ and $\delta^{18}O$ (Fig. 5.2c) (Granger, et al., 2008), and by uniformly 35‰ lower NO_2^- $\delta^{15}N$ values (Suppl. Info. Fig. 5.5). While larger than expected for OMZ denitrification (ε ~ 20 to 30‰), most of the NO_2^- ^{15}N depletion can be explained by this process. Biogenic N_2 concentrations throughout the OMZ at Station 7 (produced by either eterotrophic denitrification or anammox) follows concentrations predicted by N′ using Richards stoichiometry (1.71 NO_3^- : 1 N_2) (Richards, 1965) throughout the OMZ and account for most of the vertically integrated signal. However, biogenic N_2 concentrations in the oxycline (50 to 80 m) where little N-loss would be expected are both high and twice as high as predicted from N′ (Fig. 5.3a). Our observations at other 'normal' offshore OMZ stations (Bristow et al. in prep.), as well as recently published data (Chang, et al., 2010), do not show this unusual feature. Because of the large background of atmospheric N_2, the N′ mass balance-calculated anomaly in the $\delta^{15}N$ of total N_2 due to biogenic N_2 production stays close to 0 (Fig. 5.3b). Measure values are in agreement except for a maximum of 0.25‰ at the biogenic N_2 maximum (Fig. 5.3b). Whereas the calculated $\delta^{15}N$ of the biogenic component alone ranges from -5 to 3‰, the measured $\delta^{15}N$ of the biogenic contribution to N_2 at this depth is ~ 5‰. This implies a source for biogenic N_2 that has experienced little isotope fractionation, likely shelf sediment denitrification as discussed below.

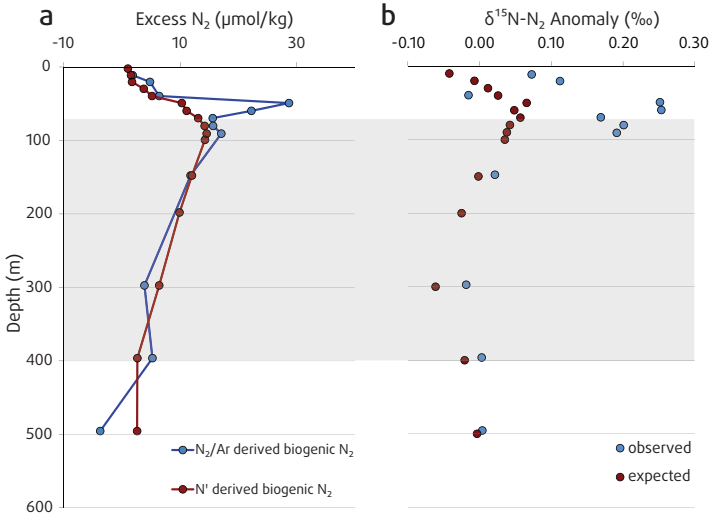

Fig. 5.3. Profiles at station 7. a) for biogenic N_2 concentration (µmol kg^{-1}) and b) the calculated and measured $\delta^{15}N$ anomaly for N_2. Expected biogenic N_2 from nitrogen anomaly (N′) assuming Richards stoichiometry (Richards, 1965) after taking into account N′ for water masses upstream of the OMZ. The deviation in N′ from actual NO_3^- removal due to PO_4^{-3} regeneration has also been adjusted for. Observed biogenic N_2 is calculated from deviations in N_2/Ar ratio from values expected at saturation with the atmosphere at in situ temperature and salinity and adjusted for physical sources of N_2/Ar anomaly by comparison with stations outside the OMZ (Chang, et al., 2010). The calculated $\delta^{15}N$ anomaly for N_2 is first based on estimation of the biogenic component from isotopic mass balance between NO_3^- laterally advected from outside the OMZ and OMZ NO_3^- and NO_2^-. Then the weighted average $\delta^{15}N$ for the biogenic and background atmospheric N_2 components is calculated to obtain the overall $\delta^{15}N$ anomaly.

Stations 7 and 29 are also associated with two coastal eddies detected in the January 2009 satellite map for sea-surface chlorophyll (SSC; Fig 5.4a). These eddies have low phytoplankton concentrations at their centers and high values around most of their peripheries. Sea level anomaly (SLA) reflects current structures superimposed on the mean flow and the satellite SLA map for this period confirms anticyclonic circulation within these features (Fig. 5.4b). Both anticyclonic and cyclonic eddies are important and persistent features of the circulation of this coastal upwelling system as well as the eastern tropical South Pacific as a whole (Chaigneau, *et al.*, 2008). Eddies likely impact OMZ N-loss through their transport of highly productive coastal waters offshore, visible as high SSC streamers in the January 2009 image (Fig. 5.4a). Station 7 was located within an eddy's edge and near the terminus of a

high SSC filament. Station 29 appears to have been more centrally-located, but the O_2 section at 16°S show this station to be located at the periphery of a 'bowl'-like distribution characteristic of an anticyclonic eddy's edge (same for station 7, Suppl. Info. Fig. 5.1). This apparent discrepancy is likely the result of eddy translation during the month-long period over which the SSC and SLA maps were averaged. Very high inshore productivity is associated with intense upwelling of nutrient-rich (NO_3^-, PO_4^{-3}, and silicate) waters on the shallow shelf coupled with sediment contact that relieves Fe limitation (Bruland, *et al.*, 2005). Given the observed eddy size and an estimated swirl velocity of ~ 20 km d^{-1} from ADCP measurements, it would take 20 days to transport coastal water to the location of Station 7 and even less time to Station 29. With an average eddy lifetime of ~1 month, there is sufficient time for these eddies to impact offshore waters. The very high biogenic N_2 (relative to N') observed within the oxycline at station 7 is therefore best explained as a feature produced by denitrification in shelf sediments and transported offshore. The high $\delta^{15}N$ value of the biogenic N_2 maximum is also consistent with a sediment source, where complete N-removal produces N_2 with little or no signal of isotope fractionation (Brandes and Devol, 1997).

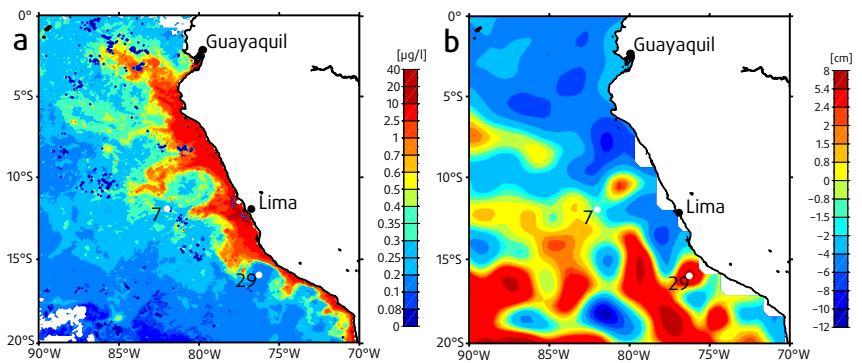

Fig. 5.4. Satellite observations averaged for January 2009, the month during which stations 7 and 29 were occupied (locations as indicated). a) for sea surface chlorophyll (ssc; µg l^{-1}) and b) sea level anomaly (SLA; cm). SSC reflects surface ocean phytoplankton concentration and productivity and was available from the NASA Giovanni website (http://gdata1.sci.gsfc.nasa.gov). SLA varies in response to barotropic velocity variation from the mean state and is available from the AVISO website (http://www.aviso.oceanobs.com).

Our new data shows that coastal eddies, through efficient offshore transport of highly productive inshore waters, enhance downward organic matter (OM) flux into the

deep OMZ thereby enhancing N-loss. Heterotrophic heterotrophic denitrification and dissimilatory nitrate reduction to ammonia processes are likely stimulated by these pulses in OM supply. While anammox is autotrophic, it is also dependent on NH_4^+ and NO_2^- supplied by heterotrophic denitrification and dissimilatory nitrate reduction to ammonia. Thus dissimilatory NO_3^- reduction and concomitant production of biogenic N_2 is likely controlled by OM flux (Thamdrup, et al., 2006). Highly productive filaments transiting offshore will inject large pulses of OM into the deep OMZ that would otherwise have been captured by inner shelf sediments. By providing fuel for deep-ocean microbial N-loss processes, eddies thereby enhance the system's overall N-loss relative to OM production. Assuming conventional Redfield (1958) and Richards (1965) stoichiometry, photoautotrophic conversion of 30 μmol kg^{-1} of NO_3^- in the upper 30 m of upwelled water would produce enough OM to deplete 20 μmol kg^{-1} of NO_3^- from the upper 250 m of the offshore OMZ. Eddy lifetime and swirl velocity appear sufficient for this OM to be both produced within the streamer structure and sink into the OMZ. When added to the 'background' NO_3^- removal observed throughout the Peru OMZ (Fig. 5.1), the magnitudes of the extreme indicators observed at Stations 7 and 29 are readily explained.

The observed extreme enrichments of NO_3^- ^{15}N and ^{18}O imply that important revisions to global ocean N and N isotope budgets are required. Because sedimentary denitrification produces little isotopic fractionation (Brandes and Devol, 1997), the ratio of the average ^{15}N enrichment in the whole ocean (~ 7‰ compared to sources) to the OMZ denitrification effect (~ 25‰) has been used to estimate the relative contribution of OMZ to sedimentary N-loss (Brandes and Devol, 2002). However, the extreme NO_3^- ^{15}N and ^{18}O enrichments resulting from extreme NO_3^- depletion reported here, requires by mass balance a less depleted N_2 product, Indeed, the calculated depth integrated average $\delta^{15}N$ for biogenic N_2 at Station 7 is ~ -1‰ only 6‰ less than the oceanic average for the $\delta^{15}N$ of NO_3^-. The resulting lower effective fractionation effect for OMZ N-loss when applied to global N isotope budgets would lead to OMZ's accounting for a larger portion of overall oceanic N-loss than previously thought (Altabet, 2007).

Our observations reveal that coastal eddies create previously unrecognized spatial as well as temporal variability in deep Peru OMZ biogeochemistry. Apparently contradictory results among prior studies (Bulow, et al., 2010, Lam, et al., 2009, Thamdrup, et al., 2006, Ward, et al., 2009) might be explained by experimental

station positions that varied relative to the eddy field. Pulses of OM from eddy streamers would also produce temporal successions in the underlying OMZ microbial community. In the oxycline and above, remineralization of organic matter, production of NH_4^+, and nitrification (and perhaps N_2O production) would be transiently enhanced as suggested by earlier observations (Friederich and Codispoti, 1987). Subsequent sinking of OM into the OMZ would stimulate heterotrophic processes supported by NO_3^- reduction leading to the observed enhanced N' and accumulation of NO_2^-. Pulses of heterotrophic denitrification ("stop-go denitrification") may also lead to enhancement of the production of N_2O (an intermediate in biochemistry of heterotrophic denitrification) (Naqvi, et al., 2000). NH_4^+ produced directly from OM and/or dissimilatory nitrate reduction to ammonia would in turn stimulate anammox. Overall, the Peru OMZ should be viewed as a dynamic system which is strongly affected by the physical forcing of OM flux that increases combined N-loss via transformations to biogenic N_2. This perspective may be critical to the design of future field programs.

The impact of coastal mesoscale eddies on OMZ N-loss processes is likely a general phenomenon operating in the other large OMZ's off Mexico and in the Arabian Sea where the number of eddies is even larger than off Peru (Chelton, et al., 2007). However, OMZ's extend geographically far beyond the region of direct influence by coastal eddies, especially the one off Mexico (Codispoti and Richards, 1976). In oligotrophic open ocean regions, mesoscale eddies are recognized as enhancing the vertical flux of nutrients and primary productivity (McGillicuddy, et al., 1998). Open ocean eddies may produce similar 'hotspots' for microbially mediated N-loss even in portions of OMZ's that are distant from productive coasts.

5.2. Supplementary Information

5.2.1. Methods

The physical, chemical, and biological dynamics of the Peru OMZ were studied in a series of cruises carried out as part of the German-led Climate - Biogeochemistry Interactions in the Tropical Ocean program (www.sfb754.de) of the German Research Foundation. At each station, water samples were collected using 12 l Niskin bottles on a CTD rosette system equipped with temperature, pressure, con-

ductivity and oxygen sensors. Nutrients and oxygen were determined according to Grasshoff et al.(1999) The isotopic composition of dissolved NO_3^- was measured using Cd-reduction to NO_2^- followed by reaction with azide to produce N_2O (McIlvin and Altabet, 2005). NaCl was added to ensure consistent quantitative yield (Ryabenko, et al., 2009). Pre-existing NO_2^- was removed at the time of collection by addition of sulfanilic acid. For NO_2^- isotopic analysis, a separate sample set was collected and preserved frozen and only the azide treatment was applied. Samples were analyzed in both Germany (ifm-geomar) and in USA (smast) using a purge-trap isotope ratio mass spectrometer (pt-irms) system. High precision N_2/Ar for detection of biogenic N_2 and $\delta^{15}N$-N_2 were determined on septum sealed samples using on-line gas extraction system coupled to a multicollector irms (Bristow et al., in prep.). These data were produced by removing O_2 in the samples prior to introduction into the mass spectrometer (Bristow et al., in prep.) to avoid artifacts associated with varying N_2/O_2 (Devol, et al., 2006). $\delta^{15}N$ N_2 data were acquired during the same analytical sessions and the anomaly reported is the difference with the value expected at equilibrium with the atmosphere at in situ temperature and salinity. Publicly available satellite data for sea surface chlorophyll (ssc) are from the nasa Govanni website (http://gdata1.sci.gsfc.nasa.gov) and sea level anomaly (sla) are from the aviso website (http://www.aviso.oceanobs.com).

5.2.2. Use of N′ to estimate NO_3^- removal and production of biogenic N_2

Outside of omz's, NO_3^- generally varies in stoichiometric proportion with PO_4^{-3} and O_2 as originally observed by Redfield (1958). Negative deviations in $[NO_3^-]$ from values expected from these proportions has been termed the NO_3^- deficit and is used to estimate net removal and production of biogenic N_2 in omz's. Here, we use a more general term, 'N anomaly'. Specific formulations have been reviewed by Devol (2008). We have used a modification of the commonly used $N^* = [NO_3^-]\text{-}16 \times [PO_4^{-3}] +2.9$) (Gumber and Sarmiento, 1997) which assumes NO_3^- as the only form of dissolved inorganic N, uses the Redfield N:P ratio, and applies an offset of 2.9 that allows for global average N* to be 0. The N anomaly, $N' = (NO_3^- + NO_2^- - 16 \text{ x } PO_4^{-3})$, takes into account NO_2^- (which can be found at significant concentrations in omz's), and forgoes the global offset as not being relevant regionally. N′ overestimates slightly actual NO_3^- removal because of PO_4^{-3} release from organic matter breakdown by about 16% (Devol, 2008). Accordingly,

biogenic N_2 ($N_{2\ biogenic}$) assuming equivalence with NO_3^- removal as well as Richards' stoichiometry (1.71 NO_3^-: 1 N_2) (Richards, 1965) (which takes into account conversion of organic N to N_2) can be calculated as;

$$1)\ N_{2\,biogenic}\ (\text{as } \mu\text{mol } N_2) = \frac{(N'_{source} - N'_{OMZ}) \times 0.86}{1.71}$$

$$2)\ N_{2\,biogenic} \sim (N'_{source} - N'_{OMZ}) \times 0.5$$

Because the corrections for PO_4^{-3} production and N_2 produced from organic N breakdown assume the same elemental stoichiometry for organic matter, they effectively cancel each other. The N'_{source} term accounts for source waters not necessarily having zero N anomaly. It was measured at stations upstream from the OMZ on isopycnal surfaces corresponding to those bounding the Peru OMZ and is about -5 μmol kg^{-1} in this system. Fig. 5.3a compares biogenic N_2 calculated in this fashion (N′ derived) with measured values (from N_2/Ar).

5.2.3. Anomaly in the $\delta^{15}N$ of N_2

The $\delta^{15}N$-N_2 anomaly reported is the difference with the value expected at atmospheric equilibrium at in situ temperature and salinity (between 0.6 and 0.8‰). For the measured anomaly, the difference between measured $\delta^{15}N$-N_2 and the equilibrium value is reported (Fig. 5.3b). For the expected anomaly, the $\delta^{15}N$ of biogenic N_2 is first calculated from isotope mass balance between source NO_3^- and OMZ NO_3^- and NO_2^- assuming differences are accounted for by production of biogenic N_2 ;

$$(3)\ \delta^{15}N - N_{2\,biogenic} = \frac{\delta^{15}N - NO_{3\,source} \times [NO_3^-]_{source} - [NO_3^-]_{OMZ} \times \delta^{15}N - NO_{3\,OMZ} - [NO_2^-]_{OMZ} \times \delta^{15}N - NO_{2\,OMZ}}{[N_{2\,biogenic}]}$$

$$(4)\ [NO_3^-]_{source} = 16 \times PO_{4\,OMZ}^{3} + N'_{source}$$

As for N'_{source}, $\delta^{15}N$-$NO_3^-{}_{source}$ is measured at stations upstream of the Peru OMZ and is about 7‰. Not included is the isotopic signal from the small amount of biogenic N_2 produced from organic N_2 which would be expected to produce a modest increase in its $\delta^{15}N$ value in this system.

The expected $\delta^{15}N\text{-}N_2$ anomaly is calculated by addition of the biogenic N_2 signal with the background N_2 of atmospheric origin ($N_{2\ atm}$; calculated assuming equilibrium at in situ temperature and salinity) with zero $\delta^{15}N$ anomaly;

$$5)\ \delta^{15}N - N_{2\ anomaly} = \frac{([N_{2\ atm}] + [N_{2\ biogenic}] \times \delta^{15}N - N_{2\ bioenic})}{([N_{2\ atm}] + [N_{2\ biogenic}])}$$

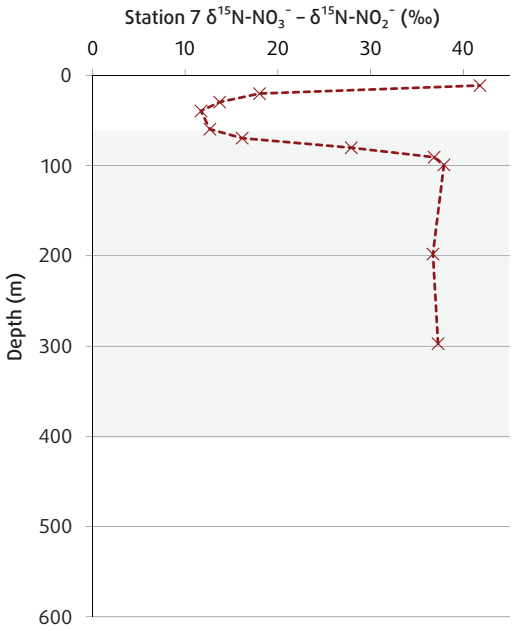

Fig. 5.5. Profile for the offset between $\delta^{15}N\text{-}NO_3^-$ and $\delta^{15}N\text{-}NO_2^-$ at Station 7. O_2^- is ^{15}N depleted relative to NO_3^- (e.g. low $\delta^{15}N\text{-}NO_2^-$) particularly in the OMZ below 90 m. The corresponding large and near steady offset within the OMZ is consistent with isotopic fractionation during dissimilatory NO_3^- reduction to NO_2^-.

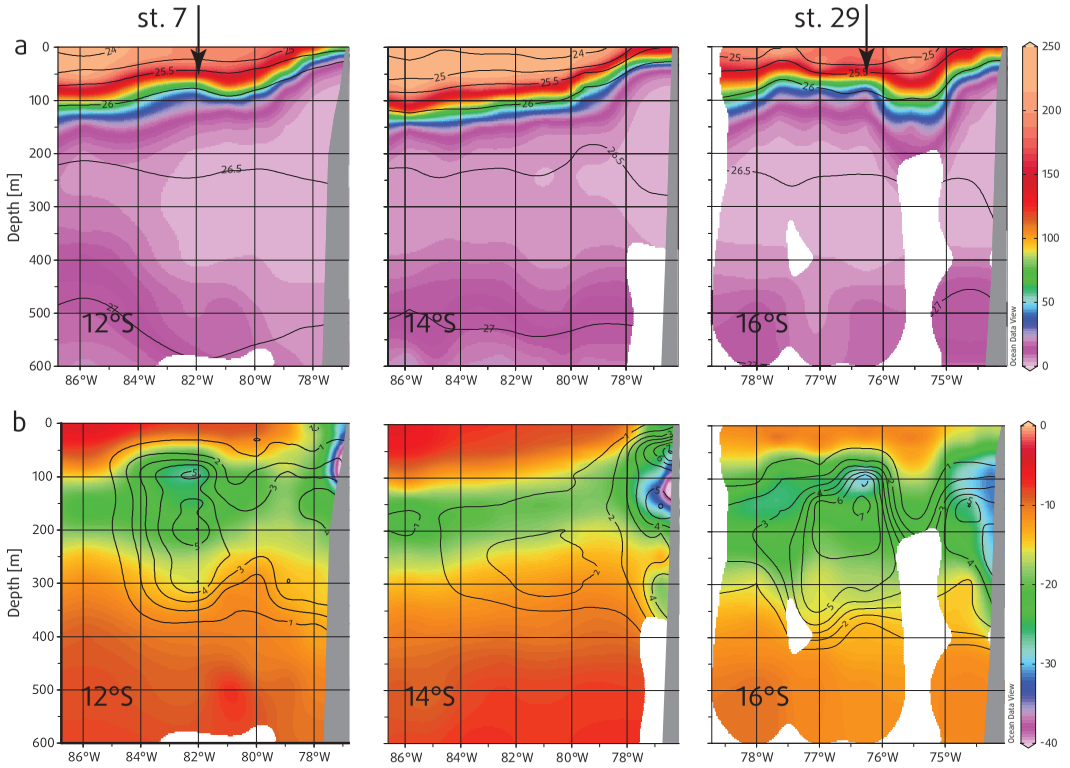

Fig. 5.6. Parameter distribution off the Peru coast. a) O_2 concentration (µmol kg^{-1}; color shading) and σ_θ (contour lines) sections at 12°S, 14°S and 16°S latitude (see station positions in Fig. 5.1). Stations 7 and 29 are part of the 12°S and 16°S sections, respectively, and their positions are marked. b) Corresponding N' (color shading) and NO_2-concentration (contour lines) sections at 12°S, 14°S and 16° S. Units are in µmol kg^{-1}.

6
Conclusions and Outlook

As a limiting element for biological productivity, nitrogen occupies a central role in ocean biogeochemistry. It exists in more chemical forms than most other elements, with a myriad of chemical transformations that are unique to this element. Nearly all these transformations are undertaken by marine organisms as part of their metabolism, which involves isotopic fractionation. Thus nitrogen stable isotopes carry important information on sources and sinks of nitrogen and its transformation within the oceanic cycle. Oxygen Minimum Zones are very important for nitrogen cycle being associated with the most nitrogen loss in the ocean. Models predict an expansion of OMZ under global warming conditions, which would have a direct influence on the global nitrogen cycle. Better understanding of nitrogen transformation in the OMZ is needed to estimate their global impacts nowadays and in the future.

In Chapter 2, the influence of chloride concentration on the performance of the chemical reduction method for measurement of the nitrogen isotopic ratio ($\delta^{15}N$) in NO_3^- in natural waters is discussed. The result of this study suggest that Cd reduction method of McIlvin and Altabet (2005) shows a variable conversion efficiency (both under- and overreduction were observed) and significant variation in $\delta^{15}N$ determination under low-salinity ($S < 30$) conditions. Addition of 5 M NaCl to all samples resulted in rapid (< 4 h) and quantitative (> 99%) reduction of NO_3^- to NO_2^- as well as stable $\delta^{15}N$ values that closely matched expected values for standards (within 0.3‰ of standard value). The positive effect of NaCl is likely due to a decrease in free Cd^{2+} produced over the course of the reaction due to formation of $CdCl_2$. This method was used for the nitrogen isotope analyses used for this dissertation.

Future work will include the development and improvement of the method not only for dissolved nitrate and nitrite $\delta^{15}N$ analysis but also for other nitrogen species, such as ammonium, and particulate organic nitrogen. It would be especially helpful to meas-

ure oxygen isotope ratios of the nitrogen-containing species as this carries additional information and could reduce ambiguity in the interpretation of N-transformations.

Chapter 3 focuses on nitrogen isotope and N_2O distribution in the Atlantic and Pacific OMZs. In this work an extensive amount of new data for nitrogen isotope and key nitrogen species collected from two regions is presented. The Atlantic region has higher oxygen levels (~ 40 μmol/l) but lower concentrations of DIN (maximum of ~ 40 μmol/l) in comparison to the Pacific region (< 2 μmol/l oxygen and ~ 50 μmol/l DIN). The N:P ratios show deviation from Redfield stiochiometry in both regions but in opposite directions, which is asign that the nitrogen cycles in the two regions are very different. The Atlantic Ocean is mostly known for N_2-fixation, while the Pacific for N-loss processes (denitrification/anammox). Indeed N' has the opposite sign in the regions: positive in the Atlantic and negative in the Pacific. The $\delta^{15}N$ in the two OMZ regions showed very different distributions. In the surface water of Atlantic very low values $\delta^{15}N$ were detected, originated from $\delta^{15}N^{-}[NO_3^-]s_{ahara\ dust}$ in the surface waters south of the Cape Verde Islands. The low $\delta^{15}N$ values from the dust deposited in the water column can influence the complete nitrogen budget, for example, decreasing N_2-fixation, estimated for the region. Calculations of the apparent fractionation factor in the Pacific OMZ results in $\varepsilon_d = 11.4‰$. Dividing the stations to shelf and off-shore we observe very different fractionation factors: on the shelf it is 7.6 ‰, and in the off-shore stations it is 16‰. The deviation from 7.6 to 16‰ in the Pacific region is most probably due to different "amount" of sedimentary denitrification, with stronger effects on the shelf with lower $\delta^{15}N$. Both, Sahara dust deposition $\delta^{15}N$ signature in the Atlantic and low fractionation factor of $\varepsilon_d = 11.4‰$ in the Pacific can change our understanding of nitrogen isotope cycling and have an impact on the isotope budget.

In spite of these differences, the N_2O vs. AOU distribution under oxygen concentrations above 5 μmol/l show very similar trends in the two regions. Comparison of N_2O and $\delta^{15}N$ shows that in both basins nitrous oxide is produced via nitrification process. The switch from nitrification to denitrification process is observed in the Pacific OMZ under oxygen concentrations below 5 μmol/l.

The results from chapter 3 showed that dust deposition in North Atlantic can bring in very isotopically light nitrogen species into the water, which can shift the $\delta^{15}N$ signature in the ambient waters. To estimate the importance of deposition for the regional $\delta^{15}N$ nitrogen cycle I would like to do more work at the Tropical Eastern North Atlantic Time-Series Observatory (TENATSO) together with biologists and me-

teorologists. The TENATSO station offers the possibility of seasonal sampling of the nitrogen isotope distribution (monthly sampling is possible). The combination of water column analysis, particulate nitrogen and zooplankton $\delta^{15}N$ analysis would improve understanding of the nitrogen sources and transformations in the tropical Atlantic. TENATSO also supports atmospheric measurements and aerosol collection, and it would be very helpful to measure $\delta^{15}N$ in the aerosol samples collected at the site and compare this to the observations in the water column.

Chapter 4 and 5 are devoted to collaborative work on the nitrogen cycle of the South Pacific OMZ. Chapter 4 focuses on the comparison of water column and surface sediment $\delta^{15}N$ data along the coast of Peru and Ecuador, bringing together the benthic and water column nitrogen cycles. The study is potentially significant in linking modern measurements to the paleooceanographic interpretation of nitrogen isotope variations recorded in ancient sediments. Nitrogen isotope distributions in water column and surface sediments along the South Pacific OMZ margin were shown to parallel each other with a shift to higher $\delta^{15}N$ values south of 8°S, colocated with OMZ intensification. An apparent fractionation effect of nitrate utilization was calculated from the water column data and was used to estimate the $\delta^{15}N$ in the particulate nitrogen produced in the surface waters. The apparent fractionation effect of nitrate utilization was found to be ~ 3.8‰ for the Peruvian region, whereas the initial $\delta^{15}N\text{-}NO_3^-$ values differ in the northern (~ 5‰) and in the southern (~ 7.7‰) parts of the region. The difference of the initial values is caused particularly by enhanced N-loss in the southern part of the region, which acts to raise the values of $\delta^{15}N\text{-}NO_3^-$. The calculated $\delta^{15}N$ in the particulate nitrogen based on the water column data fits very well to the measured surface sediments values, which proved the direct connection between water column and surface sediment data.

It is believed that sedimentary denitrification has a low fractionation factor (close to zero) due to substrate limitation in the system. In future, I would like to perform experiments with benthic chambers to measure in- and out-fluxes of nitrogen species to the sediments and their isotopic composition. This would help not only to understand the nitrogen cycle in this system but also to evaluate the connection of water column and sedimentary nitrogen systems. In this connection, it would be very helpful to measure sinking particulate nitrogen from the water column to have a direct comparison of surface water OM to surface sediments.

Chapter 5 is a collaborative work linking another two different disciplines of oceanography, this time physical and chemical. Observations made from several cruise

legs in the South Pacific revealed two stations with signals of extreme N-loss (e.g. $\delta^{15}N$ values as high as 40‰). Comparison of biogeochemical maps with satellite maps of sea-surface chlorophyll (SSC) and sea level anomaly (SLA) showed that these stations were associated with anticyclonic eddies, very stable at this period at this part of the ocean. These eddies had low phytoplankton concentrations at their centers and high values around most of their peripheries. By transporting productive, nutrient-rich coastal water offshore, eddies can drive pulses of organic matter to the ocean interior which can stimulate subsurface ocean N-loss 'events' with extreme N isotope fractionation. This would then cause enhanced production of NH_4^+ and N_2O in the upper oxycline, as well as a reduction of NO_3^- and accumulation of NO_2^- and N_2O in the core of the OMZ.

The observations underscore the importance of mesoscale eddies for nitrogen cycling in the Peruvian OMZ, which should be viewed as a dynamic system which is strongly affected by the variable physical forcing of organic matter flux. The overall results from the chapter 5 show how important it is to examine the oceanic nitrogen cycle not only from the geochemical perspective but also in the context of the regional physical context in order to avoid misinterpretation of the data.

In future studies, it would particularly interesting to follow an eddy transition and examine how nitrogen cycle changes temporally within and outside it. Nitrogen and oxygen isotope analysis of dissolved inorganic nitrogen (NO_3^-, NO_2^- and NH_4^+) as well as particulate nitrogen and N_2/Ar would help to distinguish the origin of the water and the key nitrogen transformations on the way from the shelf to the open ocean.

In summary, this study showed the value of nitrogen isotopes for revealing nitrogen sources, sinks and transformations in the ocean. The different components of the study have emphasized the importance of interdisciplinary and comparative approaches, and raised a set of new hypotheses concerning nitrogen cycling. Future work should address in more detail the questions of the significance of dust deposition in the Subtropical North Atlantic, fractionations associated with benthic fluxes in the South Pacific, and the role of mesoscale eddies for biogeochemical cycling and global nitrogen budgets.

Author contributions

Chapter 2 has been published (publicly available: http://www.aslo.org/lomethods/free/2009)

Ryabenko E., Altabet M.A. and Wallace D.W.R., 2009. Effect of chloride on the chemical conversion of nitrate to nitrous oxide for $\delta^{15}N$ analysis. *Limnology and Oceanography: Methods* **7**: 545–552.

Ryabenko wrote the manuscript and conducted all experimental work. Altabet and Wallace contributed to the discussion.

Chapter 3 is a manuscript submitted to the Global Biogeochemical Cycles. Kock provided the N_2O data and calculated ΔN_2O. Bange, Altabet and Wallace contributed to the discussion. All figures and calculations were performed by Ryabenko.

Chapter 4 is a manuscript in preparation. Mollier-Vogel provided all sediment data. All water column data and calculations were performed by Ryabenko. All authors contributed to the discussion and design of the research. This manuscript is not ready for submission yet due to unavailability of some co-authors due to their cruise engagements.

Chapter 5 is submitted to Nature GeoScience. (Ryabenko is free to use the manuscript as a chapter of her dissertation, as Science place no restrictions or conditions on such use of a submission). Project formulation was by Altabet, Ryabenko and Wallace. Altabet led the writing and analysis, with writing contributions from all authors and data and analysis contributions from Ryabenko, Stramma, Grasse, and Lavik. All authors discussed the results and commented on the manuscript.

References

Abell J., Emerson S. and Renaud P., 2000. Distributions of TOP, TON and TOC in the North Pacific subtropical gyre: Implications for nutrient supply in the surface ocean and remineralization in the upper thermocline. *Journal of Marine Research* **58** (2)**:** 203-222.

Altabet M.A. and McCarthy J.J., 1985. Temporal and spatial variations in the natural abundance of ^{15}N in PON from a warm-core ring. *Deep Sea Research Part A. Oceanographic Research Papers* **32** (7)**:** 755-772.

Altabet M.A. and Francois R., 1994. Sedimentary nitrogen isotopic ratio as a recorder for surface ocean nitrate utilization. *Global Biogeochemical Cycles* **8** (1)**:** 103-116.

Altabet M.A., Francois R., Murray D.W. and Prell W.L., 1995. Climate-related variations in denitrification in the Arabian Sea from sediment $^{15}N/^{14}N$ ratios. *Nature* **373** (6514)**:** 506-509.

Altabet M.A., Murray D.W. and Prell W.L., 1999a. Climatically linked oscillations in Arabian Sea denitrification over the past 1 m.y.: Implications for the marine N cycle. *Paleoceanography* **14** (6)**:** 732-743.

Altabet M.A., Pilskaln C., Thunell R., et al., 1999b. The nitrogen isotope biogeochemistry of sinking particles from the margin of the eastern North Pacific. *Deep-Sea Research Part I-Oceanographic Research Papers* **46** (4)**:** 655-679.

Altabet M.A., 2001. Nitrogen isotopic evidence for micronutrient control of fractional NO_3^- utilization in the equatorial Pacific. *Limnology and Oceanography* **46** (2)**:** 368-380.

Altabet M.A., Higginson M.J. and Murray D.W., 2002. The effect of millennial-scale changes in Arabian Sea denitrification on atmospheric CO_2. *Nature* **415** (6868)**:** 159-162.

Altabet M.A., 2007. Constraints on oceanic N balance/imbalance from sedimentary ^{15}N records. *Biogeosciences* **4** (1)**:** 75-86.

Antia N.J., Harrison P.J. and Oliveira L., 1991. The role of dissolved organic nitrogen in phytoplankton nutrition, cell biology and ecology. *Phycologia* **30** (1)**:** 1-89.

Arp D.J. and Stein L.Y., 2003. Metabolism of inorganic N compounds by ammonia-oxidizing bacteria. *Critical Reviews in Biochemistry and Molecular Biology* **38** (6)**:** 471-495.

Arthur M.A., 1983. Oceanic nitrogen isotopes and their use in determining the source of sedimentary nitrogen. in *Stable isotopes in sedimentary geology* (Arthur, et al.) sepm short cource: 62-97

Baker A.R., Kelly S.D., Biswas K.F., et al., 2003. Atmospheric deposition of nutrients to the Atlantic Ocean. *Geophysical Research Letters* **30** (24)**:** 2296-2300.

Baker A.R., Weston K., Kelly S.D., et al., 2007. Dry and wet deposition of nutrients from the tropical Atlantic atmosphere: Links to primary productivity and nitrogen fixation. *Deep Sea Research Part I: Oceanographic Research Papers* **54** (10)**:** 1704-1720.

Bange H.W., Naqvi S.W.A. and Codispoti L.A., 2005. The nitrogen cycle in the Arabian Sea. *Progress In Oceanography* **65** (2-4)**:** 145-158.

Barber R.T. and Chavez F.P., 1986. Ocean variability in relation to living resources during the 1982-83 El Nino. *Nature* **319** (6051)**:** 279-285.

Barford C.C., Montoya J.P., Altabet M.A. and Mitchell R., 1999. Steady-state nitrogen isotope effects of N_2 and N_2O production in *Paracoccus denitrificans. Applied and Environmental Microbiology* **65** (3)**:** 989-994.

Benton M.J. and Twitchett R.J., 2003. How to kill (almost) all life: the end-Permian extinction event. *Trends in Ecology & Evolution 18* (7)**:** 358-365.

Berman-Frank I., Cullen J.T., Shaked Y., et al., 2001a. Iron availability, cellular iron quotas, and nitrogen fixation in *Trichodesmium. Limnology and Oceanography* **46** (6)**:** 1249-1260.

Berman-Frank I., Lundgren P., Chen Y.B., et al., 2001b. Segregation of nitrogen fixation and oxygenic photosynthesis in the marine cyanobacterium *Trichodesmium. Science* **294** (5546)**:** 1534-1537.

Blackburn T.H. and Blackburn N.D., 1993. Coupling of cycles and global significance of sediment diagenesis. *Marine Geology* **113** (1-2)**:** 101-110.

Blackmer A.M., Bremner J.M. and Schmidt E.L., 1980. Production of nitrous oxide by ammonia-oxidizing chemoautotrophic microorganisms in soil. *Applied and Environtal Microbiology* **40** (6)**:** 1060-1066.

Bock E., Schmidt I., Stuven R. and Zart D., 1995. Nitrogen loss caused by denitrifyling *Nitrosomonas* cells using ammonium or hydrogen as electron-donors and nitrite as electron-acceptor. *Archives of Microbiology* **163** (1)**:** 16-20.

Bourbonnais A., Lehmann M.F., Waniek J.J. and Schulz-Bull D.E., 2009. Nitrate isotope anomalies reflect N_2 fixation in the Azores Front region (subtropical NE Atlantic). *Journal of Geophysical Research-Oceans* **114:** C03003.

Brandes J.A. and Devol A.H., 1997. Isotopic fractionation of oxygen and nitrogen in coastal marine sediments. *Geochimica et Cosmochimica Acta* **61** (9)**:** 1793-1801.

Brandes J.A., Devol A.H., Yoshinari T., et al., 1998. Isotopic composition of nitrate in the central Arabian Sea and eastern tropical North Pacific: A tracer for mixing and nitrogen cycles. *Limnology and Oceanography* **43** (7)**:** 1680-1689.

Brandes J.A. and Devol A.H., 2002. A global marine-fixed nitrogen isotopic budget: Implications for Holocene nitrogen cycling. *Global Biogeochemical Cycles* **16** (4)**:** art. #1120.

Brandes J.A., Devol A.H. and Deutsch C., 2007. New developments in the marine nitrogen cycle. *Chemical Reviews* **107:** 577-589.

Breitbarth E., Oschlies A. and LaRoche J., 2007. Physiological constraints on the global distribution of Trichodesmium - effect of temperature on diazotrophy. *Biogeosciences* **4** (1): 53-61.

Bruland K.W., Rue E.L., Smith G.J. and DiTullio G.R., 2005. Iron, macronutrients and diatom blooms in the Peru upwelling regime: brown and blue waters of Peru. *Marine Chemistry* **93** (2-4)**:** 81-103.

Bulow S.E., Rich J.J., Naik H.S., et al., 2010. Denitrification exceeds anammox as a nitrogen loss pathway in the Arabian Sea oxygen minimum zone. *Deep-Sea Research Part I-Oceanographic Research Papers* **57** (3)**:** 384-393.

Capone D.G., Oneil J.M., Zehr J. and Carpenter E.J., 1990. Basis for diel variation in nitrogenase activity in the marine planktonic cyanobacterium *Trichodesmium thiebautii. Applied and Environmental Microbiology* **56** (11)**:** 3532-3536.

Carpenter E.J., 1972. Nitrogen fixation by a blue-green epiphyte on pelagic *Sargassum. Science* **178** (4066)**:** 1207-1209.

Carpenter E.J., 1973. Nitrogen fixation by *Oscillatoria (Trichodesmium) thiebautii* in the southwestern Sargasso Sea. *Deep-Sea Research* **20** (3)**:** 285-288.

Carpenter E.J., 1983. Physiology and ecology of marine *Oscillatoria (Trichodesmium). Marine Biology Letters* **4** (2)**:** 69-85.

Casciotti K.L., Sigman D.M. and Ward B.B., 2003. Linking diversity and stable isotope fractionation in ammonia-oxidizing bacteria. *Geomicrobiology Journal* **20** (4)**:** 335-353.

Casciotti K.L. and McIlvin M.R., 2007. Isotopic analyses of nitrate and nitrite from reference mixtures and application to eastern tropical North Pacific waters. *Marine Chemistry* **107** (2)**:** 184-201.

Casciotti K.L., 2009. Inverse kinetic isotope fractionation during bacterial nitrite oxidation. *Geochimica et Cosmochimica Acta* **73** (7)**:** 2061-2076.

Chaigneau A., Gizolme A. and Grados C., 2008. Mesoscale eddies off Peru in altimeter records: Identification algorithms and eddy spatio-temporal patterns. *Progress In Oceanography* **79** (2-4)**:** 106-119.

Chang B.X., Devol A.H. and Emerson S.R., 2010. Denitrification and the nitrogen gas excess in the eastern tropical South Pacific oxygen deficient zone. *Deep Sea Research Part I: Oceanographic Research Papers* **57** (9)**:** 1092-1101.

Chavez F.P. and Barber R.T., 1987. An estimate of new production in the equatorial Pacific. *Deep Sea Research Part A. Oceanographic Research Papers* **34** (7)**:** 1229-1243.

Chavez F.P., Buck K.R., Service S.K., et al., 1996. Phytoplankton variability in the central and eastern tropical Pacific. *Deep-Sea Research Part II-Topical Studies in Oceanography* **43** (4-6)**:** 835-870.

Chavez F.P., Bertrand A., Guevara-Carrasco R., et al., 2008. The northern Humboldt Current System: Brief history, present status and a view towards the future. *Progress In Oceanography* **79** (2-4)**:** 95-105.

Chavez F.P. and Messie M., 2009. A comparison of eastern boundary upwelling ecosystems. *Progress In Oceanography* **83** (1-4)**:** 80-96.

Chazen C.R., Altabet M.A. and Herbert T.D., 2009. Abrupt mid-Holocene onset of centennial-scale climate variability on the Peru-Chile margin. *Geophysical Research Letters* **36:** L18704.

Chelton D.B., Schlax M.G., Samelson R.M. and de Szoeke R.A., 2007. Global observations of large oceanic eddies. *Geophysical Research Letters* **34** (15)**:** L15606.

Cline J.D. and Richards F.A., 1972. Oxygen deficient conditions and nitrate reduction in eastern tropical North Pacific Ocean. *Limnology and Oceanography* **17** (6)**:** 885-900.

Cline J.D. and Kaplan I.R., 1975. Isotopic fractionation of dissolved nitrate during denitrification in the eastern tropical North Pacific Ocean. *Marine Chemistry* **3** (4)**:** 271-299.

Codispoti L.A. and Richards F.A., 1976. An analysis of the horizontal regime of denitrification in the eastern tropical North Pacific. *Limnology and Oceanography* **21:** 379-388.

Codispoti L.A. and Christensen J.P., 1985. Nitrification, denitrification and nitrous-oxide cycling in the eastern tropical South Pacific Ocean. *Marine Chemistry* **16** (4)**:** 277-300.

Codispoti L.A., Brandes J.A., Christensen J.P., et al., 2001. The oceanic fixed nitrogen and nitrous oxide budgets: Moving targets as we enter the anthropocene? *Scientia Marina* **65:** 85-105.

Codispoti L.A., Yoshinari T. and Devol A.H., 2005. Suboxic respiration in the oceanic water column. *Respiration in Aquatic Ecosystems*. (del Giorgio and Williams) Blackwell Scientific: 225-247

Codispoti L.A., 2007. An oceanic fixed nitrogen sink exceeding 400 Tg Na-1 vs the concept of homeostasis in the fixed-nitrogen inventory. *Biogeosciences* **4** (2)**:** 233-253.

Codispoti L.A., 2010. Interesting times for marine N_2O. *Science* **327** (5971)**:** 1339-1340.

Cohen Y. and Gordon L.I., 1978. Nitrous oxide in the oxygen minimum of the eastern tropical North Pacific: Evidence for its consumption during denitrification and possible mechanisms for its production. *Deep Sea Research* **25** (6)**:** 509-524.

Dalsgaard T., Canfield D.E., Petersen J., et al., 2003. N_2 production by the anammox reaction in the anoxic water column of Golfo Dulce, Costa Rica. *Nature* **422** (6932)**:** 606-608.

De Pol-Holz R., Ulloa O., Dezileau L., et al., 2006. Melting of the Patagonian Ice Sheet and deglacial perturbations of the nitrogen cycle in the eastern South Pacific. *Geophysical Research Letters* **33** (4)**:** L04704.

De Pol-Holz R., Ulloa O., Lamy F., et al., 2007. Late Quaternary variability of sedimentary nitrogen isotopes in the eastern South Pacific Ocean. *Paleoceanography* **22** (2)**:** PA2207.

De Pol-Holz R., Robinson R.S., Hebbeln D., et al., 2009. Controls on sedimentary nitrogen isotopes along the Chile margin. *Deep-Sea Research Part II-Topical Studies in Oceanography* **56** (16)**:** 1100-1112.

Deutsch C., Gruber N., Key R.M., et al., 2001. Denitrification and N_2 fixation in the Pacific Ocean. *Global Biogeochemical Cycles* **15** (2)**:** 483-506.

Devol A.H. and Christensen J.P., 1993. Benthic fluxes and nitrogen cycling in sediments of the continental margin of the eastern North Pacific *Journal of Marine Research* **51** (2)**:** 345-372.

Devol A.H., Uhlenhopp A.G., Naqvi S.W.A., et al., 2006. Denitrification rates and excess nitrogen gas concentrations in the Arabian Sea oxygen deficient zone. *Deep-Sea Research Part I-Oceanographic Research Papers* **53** (9)**:** 1533-1547.

Duarte C.M., Dachs J., Llabres M., et al., 2006. Aerosol inputs enhance new production in the subtropical Northeast Atlantic. *Journal of Geophysical Research-Biogeosciences* **111** (G4)**:** G04006.

Duce R.A., LaRoche J., Altieri K., et al., 2008. Impacts of atmospheric anthropogenic nitrogen on the open ocean. *Science* **320** (5878)**:** 893-897.

Dugdale R.C. and Goering J.J., 1967. Uptake of new and regenerated forms of nitrogen in marine production. *Limnology and Oceanography* **12** (2)**:** 196-206.

Echevin V., Puillat I., Grados C. and Dewitte B., 2004. Seasonal and mesoscale variability in the Peru upwelling system from in situ data duting the years 2000 to 2004. *Gayana (Concepción)* **68:** 167-173.

Echevin V., Aumont O., Ledesma J. and Flores G., 2008. The seasonal cycle of surface chlorophyll in the Peruvian upwelling system: A modelling study. *Progress In Oceanography* **79** (2-4)**:** 167-176.

Elkins J.W., Wofsy S.C., McElroy M.B., et al., 1978. Aquatic sources and sinks for nitrous oxide. *Nature* **275** (5681)**:** 602-606.

Emerson S. and Hedges J.I., 1988. Processes controlling the organic carbon content of open ocean sediments. *Paleoceanography* **3** (5)**:** 621-634.

Eppley R.W. and Thomas W.H., 1969. Comparison of half-saturation constants for growth and nitrate uptake of marine phytoplankron *Journal of Phycology* **5** (4)**:** 375-379.

Eppley R.W. and Peterson B.J., 1979. Particulate organic matter flux and planktonic new production in the deep ocean. *Nature* **282** (5740)**:** 677-680.

Farrell J.W., Pedersen T.F., Calvert S.E. and Nielsen B., 1995. Glacial-interglacial changes in nutrient utilization in the equatorial Pacific Ocean *Nature* **377** (6549)**:** 514-517.

Fiedler P.C. and Talley L.D., 2006. Hydrography of the eastern tropical Pacific: A review. *Progress In Oceanography* **69** (2-4)**:** 143-180.

Frame C.H. and Casciotti K.L., 2010. Biogeochemical controls and isotopic signatures of nitrous oxide production by a marine ammonia-oxidizing bacterium. *Biogeosciences* **7** (2)**:** 3019-3059.

Freing A., Wallace D.W.R., Tanhua T., et al., 2009. North Atlantic production of nitrous oxide in the context of changing atmospheric levels. *Global Biogeochemical Cycles* **23:** GB4015.

Freundenthal T., Wagner T., Wnezhöfer F., et al., 2001. Early diagenesis of organic matter from sediments of the eastern subtropical Atlantic: Evidence from stable nitrogen and carbon isotopes. *Geochemica et Cosmochimica Acta* **65** (11)**:** 1795–1808.

Friederich G.E. and Codispoti L.A., 1987. An analysis of continuous vertical nutrient profiles taken during a cold-anomaly off Peru. *Deep Sea Research Part A. Oceanographic Research Papers* **34** (5-6)**:** 1049-1065.

Froelich P.N., Klinkhammer G.P., Bender M.L., et al., 1979. Early oxidation of organic matter in pelagic sediments of the eastern equatorial Atlantic: suboxic diagenesis. *Geochimica et Cosmochimica Acta* **43** (7)**:** 1075-1090.

Fuhrman J.A., McCallum K. and Davis A.A., 1992. Novel major archaebacterial group from marine plankton. *Nature* **356** (6365)**:** 148-149.

Galan A., Molina V., Thamdrup B., et al., 2009. Anammox bacteria and the anaerobic oxidation of ammonium in the oxygen minimum zone off northern Chile. *Deep-Sea Research Part II-Topical Studies in Oceanography* **56** (16)**:** 1125-1135.

Galbraith E.D., Kienast M., Pedersen T.F. and Calvert S.E., 2004. Glacial-interglacial modulation of the marine nitrogen cycle by high-latitude O_2 supply to the global thermocline. *Paleoceanography* **19** (4)**:** PA4007.

Gallon J.R., 2001. N_2 fixation in phototrophs: Adaptation to a specialized way of life. *Plant and Soil* **230** (1)**:** 39-48.

Ganeshram R.S., Pedersen T.F., Calvert S.E. and Murray J.W., 1995. Large changes in oceanic nutrient inventories from glacial to interglacial periods *Nature* **376** (6543)**:** 755-758.

Ganeshram R.S., Pedersen T.F., Calvert S.E., et al., 2000. Glacial-interglacial variability in denitrification in the world's oceans: Causes and consequences. *Paleoceanography* **15** (4)**:** 361-376.

Garcia-Fernandez J.M., de Marsac N.T. and Diez J., 2004a. Streamlined regulation and gene loss as adaptive mechanisms in *Prochlorococcus* for optimized nitrogen utilization in oligotrophic environments. *Microbiology and Molecular Biology Reviews* **68** (4)**:** 630-638.

Garcia-Fernandez J.M. and Diez J., 2004b. Adaptive mechanisms of nitrogen and carbon assimilatory pathways in the marine cyanobacteria *Prochlorococcus*. *Research in Microbiology* **155** (10)**:** 795-802.

Glessmer M.S., Eden C. and Oschlies A., 2009. Contribution of oxygen minimum zone waters to the coastal upwelling off Mauritania. *Progress In Oceanography* **83** (1-4)**:** 143-150.

Goreau T.J., Kaplan W.A., Wofsy S.C., et al., 1980. Production of NO_2^- and N_2O by nitrifying bacteria at reduced concentrations of oxygen. *Applied and Environmental Microbiology* **40** (3)**:** 526-532.

Granger J., Sigman D.M., Needoba J.A. and Harrison P.J., 2004. Coupled nitrogen and oxygen isotope fractionation of nitrate during assimilation by cultures of marine phytoplankton. *Limnology and Oceanography* **49** (5)**:** 1763-1773.

Granger J., Sigman D.M., Lehmann M.F. and Tortell P.D., 2008. Nitrogen and oxygen isotope fractionation during dissimilatory nitrate reduction by denitrifying bacteria. *Limnology and Oceanography* **53** (6)**:** 2533-2545.

Grasshoff K., Kremling K. and Ehrhardt M., 1999. Methods of seawater analysis – third, completely revised and extended version. *Seawater Analysis* Wiley-VCH.

Gruber N. and Sarmiento J.L., 1997. Global patterns of marine nitrogen fixation and denitrification. *Global Biogeochemical Cycles* **11** (2)**:** 235-266.

Gruber N. and Galloway J.N., 2008. An Earth-system perspective of the global nitrogen cycle. *Nature* **451** (7176)**:** 293-296.

Grundmanis V. and Murray J.W., 1977. Nitrification and denitrification in marine sediments from Puget Sound. *Limnology and Oceanography* **22** (5)**:** 804-813.

Hamersley M.R., Lavik G., Woebken D., et al., 2007. Anaerobic ammonium oxidation in the Peruvian oxygen minimum zone. *Limnology and Oceanography* **52** (3)**:** 923-933.

Hansell D.A. and Waterhouse T.Y., 1997. Controls on the distributions of organic carbon and nitrogen in the eastern Pacific Ocean. *Deep-Sea Research Part I-Oceanographic Research Papers* **44** (5)**:** 843-857.

Hansell D.A. and Feely R.A., 2000. Atmospheric intertropical convergence impacts surface ocean carbon and nitrogen biogeochemistry in the western tropical Pacific. *Geophysical Research Letters* **27** (7)**:** 1013-1016.

Hansell D.A., Bates N.R. and Olson D.B., 2004. Excess nitrate and nitrogen fixation in the North Atlantic Ocean. *Marine Chemistry* **84** (3-4)**:** 243-265.

Hastings M.G., Sigman D.M. and Lipschultz F., 2003. Isotopic evidence for source changes of nitrate in rain at Bermuda. *Journal of Geophysical Research-Atmospheres* **108** (D24)**:** art.# 4790.

Hebbeln D., 1992. Weichselian glacial history of the Svalbard area - correlating the marine and terrestrial records. *Boreas* **21** (3)**:** 295-304.

Helly J.J. and Levin L.A., 2004. Global distribution of naturally occurring marine hypoxia on continental margins. *Deep-Sea Research Part I-Oceanographic Research Papers* **51** (9)**:** 1159-1168.

Hendy I.L., Pedersen T.F., Kennett J.P. and Tada R., 2004. Intermittent existence of a southern Californian upwelling cell during submillennial climate change of the last 60 kyr. *Paleoceanography* **19** (3)**:** PA3007.

Hendy I.L. and Pedersen T.F., 2006. Oxygen minimum zone expansion in the eastern tropical North Pacific during deglaciation. *Geophysical Research Letters* **33** (20)**:** L20602.

Hoch M.P., Fogel M.L. and Kirchman D.L., 1992. Isortope fractionation associated with ammonium uptake by a marine bacterium. *Limnology and Oceanography* **37** (7)**:** 1447-1459.

Hoefs J., 2009. Stable isotope geochemistry. Springer Verlag.

Holmes R.M., McClelland J.W., Sigman D.M., et al., 1998. Measuring $^{15}N\text{-}NH_4^+$ in marine, estuarine and fresh waters: An adaptation of the ammonia diffusion method for samples with low ammonium concentrations. *Marine Chemistry* **60** (3-4)**:** 235-243.

Hooper A.B. and Terry K.R., 1979. Hydroxylamine oxidoreductase of *Nitrosomonas*: Production of nitric oxide from hydroxylamine. *Biochimica et Biophysica Acta (BBA) - Enzymology* **571** (1)**:** 12-20.

Hooper A.B., Vannelli T., Bergmann D.J. and Arciero D.M., 1997. Enzymology of the oxidation of ammonia to nitrite by bacteria. *Antonie Van Leeuwenhoek* **71** (1-2)**:** 59-67.

Howarth R.W., Marino R. and Cole J.J., 1988a. Nitrogen-fixation in fresh water, estuarine, and marine ecosystems. 2. Biogeochemical controls. *Limnology and Oceanography* **33** (4)**:** 688-701.

Howarth R.W., Marino R., Lane J. and Cole J.J., 1988b. Nitrogen fixation in fresh water, estuarine, and marine ecoystems. 1. Rates and importance. *Limnology and Oceanography* **33:** 469-687.

Hupfer M. and Lewandowski J., 2008. Oxygen controls the phosphorus release from lake sediments - A long-lasting paradigm in limnology. *International Review of Hydrobiology* **93** (4-5)**:** 415-432.

Huyer A., Smith R.L. and Paluszkiewicz T., 1987. Coastal upwelling off Peru during normal and El Niño times, 1981-1984. *Journal of Geophysical Research* **92** (C13)**:** 14297-14307.

Jasper J.P. and Gagosian R.B., 1989. Glacial-interglacial climatically forced $\delta^{13}C$ variations in sedimentary organic matter. *Nature* **342** (6245): 60-62.

Jetten M.S.M., Sliekers O., Kuypers M., et al., 2003. Anaerobic ammonium oxidation by marine and freshwater planctomycete-like bacteria. *Applied Microbiology and Biotechnology* **63** (2)**:** 107-114.

Johnson K.S., Elrod V.A., Fitzwater S.E., et al., 2003. Surface ocean-lower atmosphere interactions in the Northeast Pacific Ocean Gyre: Aerosols, iron, and the ecosystem response. *Global Biogeochemical Cycles* **17** (2)**:** art. #1063

Jones C.E. and Jenkyns H.C., 2001. Seawater strontium isotopes, oceanic anoxic events, and seafloor hydrothermal activity in the Jurassic and Cretaceous. *American Journal of Science* **301** (2)**:** 112-149.

Karl D., Letelier R., Tupas L., et al., 1997. The role of nitrogen fixation in biogeochemical cycling in the subtropical North Pacific Ocean. *Nature* **388** (6642)**:** 533-538.

Karl D., Michaels A., Bergman B., et al., 2002. Dinitrogen fixation in the world's oceans. *Biogeochemistry* **57** (1)**:** 47-98.

Karl D.M., Letelier R., Hebel D., et al., 1995. Ecosystem changes in the North Pacific subtropical gyre attributed to the 1991-92 El-Nino. *Nature* **373** (6511)**:** 230-234.

Karner M.B., DeLong E.F. and Karl D.M., 2001. Archaeal dominance in the mesopelagic zone of the Pacific Ocean. *Nature* **409** (6819)**:** 507-510.

Karstensen J., Stramma L. and Visbeck M., 2008. Oxygen minimum zones in the eastern tropical Atlantic and Pacific oceans. *Progress In Oceanography* **77** (4)**:** 331-350.

Kessler W.S., 2006. The circulation of the eastern tropical Pacific: A review. *Progress In Oceanography* **69** (2-4)**:** 181-217.

Knapp A.N., Sigman D.M. and Lipschultz F., 2005. N isotopic composition of dissolved organic nitrogen and nitrate at the Bermuda Atlantic time-series study site. *Global Biogeochemical Cycles* **19** (1)**:** GB1018.

Knapp A.N., Hastings M.G., Sigman D.M., et al., 2010. The flux and isotopic composition of reduced and total nitrogen in Bermuda rain. *Marine Chemistry* **120** (1-4)**:** 83-89.

Koeve W. and Kähler P., 2010. Heterotrophic denitrification vs. autotrophic anammox - quantifying collateral effects on the oceanic carbon cycle. *Biogeosciences* **7** (8)**:** 2327-2337.

Kuypers M.M.M., Sliekers A.O., Lavik G., et al., 2003. Anaerobic ammonium oxidation by anammox bacteria in the Black Sea. *Nature* **422** (6932)**:** 608-611.

Kuypers M.M.M., Lavik G., Woebken D., et al., 2005. Massive nitrogen loss from the Benguela upwelling system through anaerobic ammonium oxidation. *Proceedings of the National Academy of Sciences of the United States of America* **102** (18)**:** 6478-6483.

Lam P., Jensen M.M., Lavik G., et al., 2007. Linking crenarchaeal and bacterial nitrification to anammox in the Black Sea. *Proceedings of the National Academy of Sciences of the United States of America* **104** (17)**:** 7104-7109.

Lam P., Lavik G., Jensen M.M., et al., 2009. Revising the nitrogen cycle in the Peruvian oxygen minimum zone. *Proceedings of the National Academy of Sciences of the United States of America* **106** (12)**:** 4752-4757.

LaRoche J. and Breitbarth E., 2005. Importance of the diazotrophs as a source of new nitrogen in the ocean. *Journal of Sea Research* **53** (1-2)**:** 67-91.

Laursen A.E. and Seitzinger S.P., 2002. The role of denitrification in nitrogen removal and carbon mineralization in mid-Atlantic Bight sediments. *Continental Shelf Research* **22** (9)**:** 1397-1416.

Lavín M.F., Fiedler P.C., Amador J.A., et al., 2006. A review of eastern tropical Pacific oceanography: Summary. *Progress In Oceanography* **69** (2-4)**:** 391-398.

Lehmann M.F., Sigman D.M. and Berelson W.M., 2004. Coupling the $^{15}N/^{14}N$ and $^{18}O/^{16}O$ of nitrate as a constraint on benthic nitrogen cycling. *Marine Chemistry* **88** (1-2)**:** 1-20.

Lehmann M.F., Sigman D.M., McCorkle D.C., et al., 2005. Origin of the deep Bering Sea nitrate deficit: Constraints from the nitrogen and oxygen isotopic composition of water column nitrate and benthic nitrate fluxes. *Global Biogeochemical Cycles* **19:** GB4005.

Lehmann M.F., Sigman D.M., McCorkle D.C., et al., 2007. The distribution of nitrate $^{15}N/^{14}N$ in marine sediments and the impact of benthic nitrogen loss on the isotopic composition of oceanic nitrate. *Geochimica et Cosmochimica Acta* **71** (22)**:** 5384-5404.

Lenes J.M., Darrow B.P., Cattrall C., et al., 2001. Iron fertilization and the *Trichodesmium* response on the West Florida shelf. *Limnology and Oceanography* **46** (6)**:** 1261-1277.

Lewis M.R., Hebert D., Harrison W.G., et al., 1986. Vertical nitrate fluxes in the oligotrophic ocean. *Science* **234** (4778)**:** 870-873.

Lipschultz F., Wofsy S.C., Ward B.B., et al., 1990. Bacterial transformations of inorganic nitrogen in the oxygen-deficient waters of the eastern tropical South Pacific Ocean. *Deep Sea Research Part A. Oceanographic Research Papers* **37** (10)**:** 1513-1541.

Liu K.-K., 1979. Geochemistry of inorganic nitrogen compounds in two marine environments: The Santa Barbara Basin and the ocean off Peru. University of California.

Liu K.K. and Kaplan I.R., 1989. The eastern tropical Pacific as a source of ^{15}N-enriched nitrate in seawater off Southern California. *Limnology and Oceanography* **34** (5)**:** 820-830.

Lomas M.W. and Lipschultz F., 2006. Forming the primary nitrite maximum: Nitrifiers or phytoplankton? *Limnology and Oceanography* **51** (5)**:** 2453-2467.

Löscher C.R., Kock A., Könneke M., et al., Production of oceanic nitrous oxide by ammonia-oxidizing archaea *unpublished work*

Luyten J.R., Pedlosky J. and Stommel H., 1983. The ventilated thermocline. *Journal of Physical Oceanography* **13** (2)**:** 292-309.

Mague T.H., Mague F.C. and Holmhansen O., 1977. Physiology and chemical composition of nitrogen-fixing phytoplankton in the central North Pacific Ocean. *Marine Biology* **41** (3)**:** 213-227.

Mahaffey C., Williams R.G., Wolff G.A., et al., 2003. Biogeochemical signatures of nitrogen fixation in the eastern North Atlantic. *Geophysical Research Letters* **30** (6)**:** 1300.

Mariotti A., Germon J.C., Hubert P., et al., 1981. Experimental determination of nitrogen kinetic isotope fractionation - Some principles - Illustration for the denitrification and nitrification processes. *Plant and Soil* **62** (3)**:** 413-430.

Martinez P., Bertrand P., Calvert S.E., et al., 2000. Spatial variations in nutrient utilization, production and diagenesis in the sediments of a coastal upwelling regime (NW Africa): Implications for the paleoceanographic record. *Journal of Marine Research* **58:** 809-835.

Martinez P. and Robinson R.S., 2010. Increase in water column denitrification during the last deglaciation: the influence of oxygen demand in the eastern equatorial Pacific. *Biogeosciences* **7** (1)**:** 1-9.

Matear R.J. and Hirst A.C., 2003. Long-term changes in dissolved oxygen concentrations in the ocean caused by protracted global warming. *Global Biogeochemical Cycles* **17** (4)**:** art. #1125.

McCarthy J.J. and Carpenter E.J., 1979. *Oscillatoria* (*Trichodesmium*) *thiebautii* (*Cyanophyta*) in the central North Atlantic Ocean. *Journal of Phycology* **15** (1)**:** 75-82.

McGillicuddy D.J., Robinson A.R., Siegel D.A., et al., 1998. Influence of mesoscale eddies on new production in the Sargasso Sea. *Nature* **394** (6690)**:** 263-266.

McIlvin M.R. and Altabet M.A., 2005. Chemical conversion of nitrate and nitrite to nitrous oxide for nitrogen and oxygen isotopic analysis in freshwater and seawater. *Analytical Chemistry* **77:** 5589-5595.

Meissner K.J., Galbraith E.D. and Volker C., 2005. Denitrification under glacial and interglacial conditions: A physical approach. *Paleoceanography* **20** (3)**:** PA3001.

Messié M., Ledesma J., Kolber D.D., et al., 2009. Potential new production estimates in four eastern boundary upwelling ecosystems. *Progress In Oceanography* **83** (1-4)**:** 151-158.

Meyers P.A., 1997. Organic geochemical proxies of paleoceanographic, paleolimnologic, and paleoclimatic processes. *Organic Geochemistry* **27** (5-6)**:** 213-250.

Michaels A.F., Olson D., Sarmiento J.L., et al., 1996. Inputs, losses and transformations of nitrogen and phosphorus in the pelagic North Atlantic Ocean. *Biogeochemistry* **35** (1)**:** 181-226.

Mills M.M., Ridame C., Davey M., et al., 2004. Iron and phosphorus co-limit nitrogen fixation in the eastern tropical North Atlantic. *Nature* **429** (6989)**:** 292-294.

Monteiro F.M. and Follows M., 2006. Nitrogen fixation and preferential remineralization of phosphorus in the North Atlantic: Model insights. *Eos Trans., AGU, 87(36), Ocean Science Meeting* (Suppl)**:** OS35A– 06.

Montoya J.P. and McCarthy J.J., 1995. Isotopic fractionation during nitrate uptake by phytoplankton grown in continuous culture. *Journal of Plankton Research* **17** (3)**:** 439-464.

Montoya J.P., Carpenter E.J. and Capone D.G., 2002. Nitrogen fixation and nitrogen isotope abundances in zooplankton of the oligotrophic North Atlantic. *Limnology and Oceanography* **47** (6)**:** 1617-1628.

Moore J.K., Doney S.C., Kleypas J.A., et al., 2002. An intermediate complexity marine ecosystem model for the global domain. *Deep-Sea Research Part II-Topical Studies in Oceanography* **49** (1-3)**:** 403-462.

Morin S., Savarino J., Frey M.M., et al., 2009. Comprehensive isotopic composition of atmospheric nitrate in the Atlantic Ocean boundary layer from 65°S to 79° N. *Journal of Geophysical Research-Atmospheres* **114:** D05303.

Mulholland M.R. and Lomas M.W., 2008. Nitogen uptake and assimilation. in *Nitrogen in the Marine Environment* (Capone, Bronk, Mulholland and Carpenter) Elsevier Inc.: 303-384

Müller P.J. and Schneider R., 1993. An automated leaching method for the determination of opal in sediments and particulate matter *Deep-Sea Research Part I-Oceanographic Research Papers* **40** (3)**:** 425-444.

Müller P.J., Kirst G., Ruhland G., et al., 1998. Calibration of the alkenone paleotemperature index U-37(K') based on core-tops from the eastern South Atlantic and the global ocean (60° N - 60° S). *Geochimica et Cosmochimica Acta* **62** (10)**:** 1757-1772.

Naqvi S.W.A., Jayakumar D.A., Narvekar P.V., et al., 2000. Increased marine production of N_2O due to intensifying anoxia on the Indian continental shelf. *Nature* **408** (6810)**:** 346-349.

Naqvi S.W.A., Bange H.W., Farias L., et al., 2010. Marine hypoxia/anoxia as a source of CH_4 and N_2O. *Biogeosciences* **7** (7)**:** 2159-2190.

Nevison C., Butler J.H. and Elkins J.W., 2003. Global distribution of N_2O and the delta N_2O-AOU yield in the subsurface ocean. *Global Biogeochemical Cycles* **17** (4)**:** art. #1119.

Nevison C.D., Mahowald N.M., Weiss R.F. and Prinn R.G., 2007. Interannual and seasonal variability in atmospheric N_2O. *Global Biogeochemical Cycles* **21:** GB3017.

Nier A.O., 1950. A redetermination of the relative abundances of the isotopes of carbon, nitrogen, oxygen, argon, and potassium. *Physical Review* **77** (6)**:** 789-793.

O'Connor B.M., Fine R.A., Maillet K.A. and Olson D.B., 2002. Formation rates of subtropical underwater in the Pacific Ocean. *Deep-Sea Research Part I-Oceanographic Research Papers* **49** (9)**:** 1571-1590.

Oudot C., Andrie C. and Montel Y., 1990. Nitrous oxide production in the tropical Atlantic Ocean. *Deep Sea Research Part A. Oceanographic Research Papers* **37** (2)**:** 183-202.

Oudot C., Jean Baptiste P., Fourre E., et al., 2002. Transatlantic equatorial distribution of nitrous oxide and methane. *Deep Sea Research Part I-Oceanographic Research Papers* **49** (7): 1175-1193.

Paulmier A. and Ruiz-Pino D., 2009. Oxygen minimum zones (OMZs) in the modern ocean. *Progress In Oceanography* **80** (3-4)**:** 113-128.

Pennington J.T., Mahoney K.L., Kuwahara V.S., et al., 2006. Primary production in the eastern tropical Pacific: A review. *Progress In Oceanography* **69** (2-4)**:** 285-317.

Peters K.E., Sweeney R.E. and Kaplan I.R., 1978. Correlation of carbon and nitrogen stable isotope ratios in sedimentary organic matter. *Limnology and Oceanography* **23** (4)**:** 598-604.

Pichevin L., Bard E., Martinez P. and Billy I., 2007. Evidence of ventilation changes in the Arabian Sea during the late Quaternary: Implication for denitrification and nitrous oxide emission. *Global Biogeochemical Cycles* **21** (4)**:** GB4008.

Poth M. and Focht D.D., 1985. ^{15}N kinetic analysis of N_2O production by *Nitrosomonas europaea*: An examination of nitrifier denitrification. *Applied and Environmental Microbiology* **49** (5)**:** 1134-1141.

Pride C., Thunell R., Sigman D., et al., 1999. Nitrogen isotopic variations in the Gulf of California since the last deglaciation: Response to global climate change. *Paleoceanography* **14** (3)**:** 397-409.

Qu T., Gao S., Fukumori I., et al., 2009. Origin and pathway of equatorial 13°C water in the Pacific identified by a simulated passive tracer and its adjoint. *Journal of Physical Oceanography* **39** (8)**:** 1836-1853.

Redfield A.C., 1958. The biological control of chemical factors in the environment. *American Scientist* **46:** 205-221.

Rein B., 2007. How do the 1982/83 and 1997/98 El Niños rank in a geological record from Peru? *Quaternary International* **161** (1)**:** 56-66.

Remde A. and Conrad R., 1990. Production of nitric oxide in *Nitrosomonas europaea* by reduction of nitrite. *Archives of Microbiology* **154** (2)**:** 187-191.

Richards F.A., 1965. Anoxic basins and fjords. in *Chemical Oceanography* (Riley and Skirrow) Academic Press: 611-643

Ridame C. and Guieu C., 2002. Saharan input of phosphate to the oligotrophic water of the open western Mediterranean Sea. *Limnology and Oceanography* **47** (3)**:** 856-869.

Robinson R.S., Mix A. and Martinez P., 2007. Southern Ocean control on the extent of denitrification in the Southeast Pacific over the last 70 ka. *Quaternary Science Reviews* **26** (1-2)**:** 201-212.

Ryabenko E., Altabet M.A. and Wallace D.W.R., 2009. Effect of chloride on the chemical conversion of nitrate to nitrous oxide for $\delta^{15}N$ analysis. *Limnology and Oceanography: Methods* **7:** 545–552.

Saino T. and Hattori A., 1978. Diel variation in nitrogen fixation by a marine blue-green alga, *Trichodesmium thiebautii*. *Deep-Sea Research* **25** (12)**:** 1259-1263.

Saino T. and Hattori A., 1987. Geographical variation of the water column distrubution of suspended particulate organic nitrogen and its ^{15}N natural abundance in the Pacific and its marginal seas. *Deep Sea Research Part A. Oceanographic Research Papers* **34** (5-6)**:** 807-827.

Schepanski K., Tegen I. and Macke A., 2009. Saharan dust transport and deposition towards the tropical northern Atlantic. *Atmospheric Chemistry and Physics* **9** (4)**:** 1173-1189.

Schmidt H.L., Werner R.A., Yoshida N. and Well R., 2004. Is the isotopic composition of nitrous oxide an indicator for its origin from nitrification or denitrification? A theoretical approach from referred data and microbiological and enzyme kinetic aspects. *Rapid Communications in Mass Spectrometry* **18** (18)**:** 2036-2040.

Schott F.A., McCreary J.P. and Johnson G.C., 2004. Shallow overturning circulations of the tropical-subtropical oceans. in *Earth Climate: The Ocean-Atmosphere Interaction* (Wang, Xie and Carton) American Geophysical Union: 261–304

Schubert C.J. and Calvert S.E., 2001. Nitrogen and carbon isotopic composition of marine and terrestrial organic matter in Arctic Ocean sediments: Implications for nutrient utilization and organic matter composition. *Deep Sea Research Part I: Oceanographic Research Papers* **48** (3)**:** 789-810.

Seitzinger S.P., Sanders R.W. and Styles R., 2002. Bioavailability of DON from natural and anthropogenic sources to estuarine plankton. *Limnology and Oceanography* **47** (2)**:** 353-366.

Sigman D.M., Altabet M.A., Michener R., et al., 1997. Natural abundance-level measurement of the nitrogen isotopic composition of oceanic nitrate: an adaptation of the ammonia diffusion method. *Marine Chemistry* **57** (3-4)**:** 227-242.

Sigman D.M., Altabet M.A., McCorkle D.C., et al., 2000. The $\delta^{15}N$ of Nitrate in the Southern Ocean: Nitrogen cycling and circulation in the ocean interior. *Journal of Geophysical Research* **105** (C8)**:** 19599-19614.

Sigman D.M., Robinson R., Knapp A.N., et al., 2003. Distinguishing between water column and sedimentary denitrification in the Santa Barbara Basin using the stable isotopes of nitrate. *Geochemistry Geophysics Geosystems* **4** (5) (art. #1040)**:** 1040.

Sigman D.M., DiFiore P.J., Hain M.P., et al., 2009a. Sinking organic matter spreads the nitrogen isotope signal of pelagic denitrification in the North Pacific. *Geophysical Research Letters* **36:** L08605.

Sigman D.M., DiFiore P.J., Hain M.P., et al., 2009b. The dual isotopes of deep nitrate as a constraint on the cycle and budget of oceanic fixed nitrogen. *Deep-Sea Research Part I-Oceanographic Research Papers* **56** (9)**:** 1419-1439.

Stein L.Y. and Yung Y.L., 2003. Production, isotopic composition, and atmospheric fate of biologically produced nitrous oxide. *Annual Review of Earth and Planetary Sciences* **31:** 329-356.

Stramma L., Hüttl S. and Schafstall J., 2005. Water masses and currents in the upper tropical northeast Atlantic off Northwest Africa. *Journal of Geophysical Research* **110** (C12)**:** C12006.

Stramma L., Johnson G.C., Sprintall J. and Mohrholz V., 2008. Expanding oxygen-minimum zones in the tropical oceans. *Science* **320** (5876)**:** 655-658.

Stramma L., Johnson G.C., Firing E. and Schmidtko S., 2010. Eastern Pacific oxygen minimum zones: Supply paths and multidecadal changes. *Journal of Geophysical Research-Oceans* **115:** C09011.

Strub P.T., Allen J.S., Huyer A. and Smith R.L., 1987. Seasonal cycles of currents, temperatures, winds, and sea level over the Northeast Pacific continental shelf: 35°N to 48°N. *Journal of Geophysical Research* **92** (C2)**:** 1507-1526.

Strub P.T., Shillington F.A., James C. and Weeks S.J., 1998. Satellite comparison of the seasonal circulation in the Benguela and California current systems. *South African Journal of Marine Science-Suid-Afrikaanse Tydskrif Vir Seewetenskap* **19:** 99-112.

Suess E., Kulm L.D. and Killingley J.S., 1987. Coastal upwelling and a history of organic-rich mudstone deposition off Peru. *Geological Society, London, Special Publications* **26** (1)**:** 181-197.

Sutka R.L., Ostrom N.E., Ostrom P.H. and Phanikumar M.S., 2004. Stable nitrogen isotope dynamics of dissolved nitrate in a transect from the North Pacific Subtropical Gyre to the eastern tropical North Pacific. *Geochimica et Cosmochimica Acta* **68** (3)**:** 517-527.

Tanaka T.Y. and Chiba M., 2006. A numerical study of the contributions of dust source regions to the global dust budget. *Global and Planetary Change* **52** (1-4)**:** 88-104.

Thamdrup B., Dalsgaard T., Jensen M.M., et al., 2006. Anaerobic ammonium oxidation in the oxygen-deficient waters off northern Chile. *Limnology and Oceanography* **51** (5)**:** 2145-2156.

Van Mooy B.A.S., Keil R.G. and Devol A.H., 2002. Impact of suboxia on sinking particulate organic carbon: Enhanced carbon flux and preferential degradation of amino acids via denitrification. *Geochimica et Cosmochimica Acta* **66** (3)**:** 457-465.

van Niftrik L., Fuerst J., Sinningh Damste J.S., et al., 2004. The anammoxasome: an intracytoplasmic compartment in anammox bacteria. *FEMS Microbiology Letters* **233** (1)**:** 7-13.

Vidal M., Duarte C.M. and Agusti S., 1999. Dissolved organic nitrogen and phosphorus pools and fluxes in the central Atlantic Ocean. *Limnology and Oceanography* **44** (1)**:** 106-115.

Villareal T.A., 1994. Widespread occurrence of the Hemiaulus-cyanobacterial symbiosis in the southwest North Atlantic ocean. *Bulletin of Marine Science* **54** (1)**:** 1-7.

Voss M., Dippner J.W. and Montoya J.P., 2001. Nitrogen isotope patterns in the oxygen-deficient waters of the eastern tropical North Pacific Ocean. *Deep-Sea Research Part I-Oceanographic Research Papers* **48** (8)**:** 1905-1921.

Voss M. and Montoya J.P., 2009. Nitrogen cycle. Oceans apart. *Nature* **461** (7260)**:** 49-50.

Wada E. and Hattori A., 1978. Nitrogen isotope effect in the assimilation of inorganic nitrogenous compounds by marine diatoms. *Geomicrobiology Journal* **1** (1)**:** 85-101.

Walter S., Bange H.W., Breitenbach U. and Wallace D.W.R., 2006. Nitrous oxide in the North Atlantic Ocean. *Biogeosciences* **3** (4)**:** 607-619.

Wankel S.D., Kendall C., Pennington J.T., et al., 2007. Nitrification in the euphotic zone as evidenced by nitrate dual isotopic composition: Observations from Monterey Bay, California. *Global Biogeochemical Cycles* **21** (2)**:** GB2009.

Wankel S.D., Chen Y., Kendall C., et al., 2010. Sources of aerosol nitrate to the Gulf of Aqaba: Evidence from $\delta^{15}N$ and $\delta^{18}O$ of nitrate and trace metal chemistry. *Marine Chemistry* **120** (1-4): 90-99.

Wannicke N., Liskow I. and Voss M., 2010. Impact of diazotrophy on N stable isotope signatures of nitrate and particulate organic nitrogen: Case studies in the north-eastern tropical Atlantic Ocean. *Isotopes in Environmental and Health Studies* **46** (3)**:** 337-354.

Ward B.B., Talbot M.C. and Perry M.J., 1984. Contributions of phytoplankton and nitrifying bacteria to ammonium and nitrite dynamics in coastal water. *Continental Shelf Research* **3** (4)**:** 383-398.

Ward B.B., 1987. Nitrogen transformations in the Southern California Bight. *Deep-Sea Research Part A-Oceanographic Research Papers* **34** (5-6)**:** 785-805.

Ward B.B. and Bronk D.A., 2001. Net nitrogen uptake and DON release in surface waters: Importance of trophic interactions implied from size fractionation experiments. *Marine Ecology-Progress Series* **219:** 11-24.

Ward B.B., Devol A.H., Rich J.J., et al., 2009. Denitrification as the dominant nitrogen loss process in the Arabian Sea. *Nature* **461** (7260)**:** 78-81.

Waser N.A.D., Harrison P.J., Nielsen B., et al., 1998. Nitrogen isotope fractionation during the uptake and assimilation of nitrate, nitrite, ammonium, and urea by a marine diatom. *Limnology and Oceanography* **43** (2)**:** 215-224.

Wu J.P., Calvert S.E. and Wong C.S., 1997. Nitrogen isotope variations in the subarctic northeast Pacific: Relationships to nitrate utilization and trophic structure. *Deep-Sea Research Part I-Oceanographic Research Papers* **44** (2)**:** 287-314.

Yoshinari T., 1976. Nitrous oxide in the sea. *Marine Chemistry* **4** (2)**:** 189-202.

Zart D. and Bock E., 1998. High rate of aerobic nitrification and denitrification by *Nitrosomonas eutropha* grown in a fermentor with complete biomass retention in the presence of gaseous NO_2 or NO. *Archives of Microbiology* **169** (4)**:** 282-286.

Zehr J.P., Carpenter E.J. and Villareal T.A., 2000. New perspectives on nitrogen-fixing microorganisms in tropical and subtropical oceans. *Trends in Microbiology* **8** (2)**:** 68-73.

Zumft W.G. and Korner H., 1997. Enzyme diversity and mosaic gene organization in denitrification. *Antonie Van Leeuwenhoek* **71** (1-2)**:** 43-58.

Acknowledgements

First of all and foremost, I would like to thank Doug Wallace for his intercultural knowledge, British humor, never-ending optimism and encouragement throughout these years of my PhD. I would also like to thank Mark Altabet for his patience and substantial input during my work.

Many thanks to Gert Petrick for introducing me to the IRMS and standing by my side whenever I needed help with the equipment.

I am grateful to Annette Kock, Elfi Mollier-Vogel, Patricia Grasse, Carolin Löscher for providing me with additional data and samples, which made my work even more exciting and interesting. Many thanks to Hermann Bange, Ralph Schneider, Philippe Martinez, Lothar Stramma, Andreas Oschlies and Martin Frank for helpful discussions and critical comments. I would also like thank the captains of the L'Alalante and the Meteor, PIs, crew and scientists for two good cruises, where I could learn what an ocean is like and what it means to be an oceanographer. I am very thankful to Hansup Nam Koong for helping me with translations into German.

Many special thanks to Philipp Engewald for providing moral support and challenging me with non-oceanographer questions.

Eidesstattliche Erklärung

Hiermit erkläre ich an Eides statt, dass ich die vorgelegte Dissertation mit dem Titel “Nitrogen Isotopes in the Atlantic and Pacific Oxygen Minimum Zones”, abgesehen durch die Beratung durch den Betreuer, nach Inhalt und Form die eigene Arbeit ist, und dass ich die Arbeit weder gänzlich noch in Teilen kienem anderen Fachbereich bzw. noch keiner anderen Fakultät im Rahmen eines Prüfungsverfahrens vorgelegt habe.

Ich versichere außerdem, dass die Arbeit unter Einhaltung der Regeln guter wissenschaftlicher Praxis der Deutschen Forschungsgemeinschaft entstanden ist.

Evgenia A. Rybenko

Kiel, den 15.04.2010